Alma Mater Studiorum – Università di Bologna

DOTTORATO DI RICERCA IN

Ingegneria Civile, Chimica, Ambientale e dei Materiali

Ciclo XXX

Settore Concorsuale di afferenza: 09/D2 – SISTEMI, METODI E TECNOLOGIE DELL'INGEGNERIA CHIMICA E DI PROCESSO

Settore Scientifico disciplinare: ING-IND/24 – PRINCIPI DI INGEGNERIA CHIMICA

Novel experimental methods and modeling of solvent induced glass transition and structural relaxation in polymers

Presentata da: **Davide Pierleoni**

Coordinatore Dottorato **Supervisore**

prof. Luca Vittuari **prof. Ferruccio Doghieri**

Esame finale anno 2018

TABLE OF CONTENTS

Abstract

While glass transition and glassy dynamics, i.e. slow non-stationary dynamics occurring in amorphous solids, have been studied for long, they are still deemed to be grand challenges for science research, as well as strategic topics for technological advancement. This thesis reports scientific activities entirely devoted to the development of novel tools for advanced characterization of the glassy state, which is intended to support further work capable of knowledge improvement. The work focuses on the effects of solvent sorption in glassy dynamics, improvement of current experimental sorption analysis, but also on the relationship between sorption experiments and other classic techniques performed on dry glasses. The efforts aim at simplifying and promoting cross-analysis, and suggest wet experiments as tools for a comprehensive understanding of glassy structure. After a general and straightforward review of theories and experimental methods, novel investigation techniques and related experimental equipment are described. Special attention is given to a simple polymer-solvent system used as a model for setting up the experimental procedure, which showed complex behavior, and measured data resulted fresh enough to be reported in several national and international conferences and publications. Very topical systems as colloidal glass-formers are also subject of this work, for what concern the experimental activity carried out in the framework of an exciting period of study abroad, spent in Texas. Also in this case, productive efforts were devoted to equipment design and set up, and relevant results were obtained through the new procedure.

Chapter 1

Introduction

Despite the diffusion and common use of materials in the glassy state, there are still some gaps of knowledge concerning the nature of the glassy structure and its complex behavior. In fact, glassy materials are known from long time ago, since the first glass made artifacts were produced in the III century before Christ, according to Plinius II. [1]

A glass is apparently a solid material, presenting a lack of order on the microscopic level, that is thus referred to as amorphous structure. Theoretically, every existing liquid can be transformed in a glass through a sufficiently fast cooling process able to avoid the crystallization process, but real limitations restrict this class of materials (Glass Forming Liquids). On the other hand, as it will be specifically considered in the present thesis, different macroscopic processes may lead to formation of a glassy structure in the same material. Glasses are commonly present in nature, as vitrified lava or as parts of both flora and fauna, glasses as such are abundantly presents in our daily life, as houses and cars, but the most of employed glassy materials are represented by macromolecular glasses, especially plastics. These very different materials surprisingly share a similar behavior attributed to the glassy structure. [2]

For direct interests of the research group, as well as argument of relevant industrial interest, in this work glassy polymers were investigated. According to a report on plastic materials production from PlasticsEurope, the plastic production is still globally increasing, with 311 MT produced in 2014;

these are employed in many fundamental fields, mainly packaging, but significant quantities are employed also in constructions, automotive, electronics and agriculture [3]. This pictures a strategic use of polymeric materials, and it is easy to understand how the best knowledge of macromolecular glasses is a key to performance improvement and other research goals; even if not all these plastic materials are used in the glassy state, a good knowledge of the glassy state is fundamental for processing, for both raw materials and recycled. Beyond these aspects, the glassy dynamics are also observed in a wider range of materials, as pastes and colloidal emulsions, further increasing the interest on these complex phenomena.

This research project was focused on developing experimental methods for a new kind of response, to obtain information on glass forming material behavior directly at desired conditions, and provide better instruments for an easy and comprehensive modelling. The ultimate aim would be to supply some of the answers needed to effectively predict the phenomena related to the glassy state.

References

[1] Holland, P. The History of the World commonly called the Naturall Historie of C.Plinius Secundus, London, Printed by Adam Flip (1634).

[2] Struik, L. C. E. Physical aging in amorphous polymers and other materials. (1977).

[3] Plastics – the Facts 2015, PlasticsEurope (2015)

Chapter 2

Fundamentals of the glassy state

This chapter deals with basics on glass transition and would introduce the concept of structural relaxation. As already told, the glassy dynamics regards many kinds of materials and it has been studied for long. The multidisciplinary nature of this subject, and a description of the phenomenon that is still not complete, led to a wide range of approaches. Because of the ambitious goal of a global description of glassy dynamics set for this work, the description here given would be the most general available, and able to satisfy almost all points of view. After an introductory description of the phenomena, the sorption behavior of glasses is presented as one of the main aspects related to the experimental activity done, as well as one of the main interests of the research group, and more broadly in the context of the chemical engineering field.

2.1 The glass transition

Providing a clear and general definition for glass transition is one of the main challenges in this research field. In fact, it is not a first order transition, were a discontinuity on the first derivative of the free energy over thermodynamic variables is well understood and experimentally easy to confirm. A typical example of the clear difference that exists between the glassy and other transitions is the enthalpy behavior in isobaric experiments, where the temperature of a liquid

sample is decreased to reach a macroscopic solid state. Crystalline materials show a clean difference on the volume-temperature linear behavior among the liquid and the solid states, therefore a discontinuity on enthalpy appears; a glass forming liquid doesn't show any kind of discontinuity, and the volume behavior with temperature slowly change. This progressive evolution in the material behavior is one of the glass transition fingerprints, and one of the most trivial elements on the phenomenology which causes doubts on the nature of the glass transition. Indeed, it could be considered as a special case of a general behavior, and, conversely, a completely different process that is worthy of being described separately. This is a conceptual and theoretical problem as well as an actual complication causing real difficulties on experimental practice. Without proper transition starting from the liquid state, and in absence of a long-range order in the structure, the glassy structure can only be referred to as a liquid behaving as a solid-like state, due to the large increment of viscosity associated to the transition.

Continuing the counterpart of described cooling down phenomenon, crystallization and glass transition, the former is well characterized by characteristic conditions as the melting point, while the latter does not show precise characteristic values. And of course, the lack of a well determined transition point during glass formation make the equivalent characterization much more complicated. A typical parameter used to describe the transition due to thermal effect is the glass transition temperature (T_g). This is a value lying in the range of the typical slow-change behavior, bringing with it the need to define a method for its determination. Furthermore, these values can be sensitive to the experimental conditions, the kind of test itself, or just the type of response. Details on this will be treated in the experimental chapters.

Long time ago it was established that, in cooling experiments, the glass transition occurs when the rate of the configurational rearrangements of molecules becomes of the same order of the cooling rate, and consequently the glass transition controlled by a sort of freedom of movement, defined as molecular mobility [1]. This concept extends the dependency of materials behavior even to other

variables besides temperature used in the most diffused idea of the pseudo-solidification process; as example, Frenkel first noted that viscosity of liquids must depend on the specific structure rather than the temperature alone. [2] These simple elements are the basis for theories developed in the course of time, and these could be mainly divided into purely kinetic explanation, by which the glass transition is just an apparent phenomenon resulting from peculiarities in the viscoelastic behavior, and other approaches considering the glass formation to another transition order. The kinetic explanation is nevertheless insufficient to explain all aspects of the glassy systems, as discussed by Kauzmann [3] [4]. Within this frame, several authors spent their efforts to relate the molecular mobility to order parameters, especially excess volume, enthalpy, entropy, or configurational free energy. [4] [5] Although these approaches led to good descriptions of experimental observations, current capability for predictions is unsatisfactory and the glassy structure dynamic is still an open question [6].

Through experimental practice, relevant findings were reported on factors influencing the glass transition, sometimes supporting the already developed theories, but in some cases rising other questions. And this is a further evidence of how the research on glassy state is topical and a comprehensive description is needed. Some of the main results from these experimental advances over the last fifty years are represented by evidences of glass transitions induced by pressure at isothermal conditions, and by temperature at isochoric state; the latter will be addressed in more detail in Chapters 3, 6 and 8, where properly designed experiments will be described. [7] [8]

2.2 Structural relaxation

It is well established that amorphous materials below the glass transition are not in their thermodynamic equilibrium state, from the earliest discoveries about glasses [9]. A clear and traditional picture of the glassy state comes out from the change of specific volume as a function of

temperature. While both in higher temperature liquid and in glassy states a substantial linear dependency is shown, the glass transition is underlined as a change in this linear behavior, given that the glass shows a lower rate of change of volume with temperature with respect to the liquid phase. Dealing with the concept of molecular mobility, as already discussed, the glass transition occurs when the rate of configurational rearrangement becomes of the same order of a characteristic rate of change on the glass-inducing variable, e.g. temperature decreasing rate in the most common vitrification process. Thus, the molecular mobility is not null in the glassy state, and the latter represents an out-of-equilibrium condition due to a lack of time on structural reorganization; in the simple case of specific volume over temperature, while the glass follows a characteristic behavior (that is therefore dependent from the cooling rate), a theoretical equilibrium condition is represented by the extrapolation of the liquid behavior at temperatures lower than T_g. Hence the thermodynamic system at glassy state is continuously trying to improve its degree of order, the material slowly evolving towards a pseudo-equilibrium condition [10] [11]. Since this out-of-equilibrium behavior was first revealed from dilatometry, the phenomenon is usually referred as volume relaxation, or generally speaking as physical aging. However, other kind of relaxation phenomena were addressed through different kind of experiments and they will be described in the next chapters.

As for the glass transition per se, the importance of a good knowledge of the relaxation dynamics extends beyond a merely investigation on molecular motions, because this rearrangement influences dramatically the material properties, as brittleness increment, dielectric and viscoelastic properties, and so on: the “physical aging is a gradual continuation of the glass formation”, and then all the properties affected by the glass-inducing variables are interested by time dependency.

One of the most perplexing aspects of the aging phenomenon is represented by the dynamics occurring well below the glass transition. This is one of the most recent research field since some contrasting theories exist, but exhaustive tests have been hampered by experimental limitations, such as the need of old enough (densified) materials [12]. Persistency for very long times is a

physical aging characteristic, long time ago addressed by Struik, who gave an enormous contribution on the comprehension of physical aging, especially developing experimental protocol still in use; a summary of results is reported in a paper in bibliography [10]. Among those reported in the latter, an important aspect for the purposes of the present thesis is the reversibility. Experiments show that the history on an aged sample is fully erased when the material reaches the thermodynamic equilibrium in the liquid state after any transition and aging path. A reference condition can be then restored in a glass-forming material just restarting from the same equilibrium conditions (e.g. the same temperature above T_g), and the same sample can be used an arbitrary number of times.

2.3 Anomalous sorption behavior

There are a lot of similarity elements between the aforementioned glassy dynamics and the characteristic sorption behavior observed in glassy polymers. But as already told for other concepts, a discussion on experimental evidences is still open and a lot of different approaches to the problem are available. This paragraph would just summarize the most common and well-known arguments, in order to introduce main concepts that will be exploited in the interpretation of data which follows.

Polymers show a rapid response on sorption above the glass transition, when the applied conditions are changed as the solvent activity in the environment surrounding the sample. Furthermore, as for other materials, the transport mechanism follows the Fick's law. Glassy polymers represent an interesting case of apparent violation of the so called Fickian diffusion. The structural instability of glassy materials (physical aging) affects all the structure-dependent properties other than mechanical, diffusivity and the solubility to a penetrant among others [13].

A possible explanation on this influence involves the free volume concept, that acts as a connecting ring between the glassy dynamics and mass transport theories. Toward sorption modelling, several different theories based on free volume ideas were developed. However, these are all founded on the assumption that excess free volume on glassy polymers creates active sites for the mass transport process [14]. This conceptual volume is the same surplus of volume with respect to the theoretical equilibrium value involved in the physical aging discussion, and from this the effect of glassy dynamics on mass transport phenomena [15].

A possible classification for diffusion mechanism in glassy polymers was proposed by Frisch, depending on the difference between the characteristic times affecting the penetrant diffusion and the relaxation process running into the glassy structure [16].

Intuitively, when the relaxation process is much faster than the rate of diffusion the behavior is Fickian, and it is classified as Case I in this context. Conversely, when relaxation is much slower than diffusion, several different behaviors may result. When the kinetic order of the sorption process approaches one the phenomenon is classified as Case II, but even higher order kinetics may be observed, in so called Super Case II, as explained by Jacques, Hopfenberg and Stannett [17]. In the case both diffusion and relaxation processes have similar characteristic time, the sorption response became much more complicated due to the superposing phenomena and is generally classified as Non-Fickian or anomalous diffusion, where solubility over time is almost impossible to know even just qualitatively beforehand.

When the penetrant specie is capable of specific interactions with the polymer molecules, as example when the penetrant is a good solvent, the mobility of chains increases, and in some cases even the free volume depending on the solute concentration itself [18] [19]. Therefore, the sorption process of these species defined as “plasticizers” have some additional elements to consider, as characteristic times for both relaxational and diffusive mechanism affected by the penetrant concentration. This “plasticization” effect can be so relevant to induce a glass-to-rubber transition at

conditions far below to the “dry” glass transition temperature, and it has multiple implications in cases where the plasticizer concentration in a sample increases significantly over time, as it will be discussed in the introductory chapter for experimental methods.

An example of this implications is a transition between sorption cases as the plasticizer concentration changes the characteristic times to such an extent that it can be considered as a new glass-inducing variable. Based on the plasticization effect, Non-Fickian sorption behavior was empirically described by Berens and Hopfenberg, with a model that was also called “diffusion-relaxation” [20]. For the first time, they formalized the superposition of diffusive and solvent-induced relaxation phenomena, interpreting the varied sorption kinetics as a linear mathematical superposition of phenomenologically independent relaxation terms over the diffusion term. This approach led to postulate that the diffusion is a purely ideal Fickian process, and the anomalies for Non-Fickian behaviors in glassy polymers are ascribed to relaxation. This idea of process separation will be also supported by experiment results in the present thesis.

As already mentioned, plasticizers can also increase the free volume depending on their concentration. A sorption process starting from dry condition and increasing the solvent content can shows well distinct dynamics. Firstly, the penetrant molecules can be trapped into the free-volume already present in the glassy structure at dry state, until these are saturated. Specific positive interaction between molecules and an improved molecular mobility can then trigger another mechanism: the new condition at high solvent content can be “energetically convenient” for solvent penetration in “new holes” that are formed among macromolecules, and this lead to an increment of volume [21]. This process is usually referred to as sorption/swelling, and is an interesting phenomenon since represents a contrasting mechanism to the volume relaxation that can occur at the same time of usual relaxation dynamics. Such superposition will be deeply discussed in the results chapters.

It is clear from all the above that the glass dynamics in presence of penetrants, or the mass transport in glassy polymer as the other side of the coin, are quite complex processes where a number of variables are involved. After great scientific achievements obtained over the last 70 years, significant improvements could be now reached through novel robust experimental protocols exploiting the current framework on the subject. And this will be discussed in the next sections.

References

[1] Kovacs, A. Applicability of the free volume concept on relaxation phenomena in the glass transition range. *Rheologica Acta* **5**, 262-269 (1966).

[2] Frenkel, Y. I. Kinetic theory of liquids. (1955).

[3] Kauzmann, W. The nature of the glassy state and the behavior of liquids at low temperatures. Chemical Reviews 43, 219-256 (1948). [4] Gibbs, J.H. and DiMarzio, E.A. Nature of the Glass Transition and the Glassy State, J. Chem. Phys. 28, 3 (1958).

[5] Kovacs, A., Stratton, R. A. & Ferry, J. D. Dynamic mechanical properties of polyvinyl acetate in shear in the glass transition temperature range. The Journal of Physical Chemistry 67, 152-161 (1963).

[6] Debenedetti, P. G. & Stillinger, F. H. Supercooled liquids and the glass transition. *Nature* **410**, 259-267, doi:10.1038/35065704 (2001).

[7] Reiser, A., Kasper, G. & Hunklinger, S. Pressure-induced isothermal glass transition of small organic molecules. *Physical Review B***72**, 7, doi:10.1103/PhysRevB.72.094204 (2005).

[8] Colucci, D. M. *et al.* Isochoric and isobaric glass formation: Similarities and differences. *Journal of Polymer Science Part B-Polymer Physics* **35**, 1561-1573, doi:10.1002/(sici)1099-0488(19970730)35:10<1561::aid-polb8>3.0.co;2-u (1997).

[9] Kovacs, A. J. La contraction isotherme du volume des polymères amorphes. *Journal of Polymer Science Part A: Polymer Chemistry* **30**, 131-147 (1958).

[10] Struik, L. C. E. Physical aging in amorphous polymers and other materials. (1977).

[11] Menges, G. & Thienel, P. Pressure-specific volume-temperature behavior of thermoplastics under normal processing conditions. *Polymer Engineering & Science* **17**, 758-763 (1977).

[12] Zhao, J., Simon, S. L. & McKenna, G. B. Using 20-million-year-old amber to test the super-Arrhenius behaviour of glass-forming systems. *Nature Communications* **4**, 6, doi:10.1038/ncomms2809 (2013).

[13] Paul, D. Gas sorption and transport in glassy polymers. *Berichte der Bunsengesellschaft für physikalische Chemie* **83**, 294-302 (1979).

[14] Vrentas, J. S., Duda, J. L. & Ling, H. C. Free-volume theories for self-diffusion in polymer solvent systems .1. Conceptual differences in theories. *Journal of Polymer Science Part B-Polymer Physics* **23**, 275-288, doi:10.1002/pol.1985.180230204 (1985).

[15] Struik, L. C. E. Physical Aging in Plastics and other Glassy Materials. *Polymer Engineering and Science* **17**, 165-173, doi:10.1002/pen.760170305

(1977).

[16] Frisch, H. Sorption and transport in glassy polymers–a review. *Polymer Engineering & Science* **20**, 2-13 (1980).

[17] Jacques, C., Hopfenberg, H. & Stannett, V. in *Permeability of Plastic Films and Coatings* 73-86 (Springer, 1974).

[18] Bos, A., Punt, I. G. M., Wessling, M. & Strathmann, H. CO2-induced plasticization phenomena in glassy polymers. *Journal of Membrane Science* **155**, 67-78, doi:10.1016/s0376-7388(98)00299-3 (1999).

[19] Visser, T. & Wessling, M. When do sorption-induced relaxations in glassy polymers set in? *Macromolecules* **40**, 4992-5000, doi:10.1021/ma070202g (2007).

[20] Berens, A. & Hopfenberg, H. Diffusion and relaxation in glassy polymer powders: 2. Separation of diffusion and relaxation parameters. *Polymer* **19**, 489-496 (1978).

[21] Bonavoglia, B., Storti, G., Morbidelli, M., Rajendran, A. & Mazzotti, M. Sorption and swelling of semicrystalline polymers in supercritical CO2. *Journal of Polymer Science Part B: Polymer Physics* **44**, 1531-1546 (2006).

Chapter 3

Common experimental techniques

In this chapter most of the techniques are briefly introduced that are commonly used to characterize the glass transition and the evolution over time of the glassy structure. This short review would be a state-of-art on experimental methods that will be compared to the methodologies subject of this thesis. A brief discussion on evidences of the phenomena mentioned in the previous chapter will be provided, through the description of experimental methods, and typical results obtained from glassy materials.

3.1 Calorimetric techniques

One of the most diffuse technique for T_g determination is Differential Scanning Calorimetry (DSC). Developed on the early 1960s, the method involves temperature increase and decrease, measuring the difference of heat flux necessary to maintain the same temperature for the sample and a reference (as an empty pan). The DSC output is an isobaric curve (commonly acquired either heating or cooling at constant rate) used to describe the heat flux behavior over temperature; this is commonly named “thermogram”. On a common transition, as melt or crystallization, the physical phase change has a thermic effect, endothermic and exothermic respectively in these cases. This character is clearly identified on thermogram as maximum and minimum peaks. Conversely, any quiescent thermal effect is associated to the glass transition (as explained on Chapter 2), but the glassy structure shows a sudden change on heat capacity as characteristic thermal behavior, then the glass transition can be detected on the thermogram as a sigmoid. Identify a good range representative of the real transition requires good control on heating and cooling rates (5 K/min is in

the order of rate commonly applied), or even perform runs at different rates, being the DSC a dynamic technique, and the glass transition temperature spread over a temperature range.

Experiments starting from aged glassy structure typically reveal a peak immediately after the transition, then immediately after the sigmoid. Several works demonstrated that this peak depends on the aging occurring into the glassy structure, and DSC-based experimental protocols were developed to the purpose of structural relaxation analysis [1] [2]. Samples are first annealed at a temperature well above the transition, in order to erase any memory effect on the sample structure, then cooled down to a temperature below the glass transition following a selected rule arbitrarily chosen; the lower temperature is selected as "aging temperature". After waiting for a prescribed aging time, the sample is then heated on DSC to acquire the thermogram referred to that specific aging condition. Superposing aged and unaged curves (as null time aging curves or the common thermogram acquired without following any specific thermal protocol) an energy value can be evaluated from the peaks obtained by aging experiments. This value is commonly known as "loss of enthalpy" during aging, since at longer aging times are associated higher peaks; in other terms, by this technique an "enthalpy relaxation" is evaluated on aged samples. Recently, Rahman and Al-Saidi described an alternative technique exploiting DSC measurements to characterize the relaxational behavior of bovine gelatin in the glassy state [3]. After a common high temperature treatment to erase the previous history followed by cooling, the sample was heated to a temperature below T_g and the heat flux measured at isothermal conditions. The evaluation of the heat flux over time showed fast flux increment, and a nearly constant value was reached waiting relatively long relaxation times.

Great contribution on this field through DSC measurement was provided by Koh, McKenna and Simon [4]. They demonstrated the possibility to measure the glass transition depression on thickness reduction for polystyrene samples, using stacks of films from bulk-like to ultrathin sizes (about 17nm). Differently from other authors, they used an alternative technique that is called "step scan" method: while in the commonly applied technique the temperature ramp follows a constant

heating rate, in this method temperature is stepwise increased by low amplitude steps as 1K and the heat value acquired over time. This latter option has the main advantage on neglecting the need of an instrumental baseline when an accurate estimation of the specific heat is required.

The rate of temperature change can dramatically influence the glassy dynamics, as widely addressed in the previous chapter. Recently, the application of new technologies to calorimeters design, as Micro and Nano Electro-Mechanical Systems (MEMS and NEMS) brought to availability on the market of Fast Scanning Calorimeters (FSCs) and a next gen experiment was introduced and named as "Flash-DSC". Specialized instrumentation can work in a wide temperature range as -95 to 450ºC with rates between 0.1 - 4000 ºC/s (cooling) or 0.5 - 40000 ºC/s (heating) [5]. These tools can thus extend the experimental range to study the effect of rate of change in temperature on glassy dynamics, but also allow to test glassy structure that are not available in other tests, like polyamides that present crystallization at mild cooling rates.

A recent alternative calorimetric technique was developed in the early 1990s as Temperature Modulated Differential Scanning Calorimetry [6]. Through this technique two different time scales are introduced into the vitrification process: a long-time scale corresponds to the same temperature ramp applied in common DSC experiments, while a short time scale is tested through a temperature modulation with defined period and amplitude. This temperature modulation (often sinusoidal) was applied to the aim of activating different mechanism, or better to obtain responses from different processes separately; however, a difficult interpretation of results limited the use of this technique and its usefulness is still debated [6].

As a last example in a non-exhaustive list, another viable path for DSC test demonstrating the experimental potential of the technique was described by Zhang et al., extending the use of this technique even to isochoric conditions [7]. Polystyrene particles were constrained in a rigid inorganic shell made by silica, and the effect of the isochoric confinement was measured on the glassy dynamics and compared to other results through variable cooling rate experiments.

In summary, the calorimetric techniques are commonly employed in dynamic scanning mode through the transition, but this is also a very versatile test used over different conditions, wide ranges, it is useful for relaxation detection, and the availability of relatively cheap commercial systems allowed a great diffusion of the method and a great data availability.

3.2 Dilatometry

The very first experimental technique used to study the structural relaxation is dilatometry, since the 1940's. Mainly used to study thermal expansion and transitions (also on other materials than macromolecules), it's generally classified as a thermo-analytical method [8] [9]. The main concept of the instrument is to measure a volume change over a temperature variation, or for the specific process under investigation.

There are different kinds of instrument, depending on the measuring technique. The oldest and most diffused one is composed by solely tubing and a capillary. The volume is filled by a confining liquid where the sample is fully immersed; volume differences are easily detected by increases or decreases on the liquid level inside the capillary, then the system requires a previous calibration, and a confining liquid must be conveniently chosen for well-known volumetric properties and stability. Hence apparatus and experiments design require special attention, depending on required sensitivity and desired measuring range. Testing polymeric glasses has also specific requirements, as the confining liquid must be conveniently selected for immiscibility or low sorption not to affect the sample response.

The whole system is heated at a temperature well above the glass transition through a controlling system like a thermostatic bath, reaching the equilibrium starting point needed in common experiments. Decreasing the temperature on the system, a linear decreasing behavior is obtained over temperature, until the rate of configurational rearrangements become smaller than the cooling rate applied. A glassy structure presents a lower thermal effect, and then during the transition the

behavior is slower and slower up to a different, linear behavior when the transition is completed, and a new structure is homogeneously obtained over the sample.

Since early times in dilatometric studies, it was clear that the glassy structure slowly evolves over time, as a volume reduction can be clearly showed also at constant temperature. Therefore, the aging phenomenon was first called “volume relaxation”. Some of the most important works on literature on volume relaxation are from Kovacs [10] [11]. These studies described that, after quenching from above to below the glass transition, the specific volume of the sample decreases linearly with the logarithm of time. And beyond that, a reasonable stable value was reached just few degrees below the glass transition range, through a self-delaying relaxation phenomenon.

As in Kovacs studies, volume relaxation curves are still widely acquired at different temperature and controlling the sample thermal history to characterize the so called “densification”; the typical outputs of a dilatometry experiment can be found in literature from Grainer and Schwarzl following different protocols [12].

Modern apparatuses have high sensitivity in measuring the displacement in the capillary by exploiting advanced techniques, but the main concept of the apparatus remained the same over years. A line on experimental possibilities is represented by the confining liquid, because in addition to the already mentioned problems for its choice, it represents a great limitation in available cooling rates for high thermal inertia, heat transfer coefficient and thermic transients. These aspects are avoided working at isothermal conditions, then the glass transition is induced by pressure. Starting at a pressure-temperature couple in the equilibrium state, the pressure is increased through the glass transition; typically, the starting pressure is in the order of few Megapascals and the glassy state is tested up to hundreds and thousands Megapascals, so the experimental equipment requires special resistance to pressure differently from “old-times” instruments. In this kind of tests, the challenge is represented by compression rate control. In facts, systems that are allowable to these experiments must be equipped with a pressurizing system, as a pressure accumulator, and the specific system used can have specific difficulties in pressure control, related to the characteristics

of confining liquid. An alternative experimental protocol was proposed by Zoller and widely applied in literature, consisting in several isothermal compressions at several temperatures. [13] Starting from the highest temperature examined, the pressure is increased acquiring the volume values up to a high-pressure value, then the system is depressurized isothermally to the lower pressure value, and the temperature decreased at constant pressure to a new value of interest. This procedure is able to give a complete characterization on the pressure-volume-temperature (PVT) behavior rapidly, but it can be criticized for a complex previous history, that in facts can compromise interpretation of results in the glassy region [14].

An alternative instrument for volume measurements is the length dilatometer. It is composed by a specimen chamber and a head where a Linear Variable Differential Transformer (LVDT) is placed. [12] [15] The sample is mounted between a transmission rod and a bottom plate, so that the former transmits a induced relative displacement to the sensor. A LVDT shall be composed of three coils placed around a tube, and a ferromagnetic cylindrical core that can slides along the axis tube as the specimen changes its length. During operation the mid coil is driven by alternating current, which induces voltage to the others depending on the ferromagnetic slide position. The sample chamber must be purposely designed to finely control temperatures, since the LVDT is sensitive to the temperature, and a temperature fluctuation acts on the sample as well as on the transmission system. With respect to other dilatometric experiments, this instrument has then a great advantage allowing severe experimental conditions as extreme temperatures, but particular geometries are required for samples because of isotropic expansion is assumed, and the temperature has to be kept constant during measurements.

Summarizing this paragraph, dilatometry experiments are very robust tests, but there is a lack of flexibility that represents a limit in experimental ranges, and consequently on the modelling possibilities for glassy dynamics.

3.3 Mechanical techniques

This class of experiments exploits a mechanical response to detect glass transition and structural relaxation, e.g. the stress response to an applied strain or vice versa. On the glass transition, it causes a strong increase of mechanical performance, that is also easy to detect even qualitatively being this a macroscopic transition between a fluid-like behavior to a solid-like behavior. While DSC measurement techniques are nowadays a standard for transitions detection, and dilatometry played a fundamental role on the very first times of glass studies, mechanical techniques were the most widely used to study the glassy dynamics since the 50's. As a matter of facts, the viscosity behavior over temperature was the subject of plenty of the most important studies in the field, modelling experimental evidences through equations still used for simplicity and usefulness; furthermore, mechanical techniques were employed by Struik, who first described the glassy state relaxation phenomena as "physical aging" on 70's of the last century [16]. Works describe creep experiments that were first conduced with a lab-made torsional rheometer equipped with a high-speed nitrogen gas thermostat [17]. After about half an hour when samples were placed at a temperature above glass transition to reach equilibrium, these were rapidly quenched below T_g (quenching time is finite, but short and well reproduced!), then aged for a prescribed time at constant temperature. After multiple aging times, samples were tested for creep as a value referred to the actual glassy material properties after aging: to this aim, creep test time was taken much shorter than aging. Due to a smaller specific volume after aging, as explained by Kovacs years before, older samples showed longer creep times, then curves shifted to right on creep compliance vs. time. These curves were also collected in master curves, showing a process linearity, and useful observations and rules came from Struiks works [16].

Besides various possible setup for creep experiments, an alternative, useful and robust tool for dynamic glass study with mechanical analysis is represented by Dynamic Mechanical Analysis (DMA). While creep experiments focus on viscous characteristics of glassy materials and specifically the behavior over experimental and aging times, DMA is used to characterize dynamic

elastic modulus (or the dynamic shear modulus, if this configuration can be preferable), namely storage and loss modulus, and consequently complex modulus and "dissipation" loss factor (commonly referred as "tan δ") [18]. In the framework of glass transition investigation, clear evidences can be obtained from DMA as glass-to-rubber transition causes a huge drop of elastic modulus of about 2-3 orders of magnitude, between typical values of 10^9 to 10^7 Pa for glasses and rubbers respectively [19]. And this makes DMA very sensitive to transitions in any case it is applied, as well-controlled tension, compression or bending. Tests are commonly performed from low temperature on tailored solid-like samples; in the case of force-controlled instruments, a sinusoidal stress is applied at assigned frequency and strain is measured, imposing prescribed heating rates to the system during test. Glass transition is then identified as a maximum peak in the loss tangent, due to dramatic decrement in storage modulus and a maximum reached by loss modulus (even if, according to Akay, the tan δ peak analysis seemed controversial) [20]. As described for other scanning experiments, e.g. DSC, the temperature rate has an influence on detected glass transitions, hence this must be well controlled and constitutes a variable of interest in investigations. But differently from other experiments, another variable influencing DMA experiments is the imposed stress frequency. It is demonstrated that in any case storage modulus and apparent transition temperature increase with frequency, but while the first is common in viscoelastic materials even out of the glassy state (as it corresponds to the effect of strain rate on elasticity), the frequency effect on transition describes peculiarity on glass transition mechanisms as frequency is able to discriminate polymer chains involved in the transition process. As a consequence, according to the transition state theories, an activation energy for glass transition can be calculated from frequency shift by Arrhenius-like relationship [21].

In summary, mechanical techniques are powerful tools for glassy dynamic measurements, for sensitivity and output relevance. But several shortcomings emerge, first on output itself: as for DSC, different types of response affect measured temperature and other effects, and this is a limit in data comparison, analysis and modelling. For DMA, there is an intrinsic effect of applied frequency

that has pros and cons, as it can be exploited for useful information, but this emerges from its perturbation. Moreover, specific requirements from experimental equipment and samples, within the limit of most diffused commercial systems, represent a limitation on possible investigations, e.g. isobaric conditions or sample strength.

3.4 Spectroscopic techniques

In the last decades other techniques were accompanied to those classic experiments previously reviewed. Following the general modern development on research technology, these new kinds of experiments are based on different kind of spectroscopy.

Dielectric spectroscopy may be the spectroscopic technique among all the others able to give new information, as the diffusive motion can be observed over more than 18 orders of magnitude in frequency or time [22]. The technique consists in complex electrical permittivity measurements. Glassy samples are placed between opportune electrodes assembling a parallel plates capacitor; then the dielectric properties of the medium are measured as a function of the applied frequency and temperature, usually performed in heating direction to characterize the glass-to-rubber transition. Relaxation phenomena are clearly distinguishable from loss factor at different conditions, as example processing or strain, and the wide experimental range make possible to detect relaxation phenomena that are out of range in other experiments; however, a direct comparison of these results with common experiments as DMA is difficult, and other issues can emerge in the experimental practice [23] [24].

Again based on dielectric properties, another available technique involves ellipsometry. The polarization of an incident electromagnetic radiation is measured as amplitude ratio and phase difference, since these depends from material properties and sample thickness. Hence the glassy dynamics can be acquired as width measurements, to obtain thermal expansivity and glass transition values. Since a fine tuning on incident angles, as well as the applied frequency on the specific sample can significantly improve the sensitivity up to hundredths of nanometers, the technique is

popular in works dealing with the confinement effects on glass transition where nanometric films are employed [25] [26].

A significant limitation in dielectric experiments is represented by the sample itself. Low polar materials, as polystyrene, show negligible dielectric loss signal, especially at short-wave frequencies [27]. As demonstrated by Bauer et al, this problem can be overcome through temperature modulation in Thermal Expansion Spectroscopy (TES) experiments: here, the capacitance change ascribed to the temperature modulation is exploited to acquire relaxational information as thermal expansion coefficient [27] [28].

An ambiguous aspect of ellipsometry is the effect of film density on the refraction index. An alternative indirect dilatometry technique exploiting spectroscopy uses X-rays. The X-ray reflectivity is a surface-sensitive technique, which produces a reflectivity curve over the grazing angle. These curves present minima values, that are exploited to reveal a surface height increment; curves can also be fitted to pull the actual thickness value [29] [30].

Positron Annihilation Lifetime Spectroscopy (PALS) is another documented technique for glassy dynamics. Using radioactive beta-decay positrons T_g values and void volume information can be obtained for bulk polymer samples; however, specific technique for surface confinement behavior were also developed [31] [32].

Summarizing this merely listed review of spectroscopic experiments, lot of ways of this kind can be followed. These are all characterized by high sensitivity, and are highly valued to carry out studies on thin samples. But these are all indirect measurements requiring hard work on calibration, expensive equipment in some cases, specifically skilled researchers, so this kind of experiments are less diffused than others and less data are available. In addition to this, a comparison between output with classic experiments is so hard, and superposition of effects on responses can invalidate results, hence these are less robust tests. Intrinsic difficulties on sample preparation joined with already cited aspects feed contradictory studies, as example the case of confinement effects [33].

3.5 Sorption techniques

3.5.1. Gravimetric techniques

The sorption behavior and the glassy dynamics were considered independent fields before joining arguments emerged over time, as addressed in the previous chapter. Furthermore, in all the discussed experimental cases from the glassy dynamics at dry conditions is very hard, sometimes even impossible, to consider the effect of penetrants in the sample or in the experimental environment. Both these aspects contributed to perform and develop glasses sorption behavior experiments different than typical glassy structures characterizations.

While the first experiments on the glassy state regarded the volumetric behavior, sorption tests were intuitively gravimetric measurements. As far back as the 1930s papers are available on literature describing anomalous water sorption behavior on complex systems, as paper-making materials [34]. These works were carried out using a very sensitive gravimetric apparatus described for the first time some years before from McBain and Bakr [35]. They built their own quartz-made helices (springs), that were accurately calibrated at different temperature on their rheological behavior. Through elastic modulus, the spring elongation can be related to the weight supported by the system, as a bucket containing the sample. The operating principle exploited at that time is exactly the same reproduced in modern apparatuses, an example of which is described by Tsvigu et al. from the DICAM laboratories; just few improvements on experimental apparatuses were made over times on environmental control and automatic acquisition [36] [37]. Calibrated quartz springs are supported by a glass hook and placed inside a closed glass tube. The closed volume is thermoset at constant temperature by an external heat exchanger system, as a glass shell where water is fluxed from a recirculating bath; if a bucket is required to store the sample, this must be attached before assembling. The spring length is then measured to set a zero value at the experimental conditions desired of temperature and vacuum, provided by a vacuum pump. A glassy polymer sample is then attached to the spring tip (or inside the bucket), and the system again vacuumed at constant temperature until the system reaches appropriate vacuum degree and the sample completely dried.

At this stage system is ready for the actual sorption test: penetrant partial pressure is increased opening a liquid reservoir valve (that is opportunely mounted to allow just vapor fluxes), pressure measured by an opportunely ranged manometer, and the spring elongation due to weight increment acquired at constant temperature. In modern systems advanced imaging techniques are exploited through opportune cameras for automatic data acquisition. In this and other gravimetric systems placed in a gaseous environment, the presence of a characteristic pressure value in the measuring environment requires a data adjustment for sample buoyancy.

The output of this sorption test is a solubility curve over time, showing the sorption kinetic; the ongoing test is completed when a stable sorption value is obtained, then the partial penetrant pressure is increased to raise the solvent content and obtain solubility isotherms for different environmental solvent activity values. Each sorption step can demonstrate if the system follows a Fickian behavior: in this case, characteristic mass transport values as diffusion coefficient can be obtained applying the Fick's law on the characteristic diffusion path length, as example the film thickness [38]. If the system shows a non-Fickian behavior as shown in the previous chapter, a data interpretation can be a hard challenge; just in case the diffusive and the relaxation processes are well separated a diffusion coefficient value can be deduced, if the diffusion-relaxation process is considered [39] [40]. And furthermore, while measurements are not affected by aging for equilibrium solubility, the glassy state sorption behavior is strongly affected as example by the thermal history, as well as other treatment undergone by specimen. Measurements typically start from the glassy state going towards higher solvent contents, and this requires high attention on sample annealing procedures after processing and opportune aging protocols for sensible results. Relaxational behavior and glass transition values can be obtained from data analysis, as will be explained in detail in the next paragraphs.

The main output of gravimetric sorption measurements is the solubility isotherm over the penetrant concentration in the environment, usually expressed as penetrant mass uptake (absorbed mass per polymer mass unit) over the solvent activity. The simple case of rubbery-equilibrium materials this

curve can be completely interpreted by thermodynamic equilibrium models and important materials parameters may be obtained, while the glassy materials sorption isotherms are non-equilibrium curves that cannot be modelled in the same way [41] [42].

Pursuing on gravimetric sorption methods, the same procedure is commonly applied also on different kind of balances. A first example of appropriate balances is the instrument patented in the 1966 by Cahn [43]. The Cahn microbalance is an electric balance, where a pivoting beam is free to rotate about a fulcrum. A weighting pan is attached to the measuring arm, which is half of a beam equilibrated through an electric motor and a displacement detector, the latter purposely set to maintain the branches horizontally. A voltmeter is then used to measure the electromagnetically generated torque from transducer circuitry, hence the volt measure is transformed into a weight measurement. The main benefit of this kind of system is an improved range of sorption values to measure: in fact, the quartz spring system has a maximum displacement in the elastic field of the helices, then a maximum weight that can be measured on the sum of the sample and the absorbed solvent; in the Cahn system the weight range depends on the maximum torque, but this can be adjusted through a weight placed in the opposite beam of the measuring one [44] [45]. This system was used during this work, then it will be addressed later on in text.

Another more recent advance was made using magnetic suspension balance [46]. It is based on the magnetic susceptibility of materials, which in this instrument are used to build a sample support: a position transducer is used to achieve a controlled suspended state on a sample holder placed inside a controlled closed volume using an electromagnet. These devices can be useful for sorption experiments in aggressive atmosphere, since the sample volume is completely separated from the measuring system [47].

Previously cited examples are all high sensitivity systems that requires specific equipment. In case of a such high sensitivity is not required, gravimetric sorption tests can also be carried out using a simple analytic balance. For solvents in the liquid state, glassy polymer samples can be simply immersed into the solvent, and the mass uptake measured by weighting the sample on the balance

after blotted dry [48]. Solubility over solvent activity values can be achieved preparing binary solution with a low solubility solvent; however, the method has great restriction on temperature control and experimental ranges, and the solubility values are difficult to obtain crossing the glass transition.

Conversely, if a higher sensitivity is required, indirect mass measurement techniques are available. One of the most diffused in the sorption tests field is based on the Quartz Crystal Microbalance (QCM). A piezoelectric crystal has a precise resonant frequency; this frequency value significantly changes with external layers on the immediate surroundings of the crystal surface. Sauerbrey demonstrated that this layer mass is proportional to the resonant frequency decrement that can be measured by an oscillating signal applied to an electromagnetic resonator made by the crystal [49]. Then a glassy polymer thin film can be deposited on the resonator surface, the dry mass measured as the resonant frequency change, and absorbed mass uptake acquired regulating the penetrant pressure in the gaseous phase surrounding the sample [50]. This can be however applied without any correction for the film sample rheology just below the glass transition, because the resonant frequency value is also sensitive to the viscoelastic behavior of the deposited layer and its thickness: significant deviations from the Sauerbrey relationship were even theoretically demonstrated [51]. The sorption experimental technique carried out with QCM will be deeply described and analyzed later, as one of the apparatuses used in the described work.

Except for special versions of previously described scales, these systems are all suitable for vapor penetration, as purposely designed for low pressure tests. As example, the quartz spring balance requires glass-made volumes for the elongation detection from the outside, and vacuum system for sample treatment and perform the zero measurement; a pressure system is usually made by steel and common glass-metal couplings are opposite for pressure and vacuum applications. So high pressure gas solubility experiments are usually performed with an indirect gravimetric method, named “pressure decay”. Prior to testing, samples are weighted in the dry state after appropriate treatments, then placed in a sealed bomb of well calibrated volume. Here the system is evacuated and charged

to an initial pressure value of the penetrant specie, measured by a manometer installed into the volume. The solvent is sorbed over time as the pressure decreases, then the mass uptake can be calculated when the pressure reaches an asymptotic value, if a well-known penetrant quantity is introduced into the system, and using the opportune equation of state, depending on the applied conditions. A characteristic solution kinetic can also be obtained at pseudo-constant pressure value, since the pressure decreases during the process. The system can be then pressurized with additional gas to reach higher final pressure values, and so forth [52]. For its relative simplicity this is a great diffused technique over laboratories specialized in sorption measurements, then it is a robust technique for both vapors and gasses and enormous amount of data are available in literature collected through the pressure decay. Furthermore, it is very flexible on range values that can be obtained, as customized instruments can be easily assembled in a cheap way; on this, times ago Koros and Paul pointed out some of the design considerations possible in this kind of apparatus [53] .As others, this is another technique used for preliminary data acquisition in this work, and it will be discussed later.

3.5.2 Other techniques

The solvent absorption causes molecular mobility increment, but also a volume increment under specific conditions, as already described in the previous sections. This allows to measure significant glassy dynamics in presence of solvents as dilatometric measurements, similarly to dry cases.

A simple instrumentation for dilation measurements is based on optical cathetometer, that is an optical telescope able to measure vertical distances on a Vernier scale, by moving along a vertical rigid column. Annealed samples are placed inside a closed volume equipped with a see-through glass window, and free to dilate. As interesting systems for processing, but also for limitations on experimental vacuum systems already addressed in the previous paragraph, this kind of configuration is abundantly reported in literature as high pressure swelling experiments, especially by carbon dioxide [54] [55].

The same step-sorption experimental protocol for gravimetric systems is applied for sorption dilation experiments, which means a penetrant pressure is applied to the system until the acquired sample volume reaches an asymptotic value, then a higher-pressure value is applied and so on. The volume uptake behaviour over time and pressure is then qualitatively similar to the mass uptake pictured in the previous chapter, but important information on aging phenomenon can be obtained by comparison between gravimetric and dilatometric experiments, as recently shown by Punsalan and Koros [55]. As can be explained by some available models for polymer sorption, while both sorption and swelling are affected by glassy dynamics, they are regulated by different mechanisms. Just by the way of example, the dual mode sorption model expresses the sorption phenomena as the sum of dissolution (Henry-like) and hole filling (Langmuir-like) mechanisms, but only the first one contributes on volume increment. Furthermore, swelling is more strongly concerned by a competing effect between faster molecular mobility and low energetic barrier for solubility, both linked to the glassy dynamics as explained in the previous chapter. As a proof of this fact, Punsalan and Koros demonstrated that acquisition and cross-analysis of physical aging from both volume and mass sorption phenomena represent a prominent tool for research [55].

Coming back to the sorption dilatometric experiments analysis, a limitation on thickness measurements by visualization is the required assumption of isotropic volume expansion, which calls for regular sample shaping. Another problem is the sensitivity, since even for the most sophisticated systems is on the order of micrometres, and then just high swelling samples can be tested, or thick samples are allowable. To overcome these issues and to perform gravimetric and swelling tests simultaneously, Rajendran et al. developed a novel strategy based on gravimetric experiments [56]. They used a Rubotherm microbalance for mass measurements, joining gravimetric and volumetric sorption experiments. After a first run following usual protocols as pressure increment test, the pressure was increased using an inert gas selected for negligible solubility into the sample. Due to the increased buoyancy, the apparent sample weight decreases, then the sample density can be easily calculated. This method was however demonstrated as reliable

just at low pressure values from the authors themselves, due to inert gas effects on sorption behavior.

On using classic dry glassy dynamics methods for solvent effects, issues on controlled environment achievement in the test equipment were already mentioned. However, the solvent effects can be studied overcoming these problems performing creep experiments as described by Struik [16]. The same approach may be followed to evaluate solvent effect on aging, controlling sample history out of the experimental equipment, then tested by common equipment, so as neglecting desorption effects during operations. As a matter of example, Zhou and Lucas published results obtained by DSC and TMA from epoxy samples immerged in water at a temperature below the dry glass transition for aging times previously chosen, and tested after water desorption [57]. Results clearly show a variation on T_g by the whole hygrothermal history, and interestingly an increase of T_g for longer aging times as the result of the structural reorganization promoted by the sorbed water. Such results have, however, a lack of precision due to a weak control on environmental conditions or the effective water content, and just the final sample condition is registered.

These problems cannot be handled without developing alternative apparatuses able to perform desired tests under well-controlled conditions. On this, a fundamental contribution to the field was given by Han and McKenna, who first set an experimental apparatus with the specific purpose of enhancing the connection between sorption and classic experiments on glassy structure; similar experimental setup was also used in other subsequent works from the same research group, extending the operative range [58] [59]. The experimental apparatus is based on a LVDT sensor, as in classic length dilatometry, and the specimen chamber was purposely designed and assembled time after time for specific condition required by the desired experiment, as a double-layer environmental chamber set for a fine control of relative humidity (RH) or high-pressure chamber for gasses, all in independent system for temperature control [60] [61].

Classic experimental protocols were also employed in these experiments. As a first notable case, Zheng and McKenna applied analogous experiments to the Kovacs' kinetic experiments as intrinsic

isopiestic, asymmetry of approach and memory, to epoxy resin samples in presence of moisture [60]. Isopiestic experiments mean structural recovery measurements (as sample shrinking) performed at constant aging RH after sample equilibration: then this protocol is the sorption-equivalent to the Kovac's volume relaxation experiment previously described. The other protocols were also applied as RH jump test analogous to the temperature-jump experiments specific to the dry glass literature, and comparable results were obtained. This was first extremely important on understanding the similar processes promoted by temperature and the presence of specific penetrants, and second interesting differences in the structural relaxation behavior emerged, opening to new opportunities in the glass research field.

Another notable experiment performed by Alcoutlabi, Briatico-Vangosa and McKenna focused on the viscoelastic behavior of epoxy resins in presence of carbon dioxide. [61] A LVDT system was set for creep compliance measurements applying a load to the sample, loading weights to the sample with a geared lift, powered by an environment- and temperature- resistance electric motor. As in the previous example reported, this allowed to perform classic tests in presence of solvent, as the Struik's protocol: after sample annealing, creep tests were performed after controlled structural recovery, obtaining creep compliance behavior as a function of carbon dioxide pressure. Even temperature-jump experiments were performed using the same apparatus, and again a useful analysis on similarities and differences between thermic and penetrant cases was made possible.

These last examples of investigations are among the most recent and important achievements in the glass research field, but as underlined by the authors themselves, much more of penetrant effect on the glass structure must be understood.

3.5.3 Issues in glass sorption experiments

As addressed in the rows above, great advances in the glassy dynamics research field were obtained from combined experiments which involve classic responses, as volume or mechanic responses, and sorption phenomena. Intuitively, a good control on the highest variables number controlling the

process of interest can increase the experimental possibilities and help on modelling activity; however, the apparatus complexity could become relevant and affect the response with significant errors. Great issues on experimental practice emerge on sorption measurement depending on specific penetrants alone; among others, Schult and Paul described some aspects on accurate measurements of water vapor sorption and permeation [62].

The best achievement in those advanced techniques is the comparison between apparently different problems that revealed similar behavior, then a successful interpretation could be carried out with similar tools. And this is the reason why in this work novel experimental methods were developed, with a special attention on reproducing similar responses to the most common experiments in dry conditions.

As previously mentioned, sorption experiments are commonly performed at isothermal conditions, and the penetrant concentration step-increased up to the glass transition and above, when this occurs. This generates in both gravimetric and dilatometric experiments multiple sorption kinetics curves and solubility isotherms over the penetrant concentration, e.g. the penetrant partial pressure in the sample environment. While in dry experiments T_g values can be directly obtained from data through well-defined analysis tools (see previous Chapter), things are much more complicated in sorption tests. As example, from mass uptake curves acquired over time by gravimetric experiments, a characteristic transition value of penetrant pressure can be obtained at tested temperature just by observing the sorption kinetic (for examples, please refer to Chapter 4). In fact, while a liquid-like structure has a fast Fickian behavior, glassy structures shows a slow Non-Fickian sorption kinetics. But these can be difficult to be recognized a priori for the unpredictability nature of the phenomena, which furthermore depends on the penetrant content, thus it evolves during the experiment. In addition to this, the experiment is performed by step increments, then a unique value is almost impossible to identify as curves are built on discrete experimental points.

Alternatively, from the solubility curve built by asymptotic values from each step, additional information can be obtained on the transition zone, but this requires theoretical models. Acquiring

an opportune amount of data in the liquid-like state (high pressure), thermodynamic equilibrium models can be applied to follow the sorption behavior [39]. The glass transition zone can be then obtained as detachment of data at low pressure from the theoretical equilibrium, similarly to what is commonly done in dry dilatometry. But this requires high data in the liquid-like state, that can be difficult to measure in a single experiment due to the low viscosity progressively achieved, or even impossible at desired measurement range, and of course this is based on assumptions and requires computational costs.

Another issue of sorption tests concerns the time required, as typical heat transfer coefficients are orders of magnitude higher than mass transport ones. In other words, since the glassy state shows slow dynamics, each sorption step can require weeks or months to reach asymptotic solubility values, depending on the sample thickness, as well as the environmental conditions of temperature and solvent concentration, and experiment design considerations can be done just for well-known materials as the diffusion coefficient can be determined just from the experiment itself. This results in low flexibility on sample preparation, preliminary data required and extremely long experimental times.

Analysis of aging induced by sorption could require even longer times. It can be indeed evaluated performing multiple experiments on different samples, instead of an online measure as commonly done in dilatometry. This requires very long times for sample preparation to observe significant differences in the sorption behavior, in addition to long experimental times already discussed, and difficulties could emerge also on finely control aging conditions [55].

An additional limitation on common practice is the need to acquire asymptotic values. First, the experimental protocol is not well-defined, since rules to set the end of sorption stage cannot be established for the unpredictability already cited; evidences of never-ending step processes were also reported on literature [39]. This of course causes a lack of reliability on these kinds of experiments.

Still on this procedure, the long times required by each step extend the aging time, then the history on the sample changes point-by-point, becoming even more complicated as also the experimental temperature and the penetrant content over the sample thickness must be accounted in the aging. And again, just poor information can be acquired on the ongoing relaxation during experiments, and long times relaxation (especially far from the glass transition, the most relevant for modelling interests) are completely avoided, these occurring well above the sorption asymptote.

Another limitation on these experiments, as well in some others already described, is to require solid glass samples. While in common dry experiments, as DSC or volume dilatometry, a sample normalization can be performed directly into the test equipment, these and other consolidated protocols require a sample annealing before sample loading. Clear disadvantages of the latter are the sample handling at room conditions, a poor control on the sample history, but also limitation on the measurements themselves as available experimental ranges.

All these are main well-known aspects on the experimental practice that limited progresses in the field so far, and represent the main motivation to this work.

In the following chapters some novel experimental protocols will be described. Each setup here described has been purposely designed to overcome some of the typical issues listed above, and other aspects as consideration previously reported for dry glass experiments has been also considered, in order to design reliable experiments able to provide useful information for analysis and modelling of glassy structures.

References

[1] Tanaka, Y., Asano, H. & Okuya, Y. Enthalpy relaxation near the glass transition for comb-like polymer: Power law relaxation revealed by DSC experiment. Journal of Non-Crystalline Solids 363, 147-151, doi:10.1016/j.jnoncrysol.2012.11.050 (2013).

[2] Koh, Y. P. & Simon, S. L. Enthalpy Recovery of Polystyrene: Does a Long-Term Aging Plateau Exist? Macromolecules 46, 5815-5821, doi:10.1021/ma40112361 (2013).

[3] Rahman, M. S. & Al-Saidi, G. S. Thermal Relaxation of Gelatin and Date Flesh Measured by Isothermal Condition in Differential Scanning Calorimetry (DSC) and its Relation to the Structural and Mechanical Glass Transition. International Journal of Food Properties 13, 931-944, doi:10.1080/10942912.2010.489210 (2010).

[4] Koh, Y. P., McKenna, G. B. & Simon, S. L. Calorimetric glass transition temperature and absolute heat capacity of polystyrene ultrathin films. Journal of Polymer Science Part B-Polymer Physics 44, 3518-3527, doi:10.1002/polb.21021 (2006).

[5] Mathot, V. *et al.* The Flash DSC 1, a power compensation twin-type, chip-based fast scanning calorimeter (FSC): First findings on polymers. *Thermochimica Acta* **522**, 36-45, doi:10.1016/j.tca.2011.02.031 (2011)

[6] Jiang, Z., Imrie, C. T. & Hutchinson, J. M. An introduction to temperature modulated differential scanning calorimetry (TMDSC): a relatively non-mathematical approach. *Thermochimica Acta* **387**, 75-93, doi:10.1016/s0040-6031(01)00829-2 (2002).

[7] Zhang, C., Guo, Y. L., Shepard, K. B. & Priestley, R. D. Fragility of an Isochorically Confined Polymer Glass. *Journal of Physical Chemistry Letters* **4**, 431-436, doi:10.1021/jz302002v (2013).

[8] Boyer, R. & Spencer, R. Thermal Expansion and Second-Order Transition Effects in High Polymers: Part I. Experimental Results. Journal of Applied Physics 15, 398-405 (1944).

[9] Alfrey, T., Wiederhorn, N., Stein, R. & Tobolsky, A. Some studies of plasticized polyvinyl chloride. Journal of Colloid Science 4, 211-227 (1949).

[10] Kovacs, A. J. La contraction isotherme du volume des polymères amorphes. Journal of Polymer Science Part A: Polymer Chemistry 30, 131-147 (1958).

[11] Kovacs, A. J. in Fortschritte der hochpolymeren-forschung 394-507 (Springer, 1964).

[12] Greiner, R. and Schwarzl, F. Thermal contraction and volume relaxation of amorphous polymers. Rheologica Acta 23, 378-395, doi:10.1007/BF01329190 (1984).

[13] Walsh, D. & Zoller, P. *Standard pressure volume temperature data for polymers*. (CRC Press, 1995).

[14] Briatico-Vangosa, F. & Rink, M. Dilatometric behavior and glass transition in a styrene-acrylonitrile copolymer. *Journal of Polymer Science Part B-Polymer Physics* **43**, 1904-1913, doi:10.1002/polb.20476 (2005).

[15] Tribone, J. J., Oreilly, J. M. & Greener, J. Pressure-jump volume-relaxation studies of polystyrene in the glass-transition region. *Journal of Polymer Science Part B-Polymer Physics* **27**, 837-857, doi:10.1002/polb.1989.090270409 (1989).

[16] Struik, L. C. E. Physical aging in amorphous polymers and other materials. (1977).

[17] Struik, L. Volume relaxation in polymers. *Rheologica Acta* **5**, 303-311 (1966).

[18] Ferry, J. D. *Viscoelastic properties of polymers*. (John Wiley & Sons, 1980).

[19] Rodriguez, E. L. in *Assignment of the Glass Transition* (ASTM International, 1994).

[20] Akay, M. Aspects of dynamic mechanical analysis in polymeric composites. *Composites Science and Technology* **47**, 419-423, doi:10.1016/0266-3538(93)90010-e (1993).

[21] Li, G., Lee-Sullivan, P. & Thring, R. W. Determination of activation energy for glass transition of an epoxy adhesive using dynamic mechanical analysis. *Journal of Thermal Analysis and Calorimetry* **60**, 377-390, doi:10.1023/a:1010120921582 (2000).

[22] Lunkenheimer, P., Schneider, U., Brand, R. & Loidl, A. Glassy dynamics. *Contemporary Physics* **41**, 15-36, doi:10.1080/001075100181259 (2000).

[23] Sencadas, V., Lanceros-Mendez, S., Serra, R. S. I., Balado, A. A. & Ribelles, J. L. G. Relaxation dynamics of poly(vinylidene fluoride) studied by dynamical mechanical measurements and dielectric spectroscopy. *European Physical Journal E* **35**, 11, doi:10.1140/epje/i2012-12041-x (2012).

[24] O'Donnell, K. P. & Woodward, W. H. H. Dielectric spectroscopy for the determination of the glass transition temperature of pharmaceutical solid dispersions. *Drug Development and Industrial Pharmacy* **41**, 959-968, doi:10.3109/03639045.2014.919314 (2015).

[25] Keddie, J. L., Jones, R. A. L. & Cory, R. A. Size- dependent depression of the glass-transition temperature in polymer-films. *Europhysics Letters* **27**, 59-64, doi:10.1209/0295-5075/27/1/011 (1994).

[26] Madkour, S. *et al.* Decoupling of Dynamic and Thermal Glass Transition in Thin Films of a PVME/PS Blend. *Acs Macro Letters* **6**, 1156-1161, doi:10.1021/acsmacrolett.7b00625 (2017).

[27] Fukao, K. & Miyamoto, Y. Slow dynamics near glass transitions in thin polymer films. *Physical Review E* **64**, 9, doi:10.1103/PhysRevE.64.011803 (2001).

[28] Bauer, C. *et al.* Capacitive scanning dilatometry and frequency-dependent thermal expansion of polymer films. *Physical Review E* **61**, 1755-1764, doi:10.1103/PhysRevE.61.1755 (2000).

[29] Wallace, W. E., Vanzanten, J. H. & Wu, W. L. Influence of an impenetrable interface on a polymer glass-transition temperature. *Physical Review E* **52**, R3329-R3332 (1995).

[30] Miyazaki, T., Nishida, K. & Kanaya, T. Thermal expansion behavior of ultrathin polymer films supported on silicon substrate. *Physical Review E* **69**, 6, doi:10.1103/PhysRevE.69.061803 (2004).

[31] Xie, L. *et al.* Positronium formation as a probe of polymer surfaces and thin-films. *Physical Review Letters* **74**, 4947-4950, doi:10.1103/PhysRevLett.74.4947 (1995).

[32] Jean, Y. C. *et al.* Glass transition of polystyrene near the surface studied by slow-positron-annihilation spectroscopy. *Physical Review B* **56**, R8459-R8462 (1997).

[33] McKenna, G. B. Ten (or more) years of dynamics in confinement: Perspectives for 2010. *European Physical Journal-Special Topics* **189**, 285-302, doi:10.1140/epjst/e2010-01334-8 (2010).

[34] Seborg, C. & Stamm, A. J. Sorption of Water Vapor by Paper-Making Materials I—Effect of Beating1. *Industrial & Engineering Chemistry* **23**, 1271-1275 (1931).

[35] McBain, J. & Bakr, A. A new sorption balance1. Journal of the American Chemical Society 48, 690-695 (1926).

[36] Tsvigu, C., Pavesi, E., De Angelis, M. G. & Baschetti, M. G. Effect of relative humidity and temperature on the gas transport properties of 6FDA-6FpDA polyimide: Experimental study and modelling. *Journal of Membrane Science* **485**, 60-68, doi:10.1016/j.memsci.2015.02.032 (2015).

[37] Vrentas, J. S., Duda, J. L. & Hou, A. C. Anomalous sorption in poly(ethyl methacrylate). *Journal of Applied Polymer Science* **29**, 399-406, doi:10.1002/app.1984.070290137 (1984).

[38] Crank, J. *The mathematics of diffusion*. (Oxford university press, 1979).

[39] Kruger, K. M. & Sadowski, G. Fickian and non-Fickian sorption kinetics of toluene in glassy polystyrene. *Macromolecules* **38**, 8408-8417, doi:10.1021/ma050353o (2005).

[40] Berens, A. & Hopfenberg, H. Induction and measurement of glassy-state relaxations by vapor sorption techniques. *Journal of Polymer Science Part B: Polymer Physics* **17**, 1757-1770 (1979).

[41] Camera-Roda, G. & Sarti, G. C. Mass-transport with relaxation in polymers. *Aiche Journal* **36**, 851-860, doi:10.1002/aic.690360606 (1990).

[42] Frisch, H. Sorption and transport in glassy polymers–a review. *Polymer Engineering & Science* **20**, 2-13 (1980).

[43] Cahn, L. Electromagnetic balance. United State patent (1965).

[44] Ruegg, M., Luscher, M. & Blanc, B. Hydration of native and rennin coagulated caseins as determined by differential scanning calorimetry and gravimetric sorption measurements. *Journal of Dairy Science* **57**, 387-393 (1974).

[45] Morris, D. R. & Sun, X. Water-sorption and transport properties of Nafion 117 H. *Journal of Applied Polymer Science* **50**, 1445-1452 (1993).

[46] Williams, D. A magnetic susceptibility balance suspension. *Thermochimica Acta* **24**, 243-246 (1978).

[47] Gast, T. Development of the magnetic suspension balance. *Measurement* **4**, 53-62 (1986).

[48] Kim, D. J., Caruthers, J. M. & Peppas, N. A. Penetrant transport in cross-linked polystyrene. *Macromolecules* **26**, 1841-1847, doi:10.1021/ma00060a008 (1993).

[49] Sauerbrey, G. Verwendung von Schwingquarzen zur Wägung dünner Schichten und zur Mikrowägung. *Zeitschrift für Physik A Hadrons and Nuclei* **155**, 206-222 (1959).

[50] Domack, A. & Johannsmann, D. Plastification during sorption of polymeric thin films: a quartz resonator study. *Journal of applied physics* **80**, 2599-2604 (1996).

[51] White, C. C. & Schrag, J. L. Theoretical predictions for the mechanical response of a model quartz crystal microbalance to two viscoelastic media: A

thin sample layer and surrounding bath medium. *The Journal of Chemical Physics* **111**, 11192-11206 (1999).

[52] Vieth, W. & Sladek, K. A model for diffusion in a glassy polymer. *Journal of Colloid Science* **20**, 1014-1033 (1965).

[53] Koros, W. J. & Paul, D. Design considerations for measurement of gas sorption in polymers by pressure decay. Journal of Polymer Science Part B: Polymer Physics 14, 1903-1907 (1976).

[54] Zhang, Y., Gangwani, K. K. & Lemert, R. M. Sorption and swelling of block copolymers in the presence of supercritical fluid carbon dioxide. Journal of Supercritical Fluids 11, 115-134, doi:10.1016/s0896-8446(97)00031-4 (1997).

[55] Punsalan, D. & Koros, W. J. Drifts in penetrant partial molar volumes in glassy polymers due to physical aging. Polymer 46, 10214-10220 (2005).

[56] Rajendran, A. *et al.* Simultaneous measurement of swelling and sorption in a supercritical CO2-poly(methyl methacrylate) system. *Industrial & Engineering Chemistry Research* **44**, 2549-2560, doi:10.1021/ie049523w (2005).

[57] Zhou, J. M. & Lucas, J. P. Hygrothermal effects of epoxy resin. Part II: variations of glass transition temperature. *Polymer* **40**, 5513-5522, doi:10.1016/s0032-3861(98)00791-5 (1999).

[58] Han, W. & McKenna, G. in *Proceedings of the SPE ANTEC.* 1822.

[59] Alcoutlabi, M., Banda, L., Kollengodu-Subramanian, S., Zhao, J. & McKenna, G. B. Environmental Effects on the Structural Recovery Responses of an Epoxy Resin after Carbon Dioxide Pressure Jumps: Intrinsic Isopiestics,

Asymmetry of Approach, and Memory Effect. *Macromolecules* **44**, 3828-3839, doi:10.1021/ma1027577 (2011).

[60] Zheng, Y. & McKenna, G. B. Structural recovery in a model epoxy: Comparison of responses after temperature and relative humidity jumps. *Macromolecules* **36**, 2387-2396, doi:10.1021/ma025930c (2003).

[61] Alcoutlabi, M., Briatico-Vangosa, F. & McKenna, G. B. Effect of chemical activity jumps on the viscoelastic behavior of an epoxy resin: Physical aging response in carbon dioxide pressure jumps. *Journal of Polymer Science Part B-Polymer Physics* **40**, 2050-2064, doi:10.1002/polb.10263 (2002).

[62] Schult, K. A. & Paul, D. R. Techniques for measurement of water vapor sorption and permeation in polymer films. *Journal of Applied Polymer Science* **61**, 1865-1876, doi:10.1002/(sici)1097-4628(19960912)61:11<1865::aid-app2>3.0.co;2-h (1996).

Chapter 4

Isopiestic sorption experiments

4.1 Introduction

With this chapter, the description starts of the experimental activities pursued during the doctorate program. The first experimental method used for glassy structure characterization is a common isopiestic protocol for sorption measurements, performed with a manometric apparatus previously introduced among other common methods from literature as “pressure decay”. The aim of this preliminary activity was to collect a first set of sorption data with a robust and well-recognized experiment, to characterize the same polymer-solvent system that would then be tested also with other innovative protocols in the following months. The experimental data here presented are hence reported in the next chapters for the sake of comparison between methods.

4.2 Apparatus description

The system exploited for this preliminary set of sorption experiments is a manometric apparatus purposely designed and assembled at DICAM laboratories, in order to reproduce the same experience described in the sixties by Vieth and Sladek, who exploited the technique to estimate diffusion rates in solid materials, and years later by Paul and Koros, who also described some valuable design rules that were duly noted [1] [2].

The principle of pressure decay methods is based on measuring a pressure decrement ascribed to the penetrant mass sorbed by the sample. This requires pure penetrants contained in well-known

volumes, by which gaseous specie mass can be calculated from pressure measurement and an equation of state, which must be properly chosen, according to experimental conditions.

The used system is all built by high vacuum fittings (Swagelok® VCR), that allow to evacuate the closed volume and work from vacuum to positive pressure, therefore to measure sorption kinetics of both vapours and gasses. The whole closed system that is here represented into the apparatus scheme in Figure 4.1, is mainly sectioned into three volumes: 1) penetrant reservoir 2) pre-chamber 3) sample cell.

The penetrant reservoir contains the solvent at liquid state, so it is used just for vapour sorption experiments. This must be filled with solvent before starting sorption experiments. Caution is needed in this preliminary filling procedure, as the liquid shall occupy the selected vessel to a proper level in order to avoid splatters enter into the other volumes during operations: this would lead to an out-of-control quantity of solvent inside the test volume.

The sample cell must be conveniently chosen to store desired samples amount and shape, and allow to clean the internal surfaces after tests. As sorption tests typically have long transient times due to low mass transport coefficients, samples are usually produced as self-standing films of few square centimetres area and few tens of micron thickness to reach reasonable sample mass to be measured. For this reason, the sample cell was built with a 1'' double male union fitting, that can be easily handled for loading and cleaning operations.

The pre-chamber is purposely built to have a comparable volume to that of the sample cell, and it is separated from the latter by a bellow-sealed valve. During sorption tests, the pre-chamber volume is commonly charged with the penetrant, to measure the amount of solvent before it expands into the sample cell, then the sorption phenomena starts. Here is then placed a capacitance manometer (Edwards® Barocell 600, 0-1000 mbar), which can be opportunely selected on range for desired penetrants; this is connected to the controller provided by the manufacturer, that in turn is connected to a personal computer which is used to acquire and save pressure data from the system by a purposely created Labview® Virtual Instrument. The whole experimental volume is placed inside

an independent temperature controlling system, in this case a temperature test chamber able to measure and maintain a constant temperature set with a sensitivity of 0.1 K through a PID controller, electric resistances and forced air refrigeration systems, while the adequate vacuum level is provided by a direct drive, double-staged rotary vane vacuum pump (Edwards®).

Both the pre-chamber and the sample cell volumes must be finely determined through a calibration protocol. To this aim, a nitrogen cylinder was connected to the system to temporarily replace the solvent reservoir, and the pre-chamber volume was pressurized once the whole system was evacuated. After pressure stabilization at constant temperature (the temperature set point was conveniently chosen to easily reach stable values), the nitrogen was expanded into the sample cell by opening the connecting valve, and a final stable pressure value acquired. The same kind of expansion was repeated from vacuum to different pressure values, covering almost the whole manometer range, and a similar expansion set was repeated inserting a metal cylinder with a well-known volume into the sample cell (known volume measured by a Vernier caliper). A system of two independent equations can then be built to calculate the required volumes using an opportune equation of state. As expansions were performed with low pressure nitrogen, here the ideal gas law was used. For the first set of expansions, directly from the ideal gas law the expansion pressure ratio can be expressed as:

$$\frac{p_{pre,1}}{p_{tot,1}} = \frac{V_{tot}}{V_{pre}} \qquad [4.1]$$

where $p_{pre,1}/\ p_{tot,1}$ is the ratio between the pressure before the expansion over the value after the expansion of the nitrogen into the empty sample cell, V_{pre} is the pre-chamber volume, and V_{tot} the

volume composed by the sum of V_{pre}, the sample cell volume and the valve placed between them when opened. In the same way, the pressure ratio for the last expansions set can be expressed as:

$$\frac{p_{pre,2}}{p_{tot,2}} = \frac{(V_{tot} - V_k)}{V_{pre}} \qquad [4.2]$$

where V_k is the known volume not available for the expansion into the sample cell (metal cylinder), and the subscript "2" denotes values acquired in this configuration. Average ratio values were then calculated for different starting pressure values, and volumes calculated: the system assembled and used to acquire the following sorption data has a 51.7±0.04 cm^3 pre-chamber and a total volume equal to 87.7±0.08 cm^3.

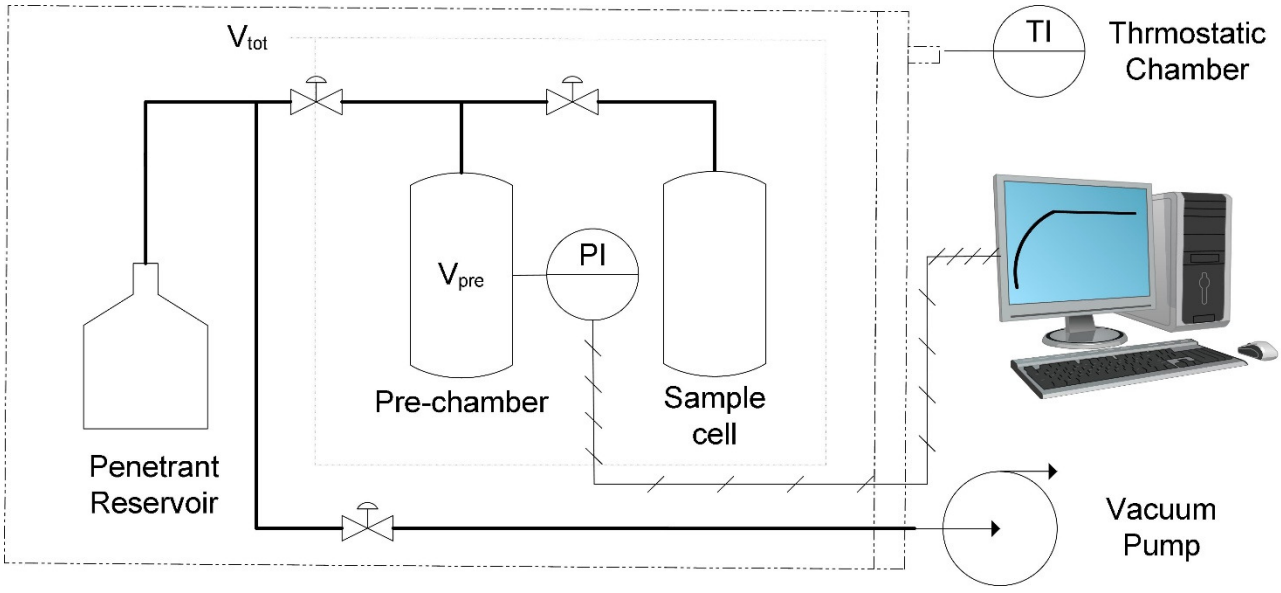

Figure 4. 1 Scheme of the pressure decay apparatus used for isopiestic experiments

4.3 Materials and methods

For glass dynamics sorption tests, in this thesis was selected the polystyrene/toluene couple, as a well-characterized system in literature [3] [4]. Atactic polystyrene (PS) was chosen as a fully amorphous glass-former product, and was kindly provided by Versalis S.p.A., Mantua (Italy), in the form of pellets, with an average molecular weight (MW) of 270 kDa and polydispersity index (MW/MN) equal to 1.1, while toluene was purchased from Sigma-Aldrich, Milan (Italy), at HPLC grade. Free-standing films were prepared by a solvent-casting technique: weighted amount of PS were dissolved in toluene, and poured into a glass Petri dish after stirring. Here solvent was casted by natural evaporation, the membrane peeled-off from the glass, and annealed following a normalized protocol. Samples were placed in a vacuum oven at 120 ºC (well above the dry glass transition, located around 101 ºC according to characterization provided by the producer) for 30 minutes, then slowly cooled down following a fixed thumb rule. The polystyrene was purposely weighted to obtain 16 µm thick membranes on average (checked by a digital double-plate Mitutoyo micrometer, sensitivity 1 µm); these were cut in large stripes, and piled alternating polystyrene with a clean metal net, to avoid sample sticking during the test steps above the glass transition. Supported thin films were also produced, to compare samples made in different ways. Aluminium foil (17 µm thick, Italchim S.r.l., Bologna, Italy) was cut in disks of 12 cm diameter and spin-coated with a 7% toluene solution of PS. The frequency of rotation was regulated on the environmental conditions to obtain 2 µm thick PS coatings on top of aluminium; average thickness was estimated by weighting preforms before and after coating with an analytical balance (Mettler Toledo, sensitivity 10^{-5} g). Samples were then annealed following the standard procedure previously described, and cut in disks of 24 mm diameter with a hollow punch, to be easily inserted into the pressure decay sample cell described above.

Pressure decay tests were performed with a classic isopiestic protocol. The latter term shall mean an experiment performed at constant solvent activity, here measured as the penetrant pressure. This

can be literally true in common gravimetric experiments where microbalances are used to evaluate the sorbed mass, as the solvent activity is exactly maintained constant (see previous chapter); although, to be fair, pressure decay experiments shall be considered as pseudo-isopiestic tests, because the change of activity constitutes the measured quantity.

Activity increase experiments were performed as commonly described in literature. Free-standing samples prepared as described above where placed into the sample cell, and the system evacuated by the vacuum pump for long time at controlled temperature, to ensure a complete desorption of solvents from the sample. Toluene was then charged into the solvent reservoir using a syringe, and air was evacuated by repeated expansions into the pre-chamber volume; solvent was trapped before the vacuum pump using a cold trap. Pure toluene was then charged into the pre-chamber and stabilized at the experimental temperature, then expanded into the sample cell and the pressure values saved until an apparent asymptotic pressure value was reached. The pre-chamber was then insulated from the sample cell (pressure increment caused by the valve closing shall be neglected), and the pre-chamber charged at higher toluene pressure. And again, after stabilization the toluene was expanded into the sample cell acquiring the pressure decrement over time.

The pressure difference between the time considered and the starting value can represent the absolute sorbed mass into the sample through an opportune equation of state. As sorption starts immediately after the expansion, initial pressure values must be calculated from system volumes. Assuming the ideal gas behavior for toluene, the initial pressure for the n-sorption step $p_{in,n}$ can be calculated as:

$$p_{in,n} = \frac{((V_{tot} - V_{pre}) \cdot p_{fin,n\text{-}1} + V_{pre} \cdot p_{pre,n})}{V_{tot}} \qquad [4.3]$$

where $p_{fin,n-1}$ is the final pressure value reached into the previous sorption step, and $p_{pre,n}$ the pressure measured into the pre-chamber volume before expansion. In these expressions, the whole volume available to the expansion was adjusted for the presence of samples, as the volume occupied by the mass introduced into the sample cell calculated from average density values.

Under the same assumption, the absolute solvent uptake referred to each sorption step $m(t) - m(0)$ can be calculated at every instant *t* as:

$$m(t) - m(0) = \frac{((p_{fin,n} - p_{in,n})\ V_{tot}\ M_{tol})}{RT} \qquad [4.4]$$

where R is the ideal gas constant, T the absolute experimental temperature, M_{tol} the toluene molar mass, and $(p_{fin,n}-p_{in,n})$ the whole pressure jump acquired. Solubility values can be then calculated, as mass ratio at pseudo-equilibrium to the final toluene pressure reached:

$$\text{mass ratio}\ (p_{fin,n}) = \frac{m_{tol}\ (p_{fin,n})}{m_{dry}} = \frac{m(t) - m(0)}{m_{dry}} + \frac{m_{tol}(p_{fin,n-1})}{m_{dry}} \qquad [4.5]$$

where m_{dry} is the sample mass measured after annealing treatment, and $m_{tol}(p_{fin,n-1})$ refers to the uptake reached into the n-*1* step.

Supported thin films were also tested to compare results. As in this case PS mass that can be fitted into the sample cell is limited by aluminium foils and low thickness, an alternated jumps protocol was applied: instead of performing successive pressure jumps for increasing monotone activity, pressure was increased and decreased alternatively. After an initial sorption step, and a following

expansion step at higher pressure value, the pre-chamber was evacuated to high vacuum, then toluene was expanded from the sample cell into the pre-chamber volume acquiring pressure over time, and so on. This allowed to have measurable pressure jumps with acceptable uncertainty.

4.4 Results

From the pressure decay method, the first achievable result consists in kinetic curves representing the sorbed mass over time during each step. Toluene uptake obtained at 40 ºC from free-standing PS sample is reported in Figure 4.2; for the sake of clarity on curve interpretation, time is here reported on square root as well as elsewhere, since Fickian sorption goes with the square root of time. Each sorption step starts from the previous asymptotic value, and ends when a pseudo-equilibrium value was recognized. These curves represent the sorption kinetic obtained for each pressure step imposed to the system, but since this output was obtained by means of pressure decay experiment, here the pressure value represents the lowest pressure value acquired during tests, and as a consequence the obtained kinetics are slightly affected by both the step increment value and the pressure decrement.

As addressed in Chapter 2, information on the sample structure can be obtained from kinetics: the behavior is a fast Fickian diffusion if the system is in the liquid-like state, while glass-like structures show slow Non-fickian kinetics. Furthermore, below the glass transition slow dynamics changes their behavior often following a specific sequence, that was described by Odani, Hayashi and Tamura for atactic PS using ethyl methyl ketone as penetrant. [5] From their experiments, low concentration runs first exhibit a sigmoid behavior, followed by a slightly faster pseudo-Fickian character. At higher concentration the behavior then showed a two-stage mechanism, then come back pseudo-Fickian and finally Fickian.

In this work, the first sigmoid behavior was not obtained, since the first pressure step was purposely performed at relatively high concentration, with the aim to speed up experiments and quickly reach

the glass-to-rubber transition. Following steps showed the same transition sequence described on literature, from pseudo-Fickian (13.6 mbar) to a two-stage sorption (19.2 mbar) and a pseudo-Fickian again. The sample behavior here introduced shows a typical uncertainty problem previously discussed in Chapter 3, as the sorption behavior slowly changes between a clear Non-fickian glassy behavior at about 23 mbar, and a clear Fickian dynamic at 28 mbar. This doesn't allow to determine a unique glass transition value, and common data elaboration strategies cannot be inherited from dry experiments, since outputs are widely different. Other critical aspects are underlined by these isotherms, as the first two steps required one month, even if pressure was purposely increased faster than required for a comprehensive test. Another important aspect that deserves to be emphasised is that the whole successive sorption test is quite difficult to be repeated: as a matter of facts, curves depends on specific conditions as pressure step and decrement during measurements, but above all the asymptotic value that ends each sorption step is left to the discretion of the operator. The latter aspect requires attention even for well-known systems as the simple PS-toluene here tested, and determines a lack of reliability on this kind of tests.

Pseudo-equilibrium sorption values obtained after each step are commonly used to build a sorption isotherm describing the solubility over the penetrant fugacity, as usually done for common mixtures; free-standing PS isotherms obtained at 30 ºC and 40 ºC are reported over solvent pressure in Figure 4.3 and 4.4 respectively. In these pictures data are reported with error bars specific for each asymptotic value obtained: these were evaluated from volumes uncertainty and instrument sensitivity, and the uncertainty propagation following general rules on Equations [4.3] [4.4] and [4.5] used for calculation. A growing uncertainty propagates step-by-step as a consequence of the successive step performed on indirect measurement, especially because of the required sum described by Equation [4.5].

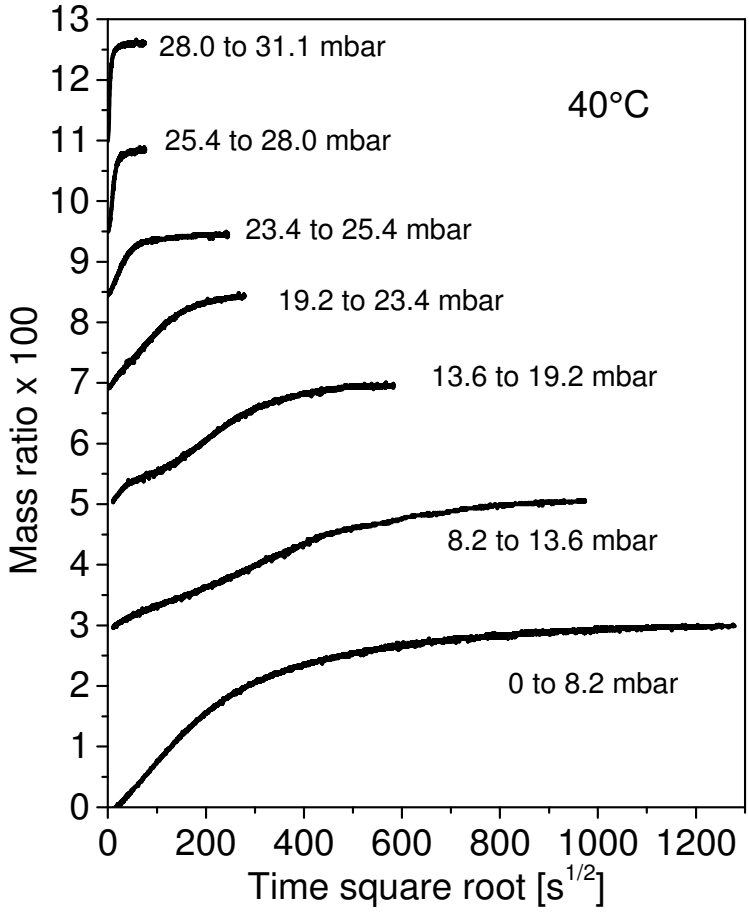

Figure 4. 2 Toluene sorption kinetic curves from free-standing polystyrene sample tested by pressure decay isopiestic experiment

Data at 30 ºC were purposely obtained at high pressure after a slow first step where the glass transition occurred; the result is then compared with literature data from Kruger and Sadowski in Figure 4.3. The obtained isotherm is very similar to that reported in the previous work, even if a different atactic polystyrene (MW 280 kDa, MW/MN = 2.94) was used in their work, and also a different experimental method, namely gravimetric isopiestic protocol based on magnetic suspension balance. This perfect superposition indicates a good reproducibility of equilibrium sorption data, which are independent on molecular variables, and a good performance of the pressure decay method, even though it is a simple and versatile indirect method.

Figure 4.4 shows previously presented sorption data at 40 ºC over the final pseudo-equilibrium toluene pressure. Differently from data acquired at 30 ºC, these are acquired both in the glassy and

liquid-like structures crossing the glass transition; while the former show a growth that could be defined as “homogenous”, in the latter two distinct solubility increase phases can be distinguished, and this pseudo-discontinuity in the behavior fells into the transition range previously identified by kinetic curves: this suggests it can be ascribed to the transition, but the difference seems not sufficiently relevant per se for a substantial analysis of glass transition.

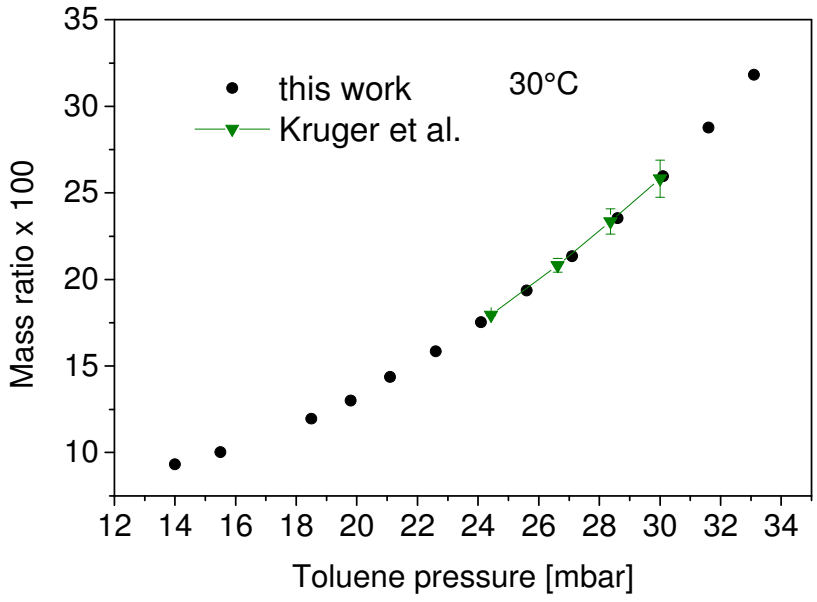

Figure 4. 3 Sorption isotherm obtained from free-standing sample at 30°C, compared with data from ref. [3] from another atactic polystyrene and toluene.

For sorption isotherm analysis, Kruger and Sadowski showed a good superposition between liquid-state sorption data previously introduced in Figure 4.3 at 30 ºC, with a simple thermodynamic equilibrium model as the Flory-Huggins. [3] They pointed out that equilibrium models can predict the curve form above the glass transition, but the characteristic S-shape from glassy materials needs another contribution, as dual-mode sorption or non-equilibrium thermodynamic models; however, a model curve could help much on data interpretation. Here a comparison was made with different equilibrium models. Results are reported in Figure 4.4 for the case of use of the Perturbed-Chain

Statistic Fluid Theory from Gross and Sadowski (PC-SAFT) on data at 40 ºC. [6] A satisfying description was obtained for equilibrium data through a good superposition, but this seemed not sufficiently good to improve the interpretation of points below the glass transition.

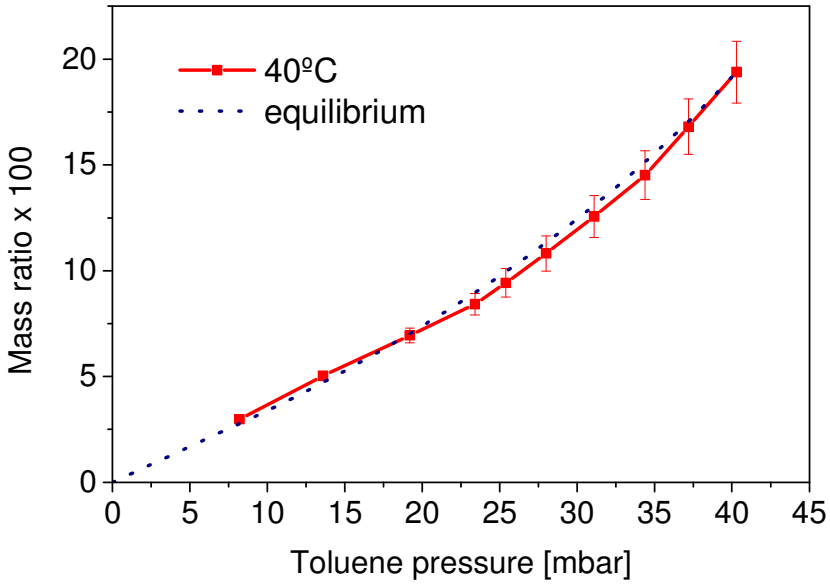

Figure 4. 4 Sorption isotherm from free-standing sample at 40ºC, compared with a thermodynamic equilibrium model result.

For the purpose of analysis improvements, more sensitive tests could be performed to erase the intrinsic uncertainty previously mentioned for this kind of tests, or other aging protocols beyond the here applied could be adopted, in order to reduce aging and increase the difference between solid-like and liquid-like sorption behavior, as demonstrated by Punsalan and Koros. [7] But this would be difficult to apply in least known systems, and inflexible as a systematic experimental procedure for glassy dynamic experiments.

As a last comparison made from pressure decay data, sorption isotherms from free-standing films and supported PS coating are reported in Figure 4.5. As indicated in "Materials and methods", supported thin films (2 µm) were obtained on aluminium foil; the thickness is orders of magnitude higher than ultrathin films were a glass transition depression was demonstrated in literature works.

However, from pressure decay experiments just equilibrium data are reported, and the bulky behavior will be rightly demonstrated by other tests reported below. As the same system used for free-standing films cannot accommodate enough cut disks, this test was performed with a much lower amount of polystyrene than the previous experiments. To compensate a consequent lower relative sensitivity on sorption measurements, pressure steps amplitude was in this case increased, in order to have an opportune pressure decrement, and steps were also performed alternately to have sufficient points for a comparable isotherm. Advantages on using supported thin films with a bulky behavior could be a faster transitory in the sorption process, that is useful in the glassy state.

When compared with data from free-standing sample, the equilibrium isotherm obtained for supported films is absolutely consistent with the previous case, within the limit represented by the uncertainty propagation resulting from the experimental method applied. This demonstrates that the equilibrium behavior of supported films is the same of free-standing films.

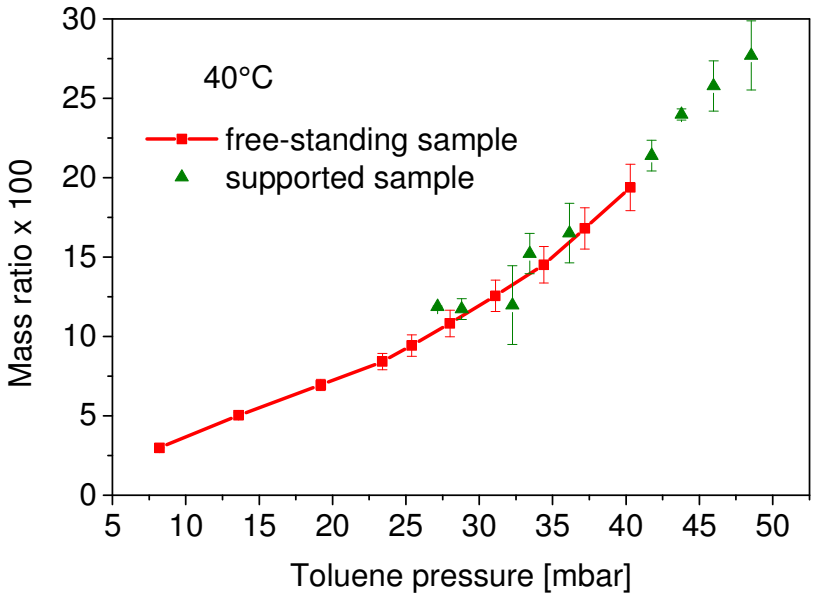

Figure 4. 5 Sorption isotherms from atactic polystyrene 16 µm thick free-standing films and 2µm supported coatings at 40°C

Furthermore, this opens to pressure decay experiments performed on supported films, but also alternating increase and decrease pressure steps, or even just decreasing steps. These modes can be useful for different determinations, as will be analysed in the next chapters; as example, performing decreasing steps on supported films allows to test materials starting from the equilibrium liquid-like state, then sample aging can be finely controlled into the experimental apparatus, and alternative aging protocols other that commons may be compared. To the author knowledge, all these modes represents an innovative solution in this field, as nobody described it before. Anyway, a good determination from supported films require longer sample production times, and a pressure decay system opportunely designed to reach sufficient accuracy, especially for good comparisons in the glassy state.

References

[1] Vieth, W. & Sladek, K. A model for diffusion in a glassy polymer. *Journal of Colloid Science* **20**, 1014-1033 (1965).

[2] Koros, W. J. & Paul, D. Design considerations for measurement of gas sorption in polymers by pressure decay. Journal of Polymer Science Part B: Polymer Physics 14, 1903-1907 (1976).

[3] Kruger, K. M. & Sadowski, G. Fickian and non-Fickian sorption kinetics of toluene in glassy polystyrene. *Macromolecules* **38**, 8408-8417, doi:10.1021/ma050353o (2005).

[4] Wong, H. C., Campbell, S. W. & Bhethanabotla, V. R. Sorption of benzene, toluene and chloroform by poly (styrene) at 298.15 K and 323.15 K using a quartz crystal balance. *Fluid phase equilibria* **139**, 371-389 (1997).

[5] Odani, H., Hayashi, J. & Tamura, M. Diffusion in glassy polymers. II. Effects of polymer-penetrant interaction; diffusion of ethyl methyl ketone in atactic polystyrene. *Bulletin of the Chemical Society of Japan* **34**, 817-821 (1961).

[6] Gross, J. & Sadowski, G. Perturbed-chain SAFT: An equation of state based on a perturbation theory for chain molecules. *Industrial & Engineering Chemistry Research* **40**, 1244-1260, doi:10.1021/ie0003887 (2001).

Chapter 5

Dynamic-step experiments

5.1 Introduction

This chapter describes research activities inherent to the first year of the doctorate program at DICAM. During this period a gravimetric apparatus previously used was restored and tailored to specific demands of a novel experimental protocol developed. The apparatus is based on a Quartz Crystal Microbalance (QCM), and experiments were performed at constant temperature on the same polymer-solvent couple previously described in Chapter 4 for pseudo-isopiestic manometric tests. The main objective of these experiments is to demonstrate that this method can be used to characterize glassy dynamics in a convenient way using sorption experiments.

5.2 Apparatus description

5.2.1 Quartz Crystal Microbalance principles

Piezoelectricity is a phenomenon occurring in certain solid materials, e.g. crystals and ceramics, which consists in electric charge accumulation due to an applied mechanical stress. In some cases, the piezoelectric effect shows reversibility because materials generate electric charge under stress (direct piezoelectric effect), as well as they develop an internal strain when crossed by an electric current (inverse piezoelectric effect); the latter was first theorized by Lippmann, then measured by Voigt on some crystals [1]. When an oscillating electric signal is applied to a piezoelectric material, a resonance phenomenon occurs, and the crystal response again oscillates with a greater amplitude at specific frequencies, these called resonant frequencies. Quartz crystals are piezoelectric

resonators highly appreciated for their ability to produce oscillations of precise frequency, and for this reason quartz resonators are used for high precision watches or microelectronics. Each crystal has a characteristic resonant frequency, mainly influenced by composition and cut, but frequency also depends upon many other variables, as temperature or aging time (which is very difficult to predict); among others, frequency depends on the resonator mass, but also a mass deposited onto the crystal surface can significantly change the resonant frequency, then crystals and particularly quartz crystals can be used to build a gravimetric system, called Quartz Crystal Microbalance (QCM) [2] [3].

Different methods are available to correlate changes in oscillation with the deposited mass for piezoelectric crystals. One of the most famous and largely used is the Sauerbrey equation, who first described frequency changes due to the mass deposited on quartz plate. Thickness-shear vibration frequency can be expressed through a characteristic propagation speed v_{prop}; operating in fundamental mode (highest amplitude) the wavelength is half of thickness, then:

$$f = \frac{v_{prop}}{2 \cdot s} \qquad [5.1]$$

From Equation [5.1] frequency f is inversely proportional to the crystal thickness s; assuming the deposited mass as an extension of supporting crystal (the Sauerbrey assumption), the relative frequency difference can be related to a mass difference as:

$$\frac{\Delta f}{f} = -\frac{\Delta s}{s} = -\frac{\Delta m}{A \cdot s \cdot \rho_{crystal}} \qquad [5.2]$$

where A is the crystal surface, f and m frequency and mass respectively, and $\rho_{crystal}$ the crystal density [4]. From Equations [5.1] and [5.2], the areal mass increment (mass per unit area) can be written as:

$$\frac{\Delta m}{A} = -\frac{v_{prop} \cdot \rho_{crystal}}{2f^2}\Delta f = -\frac{1}{C_f}\Delta f \qquad [5.3]$$

that is a form of the Sauerbrey equation [4].

The main advantage of this easy equation is that C_f is a constant value depending on the single resonator, hence the equation easily transforms frequency drop measurements into mass increments just by calibrating each sensor. But since the film was treated as a crystal extension, the equation can be applied just under restricted conditions. First, the deposited film must be homogeneously distributed on the resonator surface, and the relative frequency decrement must not exceed 2%. Greater values demonstrated non-linear frequency decrement, requiring other calculation strategies, e.g. the z-match technique. However, this requires film information that could be not available at experimental conditions desired, and this determines difficulties in applying non-linear strategies [5].

Another requirement of Sauerbrey equation is a rigid film behavior, and this represents a great limitation for viscoelastic materials as polymers. White and Schrag proposed theoretical limits for deposited film and surrounding medium parameters $\beta = 2\pi\lambda_s$, where λ_s represents the shear wavelength which depends on resonator frequency, and both density and viscosity of inherent phase: significative deviations from Sauerbrey equation can be obtained for $\beta_{film} \cdot s > 0.28$ or $\beta_{film} / \beta_{medium} > 0.2$; the first limit was also demonstrated experimentally [6] [7]. As shear wavelength increases with viscosity, and the latter is dramatically influenced by the solvent content

and the glass transition, use of QCM in sorption measurement could be questionable if a fine control on film properties at experimental conditions is not available. To this aim, in this work QCM measurements will be analysed below the glass transition; however, it is right to point out that other authors published reliable sorption data on another system PS-toluene well above the glass transition [8].

5.2.2 Experimental setup

As addressed in the previous paragraph, an oscillating electric signal must be applied to the piezoelectric resonator to obtain an amplified output at resonant frequency. In this work, AT-cut 9MHz quartz crystal resonators (diameter = 0.5 cm, with double-sided gold electrodes) in HC-49 package (with removable can, Figure 5.1) were used combined into a commercial oscillating circuit (Elbatech, Isola D'Elba, Italy); external connections were purposely insulated and regulated to reduce noise. The circuit is driven by a National Instrument boards, and data are collected with a PC and a purposely designed software. The sensitivity of the instrument on frequency measurements is 0.1 Hz and accuracy about 0.5 Hz; on mass, accuracy on this kind of instruments is on the order of nanograms per square centimetre, then a fine calibration requires specific techniques not available in our lab. For this reason, the resonator constant was estimated through theoretical calculation of propagation speed v_{prop} from values of quartz density and shear modulus of quartz μ_{quartz} for AT-cut crystals:

$$v_{prop} = \sqrt{\frac{\mu_{quartz}}{\rho_{quartz}}} = \sqrt{\frac{2.947 \cdot 10^{11}\, g \cdot cm^{-1} \cdot s^{-2}}{2.648\ g \cdot cm^{-3}}} \qquad [5.4]$$

and merging this equation with the Sauerbrey method (Equation [5.3]):

$$\frac{\Delta m}{A} = -\frac{v_{prop} \cdot \rho_{crystal}}{2f^2}\Delta f = -\frac{\sqrt{\rho_{quartz} \cdot \mu_{quartz}}}{2f_0^{\,2}}\Delta f \qquad [5.5]$$

where f_0 represents the unloaded frequency, measured for each resonator before mass deposition. Mass accuracy then results $3 \cdot 10^{-9}$ g/cm^2 (or $7 \cdot 10^{-10}$ g), except for slight difference depending on f_0 values from each resonator.

Measurements were performed in a well-controlled closed volume, that has the same characteristics of the pressure decay apparatus previously described: the setup represented in Figure 5.2 will be briefly described for the sake of clarity. The system is built by high-vacuum fittings and shall consists into 3 main chambers separated by opportune valves: 1) penetrant reservoir 2) pre-chamber 3) sample cell. Quartz crystal is inserted into the sample cell volume through purposely designed vacuum and solvents-resistant connections and cable seals; also a J-type thermocouple is placed close to the crystal for temperature measurement.

The penetrant reservoir is composed by a vessel where liquid-state solvent is poured before tests. As in pressure decay apparatus, the solvent level here must be kept opportunely low, in order to avoid drops enter into the system: this allow a good control on experimental conditions, here fundamentals as will be described for the experimental protocol.

The pre-chamber volume separates the penetrant reservoir and the sample cell. This is composed by a purposely made vessel where the penetrant is charged for preliminary measurement and stabilization at desired conditions; to this aim, a capacitance manometer (Edwards® Barocell 600, 0-100 mbar) is here installed to measure the solvent pressure in the gaseous phase.

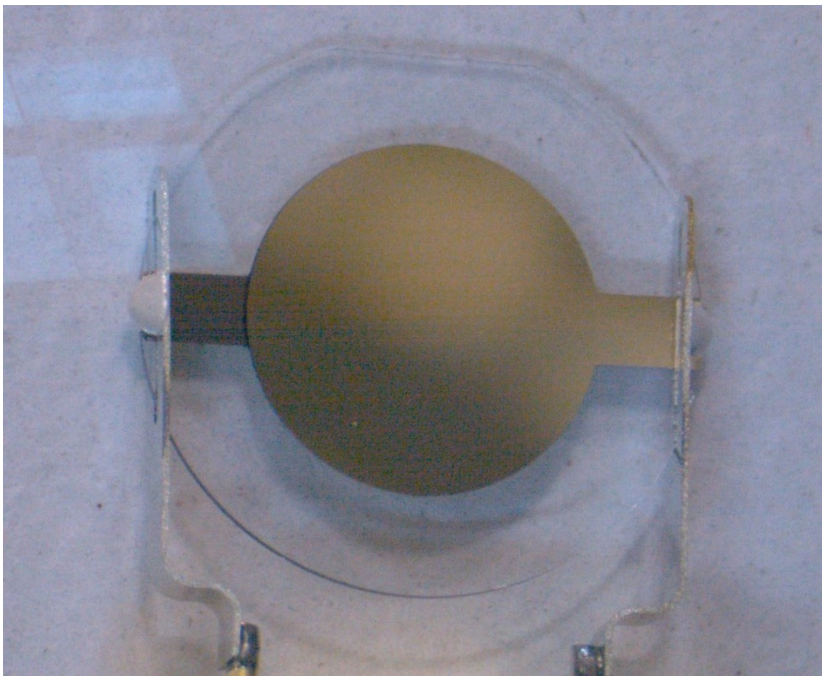

Figure 5. 1 Detail of a Quartz Crystal resonator in HC49 package [9]

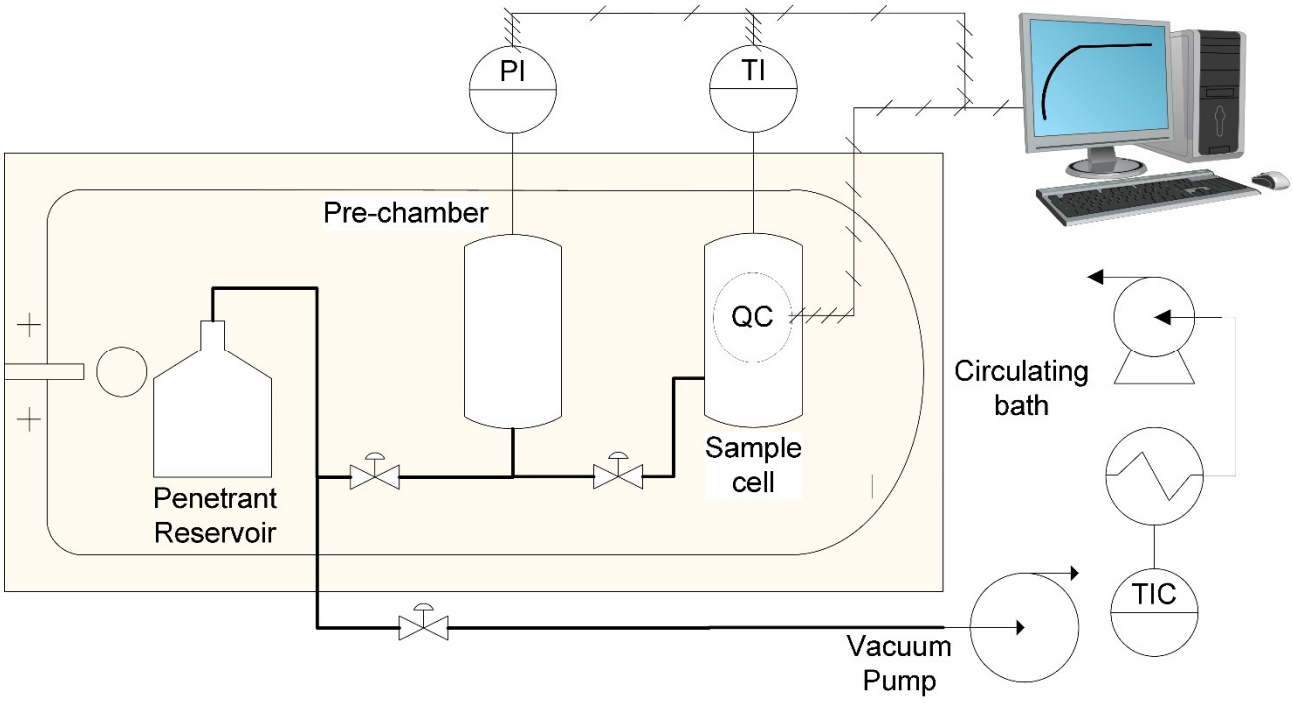

Figure 5. 2 Scheme of the designed experimental apparatus for dynamic-step experiments, based on a Quartz Crystal Microbalance (QCM)

While pre-chamber and sample cell volumes (and their ratio) are fundamentals for manometric sorption experiments, in this kind of gravimetric experiments they must be just large enough to neglect pressure decay into the environment during sorption, thus achieving almost constant boundary conditions. Anyway, due to high sensitivity and weight limits of QCM sample, polymer amounts used in systems lie this are small enough to allow for the problem to be ignored.

The apparatus is complemented by a direct drive, double-staged rotary vane vacuum pump (Edwards®) to evacuate the system to high vacuum, and a water tank where the whole closed system is immerged for temperature control, provided by a recirculating bath equipped with a heating head and water refrigerator (Thermo Fisher Scientific®, temperature stability = 0.1 K measured inside the closed volume).

5.3 Materials and methods

Atactic polystyrene (PS, kindly provided as pellets by Versalis, Mantua, Italy) with an average molecular weight of 270 kDa and polydispersity index of 1.1 was first dissolved in toluene (HPLC grade, Sigma-Aldrich, Milan, Italy) to obtain a 2% weight solution. AT-cut 9 MHz quartz crystals were first polished with toluene in ultrasonication bath for 2 minutes, then unload frequency was measured at controlled temperature and high vacuum. Crystals were then coated by a spin-coater with the toluene solution, regulating the rotational speed in order to obtain the desired thickness at environmental conditions; thickness was evaluated by weighting samples by the same gravimetric technique here described, assuming a polystyrene density value equal to 1.05 g/cm^3 as stated by the producer and homogeneous coverage.

On the coating process a great deal of attention was paid to obtain homogeneous distribution of polymer on the crystal plate surface; as this is stopped by vacuum on the spin-coater rotator, just the opposite side of the resonator can be covered. But small area and viscous forces were showed to cause borders accumulation or leakages into the outer surface, and therefore unreliable

measurements. This problem was solved modifying the common spin-coating protocol: instead on depositing the liquid phase before spinning the quartz plate, controlled amount of the PS solution were injected onto the spinning surface, rotating at constant speed, then thin PS films were obtained without macroscopic defects.

Each coated crystal was then aged before being tested, following the same high temperature protocol previously described for pressure decay samples: specimens were placed in a vacuum oven, at high vacuum and above the glass transition temperature at 120 ºC for 30 minutes, in order to anneal the structure and desorb trace amounts of trapped solvent. Then controlled aging was performed by slow cooling down to room temperature following a well-reproducible thumb rule. A preliminary test was performed on unloaded crystals to ensure the aging protocol effect on resonators here used, as suggested in literature; since the fundamental frequency was apparently unchanged after treatment, adjustment on calculation were not considered [10].

After aging treatment, sample was connected to the electrodes inside the sample cell, the system closed and evacuated overnight to reach stable conditions. Before starting, toluene was charged into the penetrant reservoir and several expansions into the pre-chamber were performed, followed by evacuation with the vacuum pump, in order to have pure solvent into the reservoir; solvent moisture was collected into a cryogenic trap working with liquid nitrogen, and special attention was paid to avoid any solvent leakage into the sample cell during operations.

After these preliminary operations, gravimetric sorption measurements were performed following a purposely designed protocol able to account for glassy dynamics, here referred as “dynamic-step sorption experiment”. It consists in consecutive step sorption measurements, during which the mass increment caused by solvent penetration into the glassy sample is acquired for increasing solvent pressure steps. Toluene vapour was charged into the pre-chamber where temperature was stabilised, and pressure adjusted to a well-controlled value. The penetrant was then expanded into the sample cell at fixed time intervals, reaching a prescribed toluene pressure that can be easily planned by accounting for pre-chamber pressure and volumes ratio.

Instead of moving forward to the next step waiting for asymptotic pressure values, in these experiments pressure steps were performed to follow an average constant rate of pressure increase. Experiments were performed at different values for the rate of pressure increase, all consistent with a reasonably uniform value of solute fugacity reached across the sample thickness at the end of each sorption step, namely ensuring the completion of diffusion process. As described in Chapter 2 as theoretical aspects, and Chapter 3 concerning common dry experiments, the rate of variation for the promoting external variable for glass-rubber transitions is one of the main players regulating the glassy dynamics, e.g. temperature and its rate of change in dilatometry [11]. These experiments were purposely designed to combine the sensitivity of dynamic changes, a typical prerogative of classic tests for glasses, and the opportunity to get information on mass transport, as required for sorption tests. The output is of the same kind of classic sorption experiments, as the pressure decay test described in the previous chapter, which means a kinetic isotherm for each sorption step, and a sorption isotherm built by final solubility values per kinetic curve. Since each run follows constant pressure rate previously chosen, multiple isotherms can be obtained, each one representing an iso-rate test. The main goal of this set of experiments is to demonstrate the existence and consistency of these iso-rate isothermal curves, then this would be a preliminary activity for further modelling efforts, able to describe and quantify the glassy dynamics in presence of solvent.

On experiments design, particular attention was paid on collecting terminal sorption values much later than mass transport transients, as iso-rate isotherms shall never be affected by transport, but solely by relaxational behavior. In order to ensure short transients, even in the dry glassy state where diffusion coefficients are relatively low, thin samples were tested for multiple benefits. First, a thin sample is required to perform fast experiments as the diffusion time goes with the square of thickness; as the PS-toluene system is largely characterized in literature, available data was used for calculation, in order to plan the desired set of experimental pressure rates [12]. Another advantage on working with thin samples is the chance of getting meaningfully kinetic curves, where pure Fickian and relaxational sorption behaviours are well separated. This requires specific conditions on

characteristic times, as in thin glassy samples the relaxation process may result much slower than diffusion.

The enhancement of diffusion process is then fundamental for this investigation. This kind of output has many advantages: firstly, it can demonstrate the overlap of Fickian sorption and relaxation composing the global Non-fickian response, as stated time ago by Berens and Hopfenberg [13]. A well-separated Fickian sorption stage is easy to detect for kinetic characteristic curve shape, but can also easily modelled as demonstrated by Crank through the following equation:

$$\frac{m}{m_{t\to\infty,Fickian}} = 1 - \sum_{n} \frac{8}{(2n+1)^2 \cdot \pi^2} \exp\left[\frac{-\mathfrak{D} \cdot (2n+1)^2 \cdot \pi^2 \cdot t}{4 \cdot s^2}\right] \qquad [5.6]$$

where $\mathfrak{D}$ is the diffusion coefficient and $m_{t\to\infty,Fickian}$ represents the asymptotic sorbed mass for a solely Fickian sorption stage; Equation [5.6] is written for membranes at initial uniform concentration and isopiestic Fickian sorption [14]. By adjustment on $\mathfrak{D}$ and $m_{t\to\infty,Fickian}$ (the latter recognized as an intermediate sorbed mass value where the Fickian diffusion ended), the model curve can be superposed to data for a better interpretation, and to finely evaluate a "real" pure Fickian diffusion coefficient value at conditions applied, which means without any influence of relaxation phenomena.

Another aspect considered in experiments design is the effect of thickness on glassy dynamics. As already discussed, nanoconfinement showed influences into glass dynamics and the scientific community is still debating on this [15]. This being the first example of experiments performed following the proposed protocol, samples were purposely prepared with high thickness for bulky behavior, to gather experience in relatively simple systems. Among available interpretations for nanoconfinement effects, Bodiguel and Fretigny demonstrated on low molecular weight PS that dynamics are affected just along few nanometres in proximity of surface, then on a characteristic

tube diameter length instead of the radius of gyration of molecules R_g (typically higher) commonly considered as a reference; here the radius of gyration was considered as a reference limit for the sake of caution [16]. For PS-toluene system Fetters proposed the following expression:

$$R_g = 0.012 \cdot MW^{0.595} \quad [5.7]$$

thus, R_g was estimated for the system here analysed as 20.5 nm [17]. Samples were then selected to be thicker than 400 nm, in order to simply leave confinement effects out of our considerations; however, an experimental demonstration of the bulky behavior in this thickness range will be addressed in the next chapter, where purposely designed experiments for thickness influence will be described.

5.4 Results

Figure 5.3 shows kinetic curves obtained from a dynamic-step sorption experiment, performed on a 480 nm thick PS sample at 30 ºC, and steps of toluene pressure increment of 2.45±0.1 mbar every 12 hours, namely a constant rate of pressure increment of 4.90±0.1 mbar/d or 10% per day in terms of toluene activity increment. These experiments were performed at shorter pressure amplitude steps than pressure decay tests reported in the previous chapter, due to the high sensitivity of QCM system. Perform many short steps helps to get high definition sorption isotherms, but this is commonly undesirable in common experiments due to long times required for each step, while this is not a limit following the proposed protocol since short times are required as the asymptotic value is not followed. Another great advantage on limiting the step process to non-asymptotic values is a reproducibility improvement of sorption experiments, as the same protocol at the same conditions

can be performed regardless of operator or unconventional stability rules. A second experiment performed following the same step sequence confirmed the great reliability of this method.

As addressed into the previous paragraph, here particular attention was given to purely Fickian sorption stages. From kinetics presented in Figure 5.3 emerges a better distinction between Fickian and relaxational behaviours, with respect to the curves achieved by the pressure decay method (See Figure 4.2). The presence of slow relaxational dynamic at long times is although a proof of the glassy state structure at solvent content, and early typical transitions of Non-fickian glassy state sorption are observed.

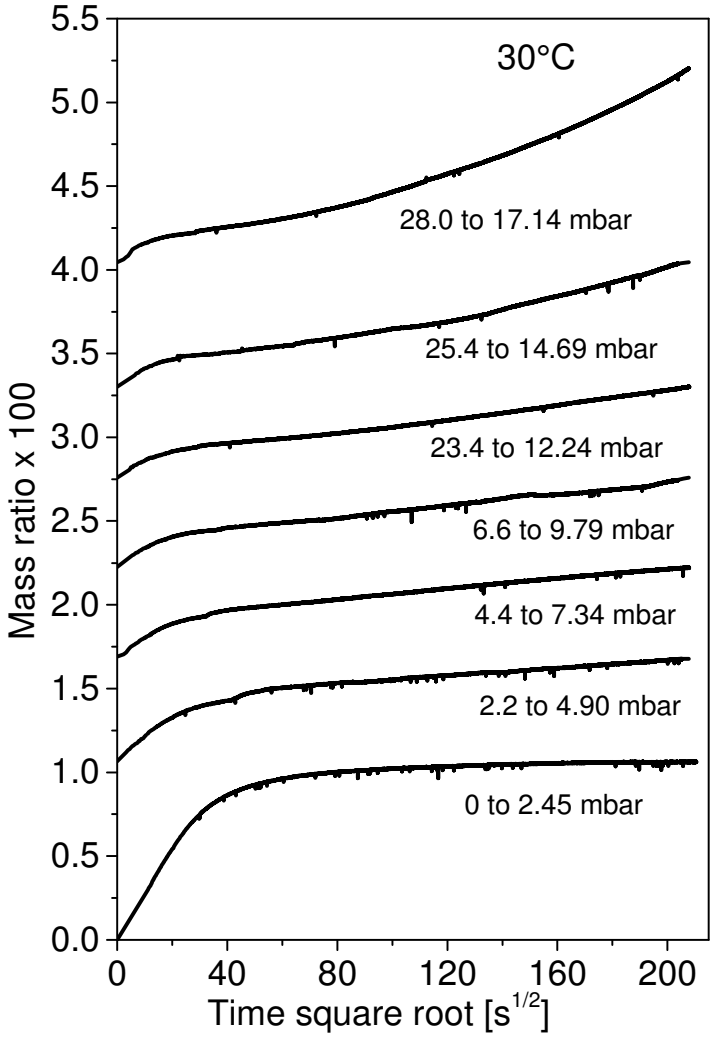

Figure 5. 3 Sorption kinetics from a dynamic-step toluene sorption experiment on 480nm PS film, at constant pressure increasing rate

Since the overall Non-fickian curve shape results from phenomena overlap, the relaxational behavior here can be supposed to be too much fast with respect to diffusion, then the glass-regulating variable shall be slowed down. The pressure rate of increment was thus decreased to obtain a better separation between sorption processes, down to 5% every 4 days. For the sake of comparison, in Figure 5.4 sorption kinetics for successive steps are reported in the time range of early Fickian sorption stages; the Fickian model curve reported was obtained by Equation [5.6], setting a diffusion coefficient equal to $4 \cdot 10^{-11}$ cm^2/s. As expected, slower iso-rate kinetic curves showed a better separation between Fickian and relaxation sorption behaviours: the typical fast mass increment can be observed in the early seconds, and a clear evidence of plateau values were obtained before the mass significantly increased due to a relaxation induced by solvent. On observed Fickian diffusion, an apparently similar behavior was obtained, without significant differences in the growing speed (regulated by the diffusion coefficient), even though each curve refers to different solvent content.

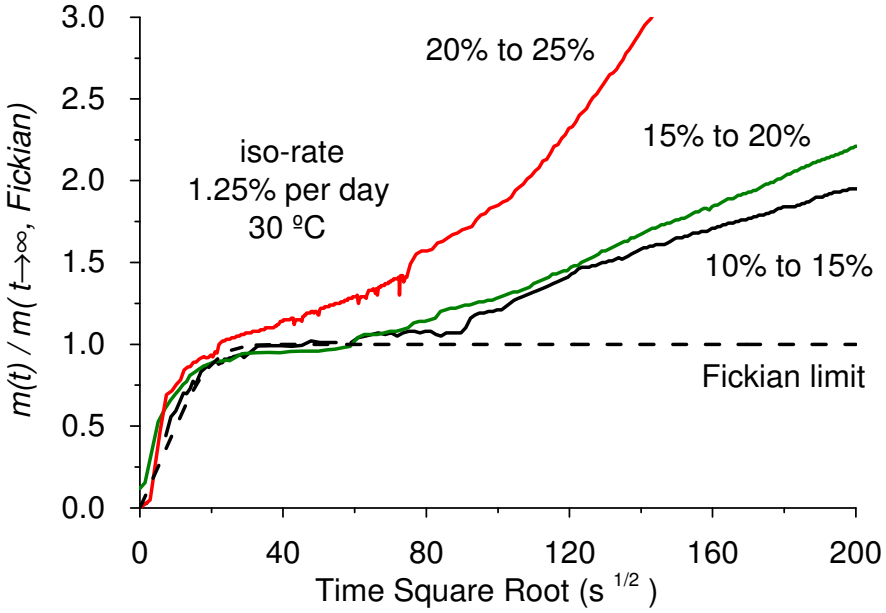

Figure 5. 4 Iso-rate kinetics obtained for successive 5% toluene activity steps performed every 4 days, on 480 nm thick PS film. Fickian model curve obtained from Equation [5.6]

Equivalent pressure increasing rates can be obtained by short as well as long steps, adjusting the step amplitude. According to Berens and Hopfenberg, diffusive and relaxational phenomena are linearly superimposed in glassy materials; as a consequence of their assumption, the general sorption behavior obtained from dynamic-step experiments cannot be influenced by step amplitude or interval, as long as the diffusion stage is almost completed during the ongoing sorption step. In order to demonstrate this, two experiments were performed on a 450nm thick sample at the same pressure increasing rate, and the rate was reached with different step protocols; for comparable measurements, the same coated resonator was used twice, and the same aging protocol was applied. A lower limit of one hour for step interval was identified from previously discussed tests, since even starting at dry conditions on about 500 nm thick samples the pure diffusive limit was apparently reached; through Fickian model, the inner surface concentration in the sample was estimated to be more than the 95% of the Fickian limit. In Figure 5.5 iso-rate kinetic curves are compared: these were both obtained at 5% activity per hour, but while in one case the experiment was carried out by the same 5% steps showed in previous results (one hour-long intervals), in the other experiment a 10% step was performed, covering the two steps-long period from the first test. The mass growing rate and pseudo-plateau values attributable to diffusion widely differ between experiments, due to a different toluene concentration in the gaseous phase; this means distinct (theoretical) equilibrium levels and driving forces to the diffusive process for each step reported. These aspects are however independent of the followed path. As also clear in Figure 5.3, first steps evidences higher solubility jumps than the following ones, even though the pressure jumps were purposely performed with the same amplitude. This phenomenon could be explained by the solvent accumulation into voids in the glassy structure, that is a material characteristic influenced by the previous history (here normalized by the aging protocol, see previous paragraph). On these rate and step-independent sorption mechanisms, relaxation dynamics runs at the same time. As the final value reached following different paths is the same, it can be stated that matching relaxation mechanisms were obtained following different paths just applying the same pressure increasing

rate. Linearity between the different sorption mechanisms can then be confirmed, and in the perspective of experiments setting a good evidence of depleted diffusion stages was provided. In addition to this, a perfect match of values can be also considered a proof of a very reliable method for routine use.

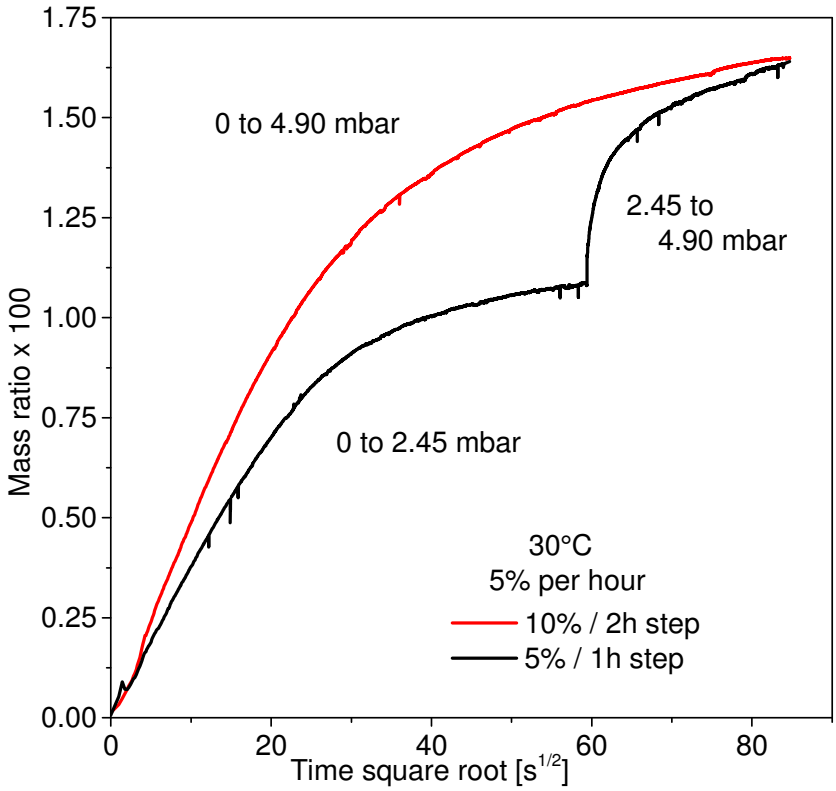

Figure 5. 5 Kinetic isotherms from iso-rate experiments performed on the same 450 nm thick PS sample, following different step protocols.

Other runs were also implemented, in order to complete the analysis with an isothermal set of iso-rate sorption curves, given in Figure 5.6. Here are reported just the solubility values obtained to the end of each step, in multiple runs performed using the same 480 nm thick PS films, each time normalizing the thermal history, and multiple step procedures. Four different applied rates are also compared with a lower theoretical limit and equilibrium values. As Fickian plateaus seemed easy to detect, these values were used to built a theoretical "not aged" curve, representing the solely

diffusion contribution to the global solubility value (green dashed curve in Figure 5.6); equilibrium references were reported, as the theoretical equilibrium value at 30 ºC from a thermodynamic model (PC-SAFT, red solid line), but also as equilibrium data from 110 ºC sorption tests from literature, as solubility experiment performed at liquid-like state at this activity range for the same polymer-solvent couple (empty stars) [12]. First, all these data seemed coherent, as for decreasing activity rates the solubility increases, due to the effect of the relaxation contribution. This was considered the main achievement from this activity, as further modelling can be performed on these iso-rates curves to deeply understand the glassy dynamics in presence of solvent, being these full-fledged reliable relaxation measurements.

Other aspects also emerged from comparison between equilibrium and non-equilibrium curves. In the first place, the theoretical as well as the real equilibrium behaviours seemed crossing the non-equilibrium curves obtained, and this occurred at every rate tested; the solubility increment showed a homogeneous grow for each test, but this nevertheless resulted clearly divided into two well-distinct zones: 1) a first left-hand side zone, where non-equilibrium solubility behavior looks like a supersaturation of the sample, and 2) a second right-hand side zone, where solubility falls under the equilibrium behavior. But as relaxation seemed to constantly increase the solubility over time, as indeed described in literature, an apparently counterintuitive phenomenon emerged as a relaxation peculiarity: while under equilibrium condition the sample solubility approaches the equilibrium value through relaxation, and this is comparable to the physical aging described by dry experiments where the volume decrement approaches a theoretical value, in supersaturated sample the relaxation contribution is apparently opposed to the molecular arrangement mechanism aimed to reach the equilibrium condition. This pictured a complex behavior, which resulted coherent in this sorption range and the polymer-solvent couple with a swelling phenomenon. Thus, the different areas identified may represent a swelling zone, where the solvent increases the volume for what could be a convenient energetic contribution, and a relaxation zone where the glassy behavior in presence of solvents resembles with the dry glass. With the view of deepening understand these dynamics and

confirm the analysis here proposed, indirect volumetric dynamic-step sorption experiments were performed in the framework of another research project. The following section is a brief comparison between results from the same PS-toluene system.

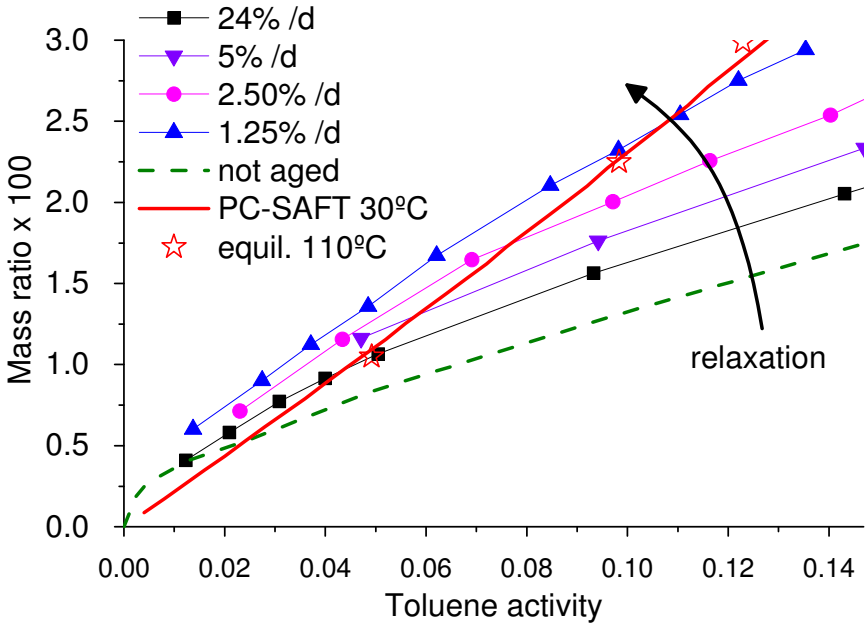

Figure 5. 6 Isotherm set of iso-rate curves, compared with theoretical equilibrium curve and Fickian plateau values (not aged curve) to evaluate the relaxation contribution to solubility in the glassy structure.

5.5 Bending beam project

The bending beam is a simple mechanical technique already developed for a wide range of purposes, as studying polymers stress state, breaking process, mechanical properties and so forth [18] [19] [20]. What here was considered is the use of the bending beam as experimental technique for Non-Fickian sorption and glass transition [21] [22].

The basic principle of this technique is the predicable deflection of a thin metallic beam, which mechanic characteristics must be well-known. This is usually coated with a thin polymeric layer that shall cause a deflection in the whole beam by a stress state, that can be then evaluated assuming the elastic properties of the metallic beam alone. Stress can be acquired over time for the influence

of mechanical stress on deflection, thermal gradients or whatever is focused in this work, namely mass transport and stress relaxation in the glassy state.

5.5.1 Materials and methods

Here follows the detailed description of experiments performed by dr. Elisa Pavesi, past student of the DICAM doctorate program, and reported into the related thesis. The experiment design starts from choice of the support material and the beam geometry; usually, small thin beams with rectangular section are used. This choice shall be carefully made in order to reach a good compromise between the instrument sensitivity, which increases with length and decreases towards thickness, and other needs requiring opposite characteristics, e.g. the total weight or the elastic range of the available material [18]. In the work subject of this section, 50 mm long spring-steel-made disposable cantilever beams were used (elastic modulus 210 GPa, Poisson coefficient 0.3); these were purposely selected with a rectangular section of 10 mm width and 0.5 mm in thickness.

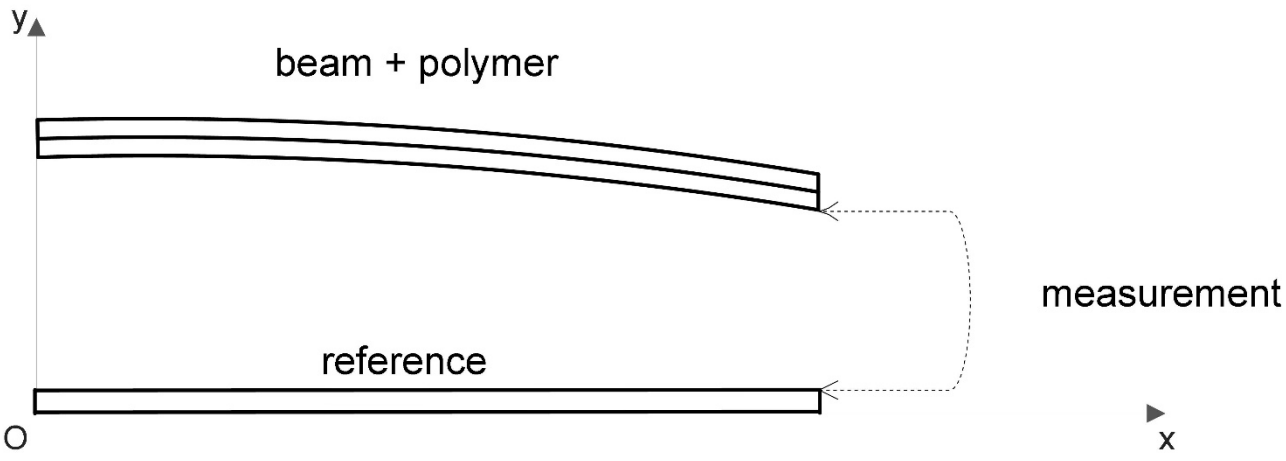

Figure 5. 7 Scheme of bending beam basis principle for stress measurement on thin polymeric films

Beams were coated by solvent casting, depositing a controlled amount of 1% wt. PS solution dissolved in toluene on pieces, and casting overnight under fume hood. Samples were then fully dried and annealed at temperature above T_g under high vacuum, then aged following the same thumb rule described for QCM experiments (Paragraph 5.3). In order to achieve reliable measurement, but preserving same experimental times from gravimetric tests, samples were purposely produced to be thinner than 5 µm, and accurate estimation of thickness was carried out by weight measurement before and after deposition, using an analytical balance (Mettler Toledo®, sensitivity 10^{-5} g). Good control in sample thickness is fundamental not only to ensure a finite isopiestic sorption step during measurement, but here above all on the stress state evaluation as will explained later.

Beam was then well-fixed inside a purposely-made sample chamber, equipped with two glass observation ports, these allowing both displacement and thickness measurements by optical micrometer. This was made by a linear Charge-Coupled Device (CCD) with image sensor CMOS (Complementary Metal-Oxide Semiconductor, Keyence model LS-7030-M, measurement range 0.3 to 30 mm, repeatability 0.15 µm); images were available for direct displaying and elaborated by a dedicated controller (Keyence LS7501) connected to a PC for acquisition and data saving.

The sample chamber was inserted in a closed-volume apparatus made of high-vacuum fittings and vessels, equivalent in all respects to the system used for QCM gravimetric sorption measurements; as here the measuring system required windows and higher volumes, a closed external chamber was purposely built for temperature control instead of water bath. This system allowed to perform step-increase pressure sorption experiments, and it was used following the same dynamic-step protocol described above, except for low steps amplitude and duration which resulted limited by high specimen thickness.

From the cantilever beam configuration, the stress state (σ) was evaluated as a function of displacement (δ) by means of radius of curvature (r):

$$\sigma(r) = \frac{E \cdot s_{substrate}^{\ 2}}{(1-\upsilon) \cdot 6r \cdot s_{polymer}}; r(\delta) \approx \frac{L^2}{2\delta} \quad [5.8]$$

where E is the elastic modulus, υ the Poisson ratio of spring steel, L the beam length, $s_{substrate}$ and $s_{polymer}$ thickness of metal beam and polymeric film respectively. Results obtained by this method could also be exploited for volume information through so-called neo-Hookian models, as described in reference; for further details on models or apparatus, please refer to dr. Pavesi's thesis [23].

5.5.2 Results

In Figure 5.8 are reported dynamic-step sorption data at 30 °C for the PS-toluene system, these acquired at two different activity increase rates, equal to 5% and 2.2% per day.

First, from reported results emerged the apparatus here used was capable of effective sorption measurements, as the response seemed a reproducible tensile stress growth ascribed to a solvent volume sorbed by the polymeric film. Furthermore, the stress behavior resulted qualitatively similar to what observed in gravimetric experiments, namely a fast growth at low activity values which slowly decrease its growing rate. Speculation could be also made on results at 2.2% per day activity increase (red dots), as a significant decrement on stress growth occurred at activity range that resulted comparable to what seemed a transition zone from swelling-to-relaxation behaviours from gravimetric data analysis; unfortunately, just few points were available to get this singularity.

Different from previous analysis, the volume-related stress function from different growing rates seemed here overlapping, but yet they corresponded to zones where mass uptake was expected to be significantly different, as demonstrated above. Physical aging in the glassy state has a strong effect on volume sorption behavior, as indeed Punsalan and Koros described from dilatometric sorption experiments, however, they never applied classic experimental protocol, and the experimental setup

is different, hence the evidence from bending beam tests needs to be confirmed through other tests [24]. The goal could be pursued by means of higher sensitivity set up and extending experimental ranges in a meaningful way.

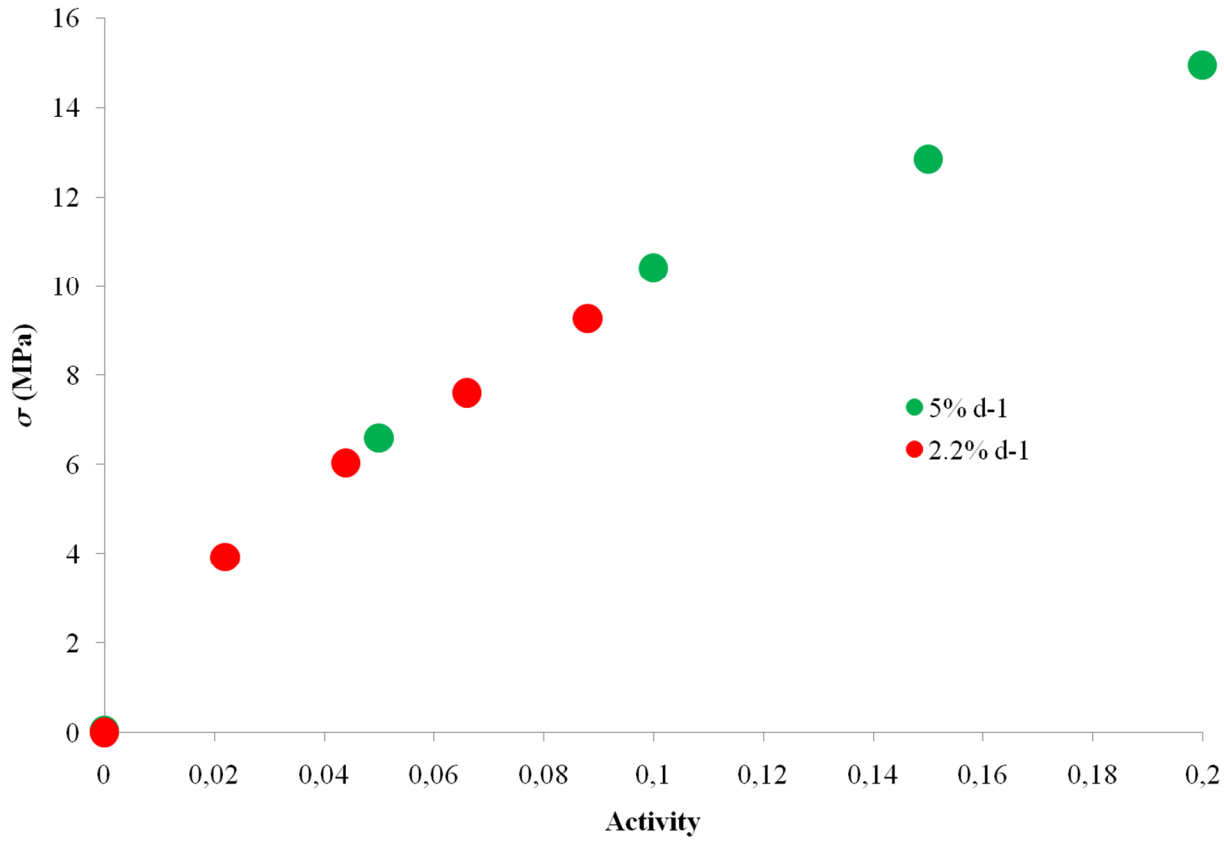

Figure 5. 8 Stress state vs. toluene activity at 30 ºC for PS-toluene system. Isotherms were collected for 5% and 2.2% activity increment rate per day, using the described apparatus based on the bending beam technique. (from [23])

References

[1] Rim, Y. S., Bae, S. H., Chen, H. J., De Marco, N. & Yang, Y. Recent Progress in Materials and Devices toward Printable and Flexible Sensors. *Advanced Materials***28**, 4415-4440, doi:10.1002/adma.201505118 (2016).

[2] Vig, J. R., Walls, F. L. & Ieee. in *IEEE/EIA International Frequency Control Symposium and Exhibition.* 30-33 (Ieee, 2000).

[3] Saeki, S., Holste, J. & Bonner, D. Sorption of organic vapors by polystyrene. *Journal of Polymer Science Part B: Polymer Physics* **19**, 307-320 (1981).

[4] Sauerbrey, G. Verwendung von Schwingquarzen zur Wägung dünner Schichten und zur Mikrowägung. *Zeitschrift für Physik A Hadrons and Nuclei* **155**, 206-222 (1959).

[5] Wajid, A. On the accuracy of the quartz-crystal microbalance (QCM) in thin-film depositions. *Sensors and Actuators a-Physical* **63**, 41-46, doi:10.1016/s0924-4247(97)80427-x (1997).

[6] White, C. C. & Schrag, J. L. Theoretical predictions for the mechanical response of a model quartz crystal microbalance to two viscoelastic media: A thin sample layer and surrounding bath medium. *The Journal of Chemical Physics* **111**, 11192-11206 (1999).

[7] Vogt, B. D., Lin, E. K., Wu, W. L. & White, C. C. Effect of film thickness on the validity of the Sauerbrey equation for hydrated polyelectrolyte films. *Journal of Physical Chemistry B* **108**, 12685-12690, doi:10.1021/jp0481005 (2004).

[8] Wong, H. C., Campbell, S. W. & Bhethanabotla, V. R. Sorption of benzene, toluene and chloroform by poly (styrene) at 298.15 K and 323.15 K using a quartz crystal balance. Fluid phase equilibria 139, 371-389 (1997).

[9] https://it.wikipedia.org/wiki/File:InsideQuartzCrystal.jpg

[10] Filler, R. L. & Vig, J. R. Long-term aging of oscillators. *Ieee Transactions on* Ultrasonics Ferroelectrics and Frequency Control 40, 387-394, doi:10.1109/58.251287 (1993).

[11] Grassia, L., Pastore Carbone, M. G., Mensitieri, G. & D'Amore, A. Modeling of density evolution of PLA under ultra-high pressure/temperature histories. Polymer52, 4011-4020, doi:10.1016/j.polymer.2011.06.058 (2011).

[12] Kruger, K. M. & Sadowski, G. Fickian and non-Fickian sorption kinetics of toluene in glassy polystyrene. Macromolecules 38, 8408-8417, doi:10.1021/ma050353o (2005).

[13] Berens, A. R., Hopfenberg, H. B. Diffusion and relaxation in glassy polymer powders: 2. Separation of diffusion and relaxation parameters, Polymer 19 (1978)

[14] Crank, J. The mathematics of diffusion. (Oxford university press, 1979).

[15] McKenna, G. B. Ten (or more) years of dynamics in confinement: Perspectives for 2010. European Physical Journal-Special Topics 189, 285-302, doi:10.1140/epjst/e2010-01334-8 (2010).

[16] Bodiguel, H. & Fretigny, C. Viscoelastic properties of ultrathin polystyrene films. *Macromolecules* **40**, 7291-7298, doi:10.1021/ma070460d (2007).

[17] Fetters, L. J., Hadjichristidis, N., Lindner, J. S. & Mays, J. W. Molecular-weight dependence of hydrodynamic and thermodynamic properties for well-

defined linear-polymers in solution. Journal of Physical and Chemical Reference Data 23, 619-640 (1994).

[18] Wilcock, J. & Campbell, D. A sensitive bending beam apparatus for measuring the stress in evaporated thin films. Thin Solid Films 3, 3-12 (1969).

[19] Zhao, J.-H., Ryan, T., Ho, P. S., McKerrow, A. J. & Shih, W.-Y. On-wafer characterization of thermomechanical properties of dielectric thin films by a bending beam technique. Journal of Applied Physics 88, 3029-3038 (2000).

[20] Shenoy, A. Single-event cracking temperature of asphalt pavements directly from bending beam rheometer data. *Journal of Transportation Engineering* **128**, 465-471 (2002).

[21] Tong, H. & Saenger, K. Bending-beam study of water sorption by thin poly (methyl methacrylate) films. *Journal of applied polymer science* **38**, 937-950 (1989).

[22] Zhao, J.-H., Kiene, M., Hu, C. & Ho, P. S. Thermal stress and glass transition of ultrathin polystyrene films. *Applied Physics Letters* **77**, 2843-2845 (2000).

[23] Pavesi, E. *Mass Transport and Stress Field in Polymer-Solute Systems: Analysis and Solutions of Coupled Problems*, ALMA MATER STUDIORUM Università di Bologna, Bologna (Italy), (2017).

[24] Punsalan, D. & Koros, W. J. Drifts in penetrant partial molar volumes in glassy polymers due to physical aging. Polymer 46, 10214-10220 (2005).

Chapter 6

Dynamic-ramps experiments

6.1 Introduction

This chapter directly refers to the paper published in the Journal of Physical Chemistry B, issue 121 (2017) in collaboration with professor Mensitieri's group, from the Department of Chemical, Materials and Production Engineering (DICMaPI) at University of Naples "Federico II", Italy [1]. Results in the same set were also the subject of communications at national and international conferences [2]. Here are described the experimental activities carried out from the author of this thesis during a period of 3 months, spent during the second year of the PhD program at the laboratories of professor Mensitieri, who kindly contributed to this work with outstanding expertise and hospitality.

The work focused on similar phenomena described in the previous chapter, but here a microbalance was used for direct gravimetric measurements, opening to chances of measurements into the equilibrium state, then the range of glass transition induced by solvent and a finely controlled aging history. Another advance introduced in this work is an alternative dynamic control of external conditions, consisting in constant rate ramps instead of step increments. As demonstrated in the previous chapter, step amplitude and frequency never influenced sorption results for a demonstrated linearity of sorption mechanisms, then results are absolutely comparable each other as ramps can be assumed as infinitesimal amplitude steps; on the other hand, kinetics output are not available as in any case the ramp allows acquisitions at isopiestic conditions. However, a great contribution can be obtained from ramps as online measurements can be performed on glassy dynamics, as local

behavior for effective transition detection, and ongoing structural relaxation. This also puts sorption experiments closer to classic dry experiments on glasses, as dilatometry or DSC; a substantial similarity on the type of outputs between wet and dry tests will be discussed into the following paragraphs.

In order to control the conditions by ramps, another experimental apparatus was purposely designed and assembled. This also allowed to perform alternative experimental protocols, where variables other than just temperature were maintained constant: novel protocols were hence proposed.

6.2 Apparatus description

A gravimetric apparatus has been set up to monitor the mass of solvent absorbed into samples from the pure component vapor phase; a complete scheme is reported in Figure 6.1. The apparatus allows one to finely control the temperature and pressure of toluene vapor inside the measuring chamber. In the apparatus, the sample is hung to the weighing arm of a CAHN-D200 electronic microbalance (produced by Thermo Electron Co., Waltham MA, USA). This is a high sensitivity instrument (up to 10^{-7} g and an accuracy of $\pm\ 3\cdot10^{-7}$g), which was gold plated in order to confer resistance to solvents and other aggressive environments.

The sample, consisting in an assembly of several hundred coated aluminium disks, piled up and hold together by a titanium wire passing through their central points, was hanged to the measuring arm of the balance. The sample and the hanging wire were located in a glass-made chamber, where the temperature was controlled by means of a thermostatic fluid circulating in a jacket surrounding the sample. The circulating fluid temperature was controlled by a programmable liquid fluid temperature bath (Julabo CF41) with an accuracy of ± 0.01 K.

The balance is connected, by service lines, to a flask dead volume (T2 in Figure 6.1), to a liquid toluene reservoir (T1 in Figure 6.1), to a combined pumping station incorporating turbopump and membrane backing pump (Pfeiffer HiCUBE 80, ultimate pressure 10^{-7} mbar, pumping speed 35 l/s;

P1 in Figure 6.1), to a pressure transducer (an MKS Baratron 121 A, absolute capacitance gauge with a full range of 100 Torr, a sensitivity of 0.01 Torr and an accuracy equal to ±0.5% of the reading) and to an electronically controlled throttle valve (MKS 653B;in Figure 6.1). Pressure of the vapor of toluene within the equipment and in the sample compartment was controlled by a MKS 651C controller (PIC in Figure 6.1), that receives the pressure value from the MKS Baratron 121 A transducer and drives the throttle valve to obtain the desired set point value of pressure, by a PID controller. Pressure is maintained at the desired value by a dynamical balance between the toluene vapor outflow through the throttle valve (separating the equipment from the vacuum pump) and the toluene vapor inflow from a solvent reservoir with a manually controlled needle valve (V1 in Figure 6.1).

The set point for the pressure controller is provided by a Labview® code that supplies to the controller the desired value of pressure at each time, enabling different desired experimental protocols. The Labview code has been also designed to acquire and record the balance reading, the throttle valve status, the pressure reading and the temperature value of the sample, with a maximum acquisition frequency of 20 points per second. The same is even used for temperature set point control for other tested protocols. Balance head, pressure transducer, solvent reservoir, dead volume flask and service lines are contained in a case where a constant temperature value of 35°C is assured by an air flow at controlled temperature (accuracy ± 0.1°C).

The liquid toluene contained in the solvent reservoir was first degassed by several freezing thawing cycles. During the desiccation stage preceding the tests, a high vacuum was attained by activating both the turbomolecular pump and the membrane backing pump. Conversely, during the tests, only the membrane backing pump is activated for pressure control purposes.

Correction for the effect of buoyancy on the measured values of weight change was quantified by first determining the apparent volume of balance system, including hanging wires, sample and counterweights. This volume was evaluated by introducing within the balance volume pure helium at several pressures, thus promoting a lift (and, in turn, a change in weight), proportional to the

density of the gas, that is related to the buoyancy effect on both arms of the balance. Using a reliable equation of state for helium gas it was then possible to determine the apparent volume of the balance, assuming that the sample and the components of the apparatus do not absorb any helium. This apparent volume was used to quantify the buoyancy effect due to toluene vapor during the test, that is needed to correct raw gravimetric results for toluene sorption in PS. It is important to note that, in the calculation of the buoyancy effect due to toluene, the variation of volume of PS as a consequence of sorption was considered negligible.

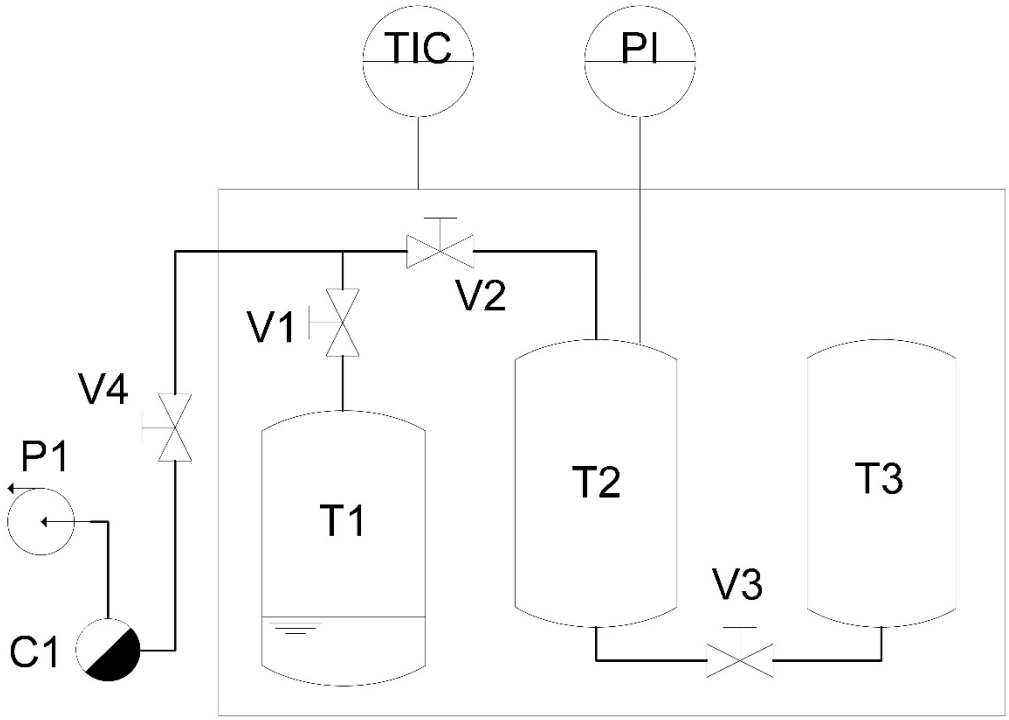

Figure 6. 1 Scheme of the apparatus assembled for dynamic sorption measurement. All controllers and data acquirements are managed by a desktop PC and a properly designed LabVIEW® Virtual Instruments. TIC: Temperature Indicator and Controller; PIC: Pressure Indicator and Controller (pressure transducer MKS 121 A and pressure controller MKS 651C); V1, V2, V3, V4 and V6: manually operated valves; V5 electronically controlled throttle valve (MKS 653B); P1 turbomolecular pump (Pfeiffer I-cube module) with membrane pump stage; T1: degassed liquid toluene reservoir; T2: dead volume flask; B1 Cahn D-200 microbalance head case; B2: water jacketed sample compartment. (from [1])

6.3 Materials and methods

Samples in the form of self-standing thick films, or supported thin layers, were prepared from the same source of atactic PS (weight-average molecular weight MW = 270000 kg/kmol; polydispersity index Mw/Mn = 1.1) kindly supplied by Versalis S.p.A., Mantua, Italy. Toluene, used either for sample preparation or for sorption/desorption tests, was used as provided by the supplier (HPLC grade, SigmaAldrich). Thin PS coatings deposited on top of aluminium foils (thickness 17 μm, Italchim S.r.l., Bologna, Italy) were obtained by a spin coating process, starting from a PS−toluene solution (PS 7% by weight). By modifying the spinning rate, it was possible to obtain thin films with different thicknesses. Two series of coating films, 430 and 750 nm thick, were actually prepared and used for the sorption experiments. Disks with a diameter of 13 mm were cut from the PS spin coated aluminium foils, using a sharp hole punch. The estimate of the average thickness of PS coating films was obtained after the evaluation of the mass of the coating: the weight of the coating film was calculated after the difference between the weight of the coated disk and the corresponding bare aluminium disk, as obtained after cleaning it by means of a solvent. A Mettler Toledo analytical balance, sensitivity 10^{-5} g, was used for the evaluation of the apparent weight of both coated and cleaned disks. The average thickness of the coating was finally estimated from its mass, based on the total area of the disk and on estimated room condition values for the mass density of polystyrene (1.04 g/cm3). Removal of residual traces of toluene was pursued by treating them at 120 °C under a vacuum for a few hours followed by overnight cooling.

The gravimetric apparatus described in the previous paragraph was used to perform different kinds of dynamic tests for toluene sorption/desorption in PS coated aluminium disks, according to the specific conditions imposed during the variation of toluene chemical potential: (1) isothermal, (2) isobaric, and (3) iso-activity.

To guarantee an adequate accuracy of the tests, around 400 PS coated disks were hung to the weighing arm of the microbalance, by piling them using a titanium thin wire. Before running any type of dynamic test, samples were preliminarily exposed to a sufficiently high toluene pressure

through an integral static sorption experiment, described in the previous section, to ensure the attainment of an equilibrium rubbery state, thus erasing any memory of previous treatment history on the sample. This constituted an essential treatment for reliable sorption tests, due to the influence of history on glassy dynamics, thus the starting point for each run.

The dynamic experiment then proceeds following the prescriptions of each specific kind of test. In particular, in isothermal tests, first a decrease in pressure of toluene vapor in the balance chamber is imposed at a controlled rate promoting desorption of toluene, and bringing the PS−toluene mixture into the glassy region; pressure is then raised at the same absolute rate, to determine the reabsorption of toluene, recovering the starting level of pressure. In the isobaric case, the temperature of the balance chamber is changed in a loop while maintaining a constant pressure of toluene vapor. In fact, the isobaric test starts from a rubbery state at low temperature proceeding then by heating the sample compartment, at a controlled rate, up to a temperature at which the sample is rubbery again (thin phenomenon will be explained in detail over the next section) and then by cooling the sample compartment, at the same controlled rate, back to the initial value of temperature. Finally, in the case of a dynamic iso-activity test, a path is followed along which temperature and pressure are both decreased at a controlled rate, in such a way that the toluene activity in the gaseous phase is kept at about a constant value for the entire duration of the experiment; toluene activity was assumed as the ratio between partial and vapor pressure, and the latter was calculated as a function of temperature by a polynomial equation.

The obtained raw data in terms of sample weight change were elaborated to evaluate the ratio of mass of absorbed toluene to that of neat “dry” polymer, referred to in the following as the “mass ratio”, or the toluene mass fraction. Experimental conditions (in terms of rate of change of pressure and/or temperature) and sample thickness were properly selected to prevent any influence on the observed behavior of kinetic effects related to toluene diffusion in the PS films. In fact, attention was paid to impose a sufficiently low rate of pressure decrease of toluene vapor and/or of temperature change to guarantee a rather uniform chemical potential within the polymer phase at

any time. Experimental proof that this is actually the case will also be provided by showing the results obtained by imposing a standard pressure decreasing ramp on samples of different thickness and by performing consecutive decreasing/increasing pressure ramps on a sample. As a consequence, when the experiments are performed on the polymer mixture in a rubbery state, it is reasonable to assume that, at each time, a uniform toluene concentration is present within the PS film, in instantaneous equilibrium with the surrounding toluene vapor phase. In fact, under these conditions, polymer relaxation is fast enough to let the polymer structure accommodate rather instantaneously to the imposed changes of pressure and/or temperature. Conversely, when experiments are performed on the polymer mixture in a glassy state, one can still assume the uniformity of toluene chemical potential within the polymer, although the system does not attain instantaneously an equilibrium state, in view of the slower relaxation dynamics: in this case, an instantaneous pseudo-equilibrium state is established between the polymer mixture and the toluene vapor phase.

6.4 Results

In this section, the experimental results of dynamic tests performed on aluminium supported PS thin films are presented and discussed, for different protocol types analysed: isothermal tests at several temperatures, isobaric tests at a pressure equal to 36 mbar, and iso-activity tests

As anticipated, for each test, samples were initially conditioned at a sufficiently high toluene pressure and for a sufficiently long time to let the polymer mixture reach a rubbery state at equilibrium with the vapor phase, thus erasing any memory effect. As will be shown, these dynamic sorption data display a discontinuity in the slope of the toluene mass ratio, within the polymer mixture phase, as a function of the pressure of toluene vapor and/or temperature. These discontinuities are attributed to the occurrence of a rubber-to-glass transition of the polymer mixture. By reporting the coordinates of these discontinuities in a temperature vs pressure plot, a contour line is obtained separating the glassy from the rubbery domains of the polymer–toluene mixture.

6.4.1 Preliminary isothermal tests

Several different factors and related characteristic times may affect mass uptake kinetics in dynamic sorption tests subject of this section, due to the continuous ramps applied: rate of change of boundary conditions, relaxation process in polymeric material, and resistance to mass transport in the solid sample.

Unlike the case of the other factors, the characteristic time of mass transport in a polymer sample is affected by the volume-to-surface ratio of the specimen. Because of that, the kinetics of the diffusion process can be manipulated by adjusting the thickness of the solid sample, without affecting the rate of any other phenomenon. The thickness of PS coating films prepared for dynamic sorption tests was designed to accelerate toluene transport to such an extent that sorption kinetics is mainly ruled by the relaxation behavior of the polymer mixture in the range of interest for the rate of change of boundary conditions. The mutual diffusion coefficient (D) in the polymer–solute system is very sensitive to solute content, and indeed, a large variation in characteristic time for diffusion was observed in static sorption experiments in the same freestanding film from dry to fully plasticized conditions. When an intermediate value D (10^{-10} cm^2/s) is considered, a characteristic time for the diffusion process lower than 1 min can be estimated for the case of a film thickness lower than 1 μm. On the basis of that, the glass-to-rubbery transition zone at 40 °C can be crossed in a dynamic sorption test at a rate as high as 0.16 mbar/min (that is the maximum value adopted in this investigation) keeping as low as a few percent the relative variation of apparent equilibrium solubility within the characteristic time for diffusion. According to the above consideration, the difference between minimum and maximum solute concentration in the polymer sample due to diffusion kinetics is limited to at the most 1% of the average value, even within the glassy region, for the rate of pressure variation mentioned above.

In order to verify the reliability of these estimates for the cases of both the rubbery and glassy states of the polymeric mixture, preliminary tests were performed to ensure that the diffusion resistance in

a dynamic sorption test is actually negligible for the rate of pressure change of interest in this work. A first test was run on PS coating film of 750 nm on thickness, performing isothermal dynamic sorption experiments at 40 °C in which toluene pressure is changed in a cyclic fashion, confined into the rubbery region. Under those conditions, the relaxation time is low enough to allow for the phenomenon to be ignored, and the difference observed for the mass ratio measured at the same toluene pressure between sorption/ desorption branches can only be attributed to diffusion resistance in the solid. Results from this kind of experiments are reported in Figure 6.2 for the case of two different values of the rate of change for toluene pressure. As one can see, the uncertainty in solute content due to diffusion resistance is lower than 1%, even for the case of the highest rate used (0.16 mbar/ min).

The same kind of test cannot be considered to verify that diffusive resistance is negligible in the glassy polymer mixture, as the significant effect of the slow relaxation phenomena would invariably affect the result of a cyclic process, performed below the glass transition. A different test was thus designed, simply comparing the result for the toluene mass ratio as a function of the toluene pressure in the gaseous phase for the dynamic desorption test run at the same pressure change rate in PS samples of different thicknesses. In case the desorption kinetics was affected by diffusive resistance, different mass ratios would result at the same values of toluene pressure for samples of different thicknesses. Experimental data were obtained at 40 °C by the same isothermal dynamic desorption test performed on 750 and 430 nm thick PS coating films, bringing both samples from rubbery conditions down below the glass transition zone, as identified from static sorption experiments. No significant difference was observed between data retrieved for the two samples (Figure 6.3), thus confirming that the diffusion resistance does not affect appreciably the dynamic sorption/ desorption tests considered in this work even when the polymer mixture is in the glassy state. Only one value for thickness was finally considered for samples used in this work, and in fact,

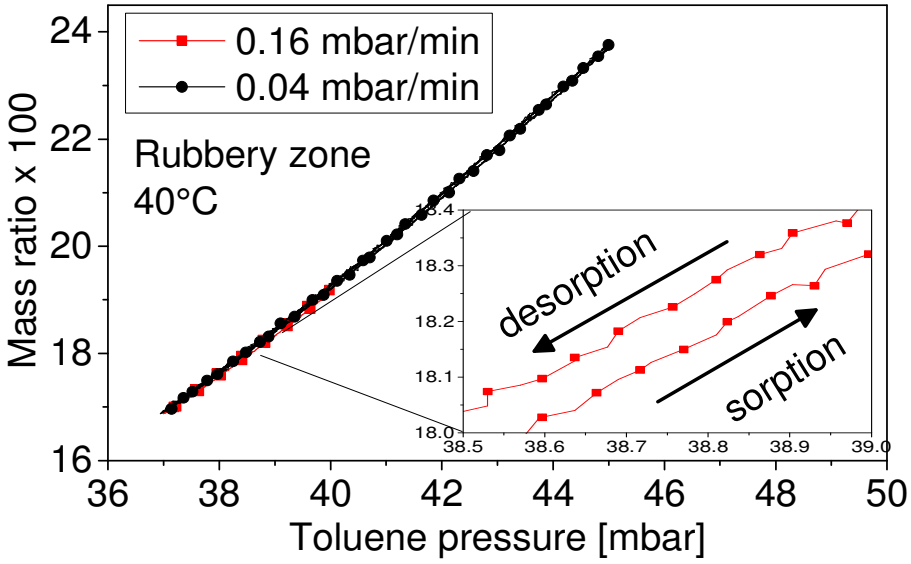

Figure 6. 2 Results of sorption/desorption tests in PS performed by cycling the pressure of toluene vapor at a controlled rate. In the inset is reported an enlargement of the results for the case of a rate of change of pressure equal to 0.16 mbar/min. A good overlap between sorption and desorption ramp confirms the limited effect of diffusive phenomena on the rate of change of toluene mass ratio in the PS-toluene mixture. (from [1])

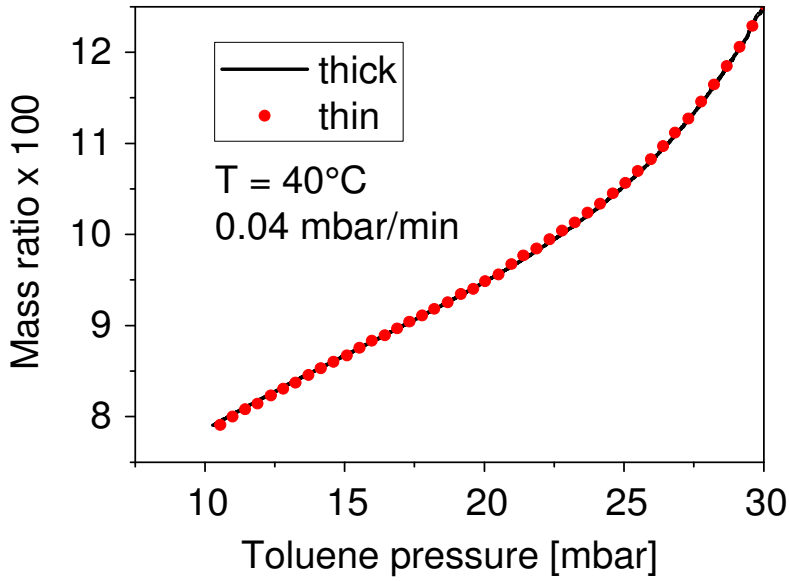

Figure 6. 3 Dynamic sorption tests at 40 °C with toluene in two PS samples of different thickness; desorbing isotherms at constant rates are thickness-independent. (from [1])

all results for dynamic experiments reported in the next sections refer to the case of toluene sorption/desorption in thin PS coating films with a thickness equal to 750 nm.

6.4.2 Dynamic isothermal tests

Different kinds of toluene sorption/desorption tests in thin PS coating films were performed in this work according to the dynamic protocol. Results for a 40 °C isothermal sorption–desorption cycle, spanning both above and below the glass transition zone already identified, are reported in Figure 6.4. Following a preliminary integral sorption experiment at a toluene pressure of 40 mbar, solute desorption was allowed by continuously decreasing the pressure of toluene vapor at a constant controlled rate of 0.16 mbar/min down to 10 mbar. After completing the pressure decrease stage, the pressure of toluene vapor is increased back to 40 mbar, at the same rate of 0.16 mbar/min. A hysteretic behavior for the desorption/sorption cycle is evident from data reported in Figure 6.4 in the region of low pressures. In fact, in this region, desorption and subsequent sorption branches do not overlap. Several relevant features of solute mass ratio, obtained from the sorption/desorption cycle in Figure 6.4 deserve to be highlighted, as they are evidenced in all similar tests performed at different temperatures or rates of change for pressure:

• A discontinuity in the value of the slope of the toluene mass ratio as a function of pressure is evident, pointed out by the arrow in Figure 6.4. In fact, a remarkable difference is evident, along the desorption stage, in the values of the isothermal solubility coefficient (i.e., the derivative of toluene mass ratio as a function of pressure) above and below a transition region, with the coefficient being higher at toluene pressure values above those marking the transition. The pressure value at which the transition is located is referred to as p_g. This discontinuity, as we will better discuss later, is assumed to identify a rubber-to-glass transition of the PS–toluene system. The exact location of the discontinuity was evaluated by using a mathematical procedure illustrated in detail later on.

• In the low-pressure range of the cycle, the solubility coefficient is higher along the desorption branch (decreasing pressure) as compared to the sorption branch (increasing pressure).

• The sorption branch recovers the mass ratio values of the desorption branch at pressure values significantly higher than those at which the transition occurs along the desorption stage.

• A small, although not negligible, difference is measured at the highest values of pressure between the solubility isotherm measured along the initial desorption path and the corresponding curve registered during the subsequent sorption run.

It is worth noting that a similar behavior was also observed by Doumenc, Bodiguel and Guerrier for toluene in polymethyl methacrylate [3].

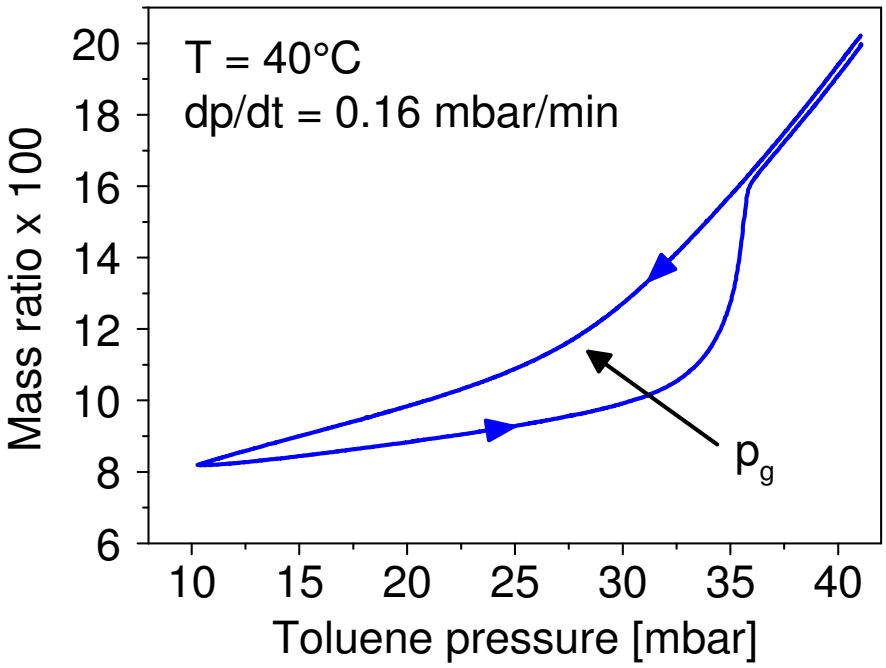

Figure 6. 4 Example of experimental results of a dynamic isothermal desorption/sorption test at 40 °C of toluene in PS: a constant rate of 0.16 mbar/min has been applied both along the decreasing and increasing pressure branches. Rubbery-to-glassy state transition is evidenced by an arrow (from [1])

While all features in the above list could be the subject of specific analysis relevant to the study of relaxation behavior in a polymer–solute system, in the present context, we focus our attention only on the features displayed by the desorption branch. In what follows, the observed transition from

rubber-like to glass-like state in dynamic desorption tests is analysed in detail, evaluating the variation of p_g with temperature and depressurization rate. Isothermal experiments were performed at 40 °C at different values of the rate of pressure decrease, from 40 mbar down to 10 mbar, and results are collectively presented in a log–log plot in Figure 6.5 along with the results of "static" sorption tests (already discussed in Chapter 4) carried out with the pressure decay apparatus, in terms of toluene mass fraction as a function of pressure of toluene vapor. It is evident that the results obtained from dynamic tests are quite different from those obtained following the classic isopiestic protocol. In fact, at pressure values above the transition region, results from static sorption and those from dynamic desorption are almost equal, since an equilibrium rubbery state for the PS–toluene mixture in contact with the toluene vapor phase is expected to be attained in both cases. Actually, a small difference in the solubility coefficient, which indeed looks a bit higher in the case of calculated static sorption tests, can be appreciated in the rubbery region. Moreover, the amount of absorbed toluene is higher in the case of dynamic desorption tests. Most likely, these features can be attributed to residual relaxation processes in the rubbery state that occur during the long static sorption tests. On the other hand, the mechanical constraint experienced by supported film used in desorption runs, as opposed to the case of free-standing films used in static sorption tests, can also be responsible for the difference in apparent solubility.

It should be finally kept in mind that two apparatuses, with manometric and gravimetric detection of mass uptake, respectively, were used for static sorption and dynamic desorption tests, and it is likely that different small systematic errors characterize the two distinct measurement techniques, as indeed it was observed in the comparison with data from literature in Chapter 4.

Conversely, at pressure values smaller than those of the transition region, data collected in the case of dynamic desorption tests markedly departed from those obtained in the case of static sorption experiments. In view of the non-equilibrium nature of the glassy state and of its history dependent behavior, this feature can be attributed to the different history of the sample in a dynamic desorption test with respect to static sorption conditions. Thanks to the advanced control of the apparatus

subject of this section with respect to more diffused protocols starting at dry conditions (e.g. the experiment described in the previous Chapter), the effect of sample history and of the non-equilibrium nature of the polymer– toluene mixture can also be recognized in the different apparent solubility measured in the glassy region for desorption runs managed at different depressurization rates. As we are able to rule out the effect of diffusive resistance on apparent solubility measured in the dynamic desorption test, we can now discuss the results in Figure 6.5 only in terms of the ratio between imposed time for variation of boundary conditions and the characteristic time for relaxation phenomena in the polymer. Indeed, the characteristic time for change of boundary conditions is kept constant in each dynamic desorption test and its value increases as the rate of change of toluene pressure decreases. On the contrary, the characteristic time of relaxation can be assumed to be roughly independent of the rate of pressure decrease, but it dramatically increases as the toluene concentration decreases in the system. At a relatively high pressure of toluene vapor, the relaxation time is much smaller than the characteristic time of variation of boundary conditions and the apparent solubility measured at an assigned toluene pressure in a dynamic desorption test is ultimately very close to the thermodynamic equilibrium value, independent of the rate of decrease of pressure. On the other hand, the apparent solubility departs from the equilibrium value when the relaxation time increases above the characteristic time of variation in boundary conditions, which occurs across the transition zone. More specifically, departure from equilibrium conditions occurs at lower toluene concentration for the case of slower depressurization experiments, because lower toluene concentration needs to be reached for the characteristic relaxation time to match the corresponding time for variation of boundary conditions in these cases. And consequently, the location of the rubber-to-glass transition occurs at lower values of p_g the lower is the rate of pressure decrease.

This behavior has remarkable analogies with the case of a pure polymer submitted to a temperature decrease at constant pressure. In such a case, the glass transition temperature (T_g) is marked by a clear discontinuity in the slope of the plot of specific volume vs temperature. If one considers the

glass transition as a II order thermodynamic transition, the T_g value should be independent of the rate of temperature decrease. However, the experimental evidence of the underlying thermodynamic transition is affected by kinetic factors. In fact, the experimentally accessible glass transition occurs at temperatures located above the purely thermodynamic glass transition, where, due to the reduction of the macromolecular mobility, the polymer structure is no more able to attain an equilibrium rubbery state. Then, the higher the cooling rate, the higher the experimentally observed glass transition temperature [4] [5] [6].

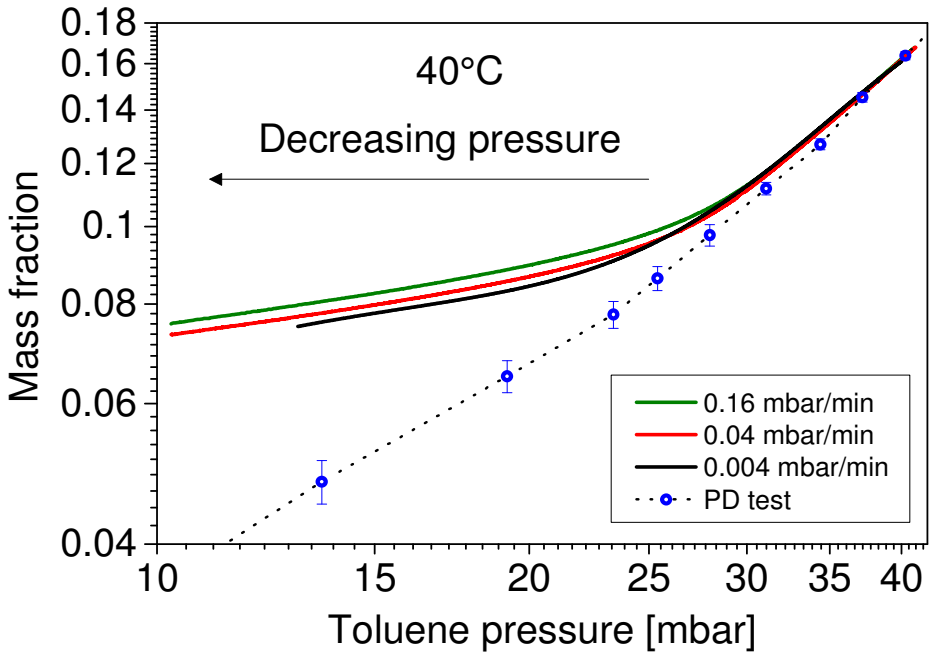

Figure 6. 5 Log–log plot reporting experimental results of dynamic isothermal desorption tests performed at several pressure decreasing rates at a temperature of 40 °C. For the sake of comparison is also reported the sorption isotherm obtained by classic isopiestic experiments carried out with the pressure decay (PD) apparatus described in Chapter 4. (from [1])

In summary, the apparent solubility isotherm retrieved from a single isothermal dynamic desorption test displays two distinct values for the solubility coefficient (slope of the apparent solubility isotherm in Figure 6.5) for equilibrium and non-equilibrium branches, with the two branches merging at a (glass) transition zone. Indeed, linear dependences of solute content from solute

pressure can be distinctly recognized above and below the transition region, with clearly higher sensitivity for the upper branch with respect to the lower one. As already mentioned, the location of the transition, in terms of the p_g value, has been evaluated by following a calculation procedure reported below. Different values of the glass transition pressure, p_g, retrieved at different values of the rate of pressure decrease, are reported in Table 6.1 along with the value of mass fraction at which the glass transition occurs at 40 °C.

Table 6.1 Values of glass transition pressure and of mass fraction of toluene at the transition, obtained at 40 °C and different pressure decreasing rate in dynamic desorption tests

pressure decrease rate [mbar/min]	0.16	0.04	0.01	0.004
glass transition toluene pressure [mbar]	28.7	28.3	27.7	26.5
toluene mass fraction (solubility @ p_g)	0.113	0.101	0.099	0.099

Together with the solute concentration, the characteristic time for relaxation also depends on the temperature and results for departure from equilibrium for apparent solubility from dynamic desorption experiments are expected to considerably change when tests are run at different temperatures. Thermodynamic equilibrium solubility isotherms as a function of penetrant pressure are also expected to be different at different temperatures; however, the equilibrium solute content within the polymer at the assigned solute activity typically shows a rather limited sensitivity to temperature, and the toluene–PS system is not an exception in this regard, as showed in literature and indeed, as made and confirmed on theoretical vs. experimental equilibrium values in Figure 5.6 (previous Chapter) [7]. For this reason, when comparing dynamic desorption results at different temperatures, it is useful to refer to plots for apparent solubility as a function of solute activity, as illustrated in Figure 6.6, with the toluene activity being calculated as the ratio between the actual pressure in the experiment and the toluene vapor pressure at the corresponding temperature.

Data are reported in Figure 6.6 for the apparent solubility in isothermal dynamic desorption runs performed in a temperature range from 20 to 90 °C, obtained at the same depressurization rate of 0.16 mbar/ min. It can be observed that, while at high toluene activity very similar solute contents are indeed exhibited by dynamic experiments run at different temperatures, rather diverse apparent solubility values are evidenced in desorption runs in the low activity region. More specifically, the positive departure of apparent solubility from the common equilibrium solubility trend is limited to the lower activity range for the case of higher temperature experiments. This feature can be easily explained considering the time associated with change in boundary conditions is the same for all experiments in focus, while the characteristic time for relaxation as a function of toluene content significantly varies with temperature and the same value of the latter is reached at lower solute contents for the case of higher temperatures. These data were analysed to determine the value of p_g at each temperature, by adopting the same mathematical procedure used in the case of isothermal tests performed at 40 °C (see below). The values of p_g determined for each isothermal dynamic desorption test, all at a depressurization rate of 0.16 mbar/min, are reported in Table 6.2 along with the corresponding toluene mass fraction.

Data in Table 6.2 show that, differently from the solute concentration, the glass transition pressure in the PS–toluene system changes with temperature in a non-monotonous way, with a maximum being shown around 60 °C. This behavior is the result of combined effects of temperature and pressure on sorption and on the associated plasticization effect. On the basis of the above evidence, it can be anticipated that, at toluene pressures below the above-mentioned maximum value, a finite temperature range exists in which the system is in a glassy state, while rubbery conditions are recognized both below a lower limit temperature or above an upper one. This also means that, when exposing a PS sample at a fixed toluene pressure, a rubbery-to-glassy transition could occur either lowering the temperature below the upper limit or raising it above the lower limit of the corresponding temperature range in which the glassy state can be observed. The latter condition is referred to as “retrograde vitrification” and it is the result of the reduction in the solute

concentration/plasticization effect occurring when the temperature is increased at constant solute pressure [8] [9]. Opposite to what happens in a high temperature/low concentration range, solute induced plasticization prevails on the temperature effect per se in the low temperature/high concentration range. A confirmation of this behavior has been looked for in this work by performing isobaric dynamic sorption/desorption processes, as described later.

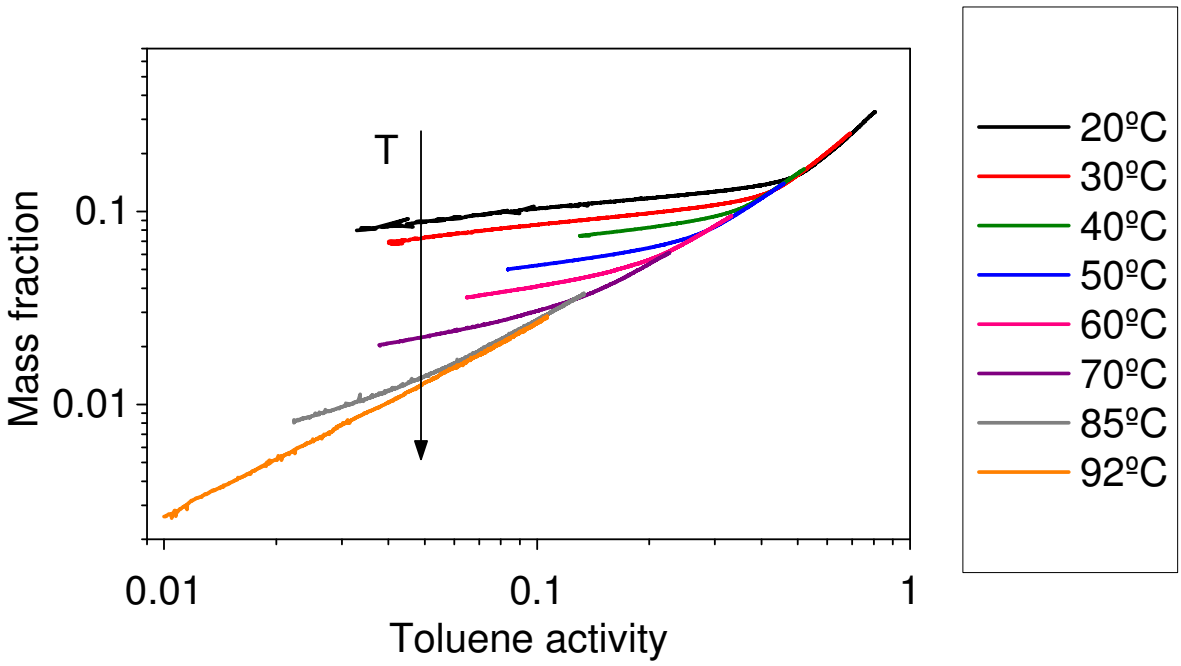

Figure 6. 6 Experimental results of isothermal dynamic desorption experiments performed at different temperatures. Values of toluene mass fraction within the polymer mixture reported as a function of solvent activity evaluated as the ratio between toluene pressure and the vapor pressure at each temperature.

Table 6.2 Values of p_g and corresponding mass fraction determined from dynamic desorption tests carried out at different temperatures and at a depressurization rate of 0.16 mbar/ min

temperature [°C]	glass transition pressure [mbar]	toluene mass fraction (solubility @ p_g)
20	15.0	0.159
30	22.0	0.135
40	30.1	0.113
50	35.7	0.081
60	40.2	0.060
70	39.1	0.039
85	30.55	0.018

6.4.2.1 Evaluation of isothermal glass transition partial pressure

As remarked in the previous section, a procedure was adopted to locate the discontinuity in a plot of mass fraction of toluene as a function of its partial pressure. However, this method was successfully applied also in later on described iso-activity curves for both pressure and temperature values at transition.

The procedure is based on the determination of the pressure at which the second derivative of the plot of toluene mass fraction vs pressure shows a maximum. In detail, the function representing the second derivative of a smoothed function built by fitting sorption data was calculated. The value of the transition pressure, p_g, was assumed as being the abscissa of the maximum in the second derivative. In Figure 6.7 is reported, as an example, the case of an isothermal test conducted at 30°C and at pressure decrease rate of 0.16 mbar/min.

In some cases, the behavior of the mass fraction vs pressure plot is linear both above and below the transition. In such cases, a simpler procedure is possible that provides the same results as the one described above. In fact, one can proceed by simply extrapolating the linear behaviours finding their intersection, that is assumed to mark the glass transition pressure (in Figure 6.8 is illustrated the case of an isothermal experiment performed at 70°C at a pressure decrease rate of 0.16 mbar/min). The value of transition pressure is the one corresponding to the abscissa of the intersection point. Its

worth noting that this linear extrapolation method is exactly the same applied in dry experiments, as example in temperature decreasing ramp dilatometry experiments at controlled rate: this represents a extraordinary achievement from the suggested experimental protocol, as the output between dry and sorption experiments on glasses are quite similar, and data can be interpret with exactly the same tools, as intended in analysis provided in Chapter 3. However, while in the dry case the linearity of experimental output is ensured by theory, and can be modelled for instance as commonly done by Tait's equation on dilatometric data, here linearity is just a reasonable approximation of the sorption curve when the glass transition occurs [10].

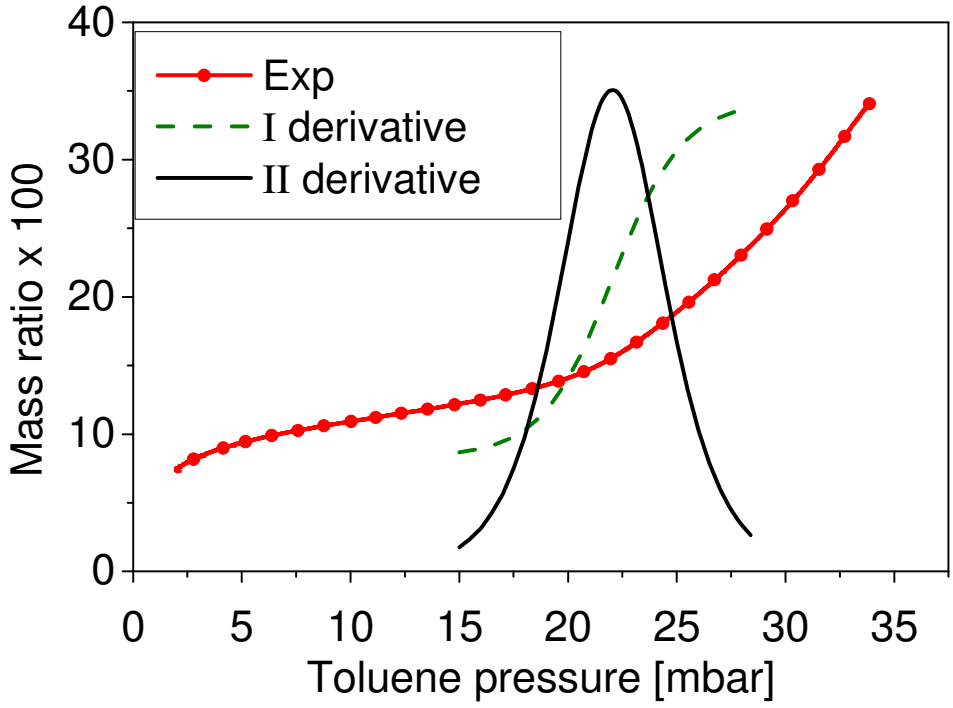

Figure 6. 7 Illustration of the procedure followed to locate the transition point (from [1])

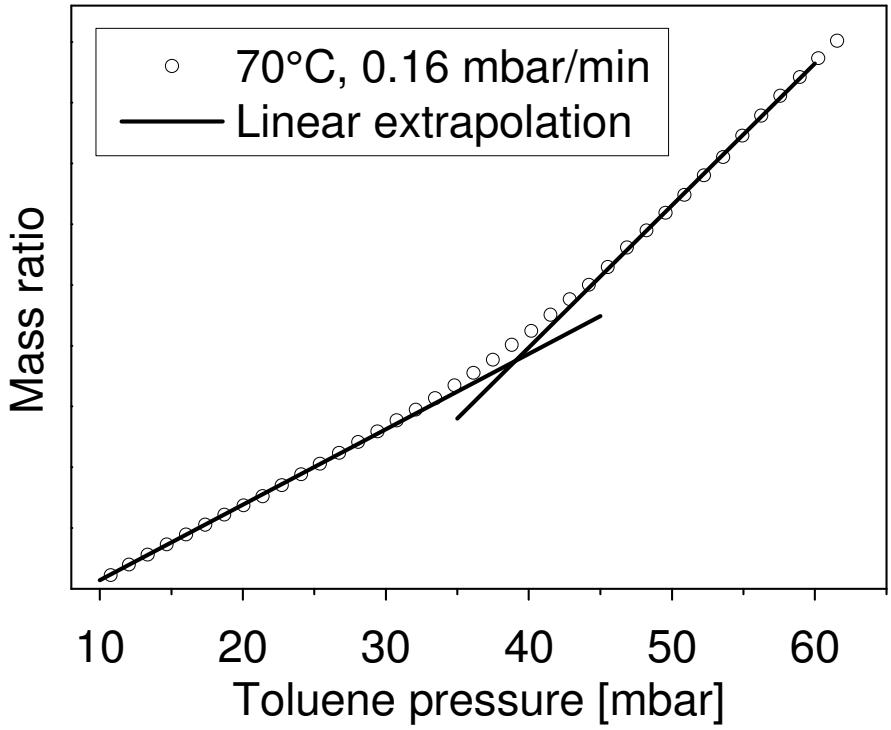

Figure 6. 8 Illustration of the procedure followed to locate the transition point for the case

6.4.3 Dynamic isobaric tests

In addition to the isothermal experiments described in the previous section, one dynamic isobaric test was performed maintaining a constant pressure of 36 mbar, by first increasing the temperature from 30 to 92 °C, at a constant rate of temperature change of 2°C/h, and then decreasing it back to 30 °C, at the same absolute rate. The apparent solubility data obtained are reported in Figure 6.9. As it refers to experimental data at lower and higher temperatures in the range explored, sorption and desorption runs show a similar solubility coefficient, consistent with the interpretation that the measured solute contents in those regions represent different parts of the same equilibrium solubility isobaric curve. At intermediate temperature, on the other hand, higher solute content is shown for the case of desorption (heating) runs with respect to that of sorption (cooling), thus confirming the existence of a non-equilibrium region at the assigned toluene pressure. The observed

behavior can be interpreted as follows. At the starting conditions (low temperature), the PS−toluene mixture is in a rubbery state, and then, as the temperature is increased, a rubber-to-glass transition occurs, promoted by the decrease in solubility accompanying heating of the system. Further increase in temperature promotes a glass-to-rubber transition. When the temperature is decreased, the mixture again displays a rubber-to-glass transition and further cooling then promotes again a glass-to-rubber transition. Different from the case of isothermal paths, the non-equilibrium glassy region along isobaric lines is confined and its limited extension does not allow for a characteristic value of glassy solubility coefficient to be retrieved.

Under these circumstances, the procedure used to identify the glass transition point after experimental data from isothermal experiments previously reported cannot be directly extended to the case of an isobaric test. To circumvent this difficulty, a different approach has been adopted in this case to estimate the two rubber-to-glass transition points (one along the heating path, the other along the cooling path), as detailed in what follows. An equilibrium thermodynamic approach based on a Non-Random compressible Lattice Fluid theory (Non-Random Hydrogen Bonding, NRHB), developed by Panayiotou et al., was used to model the phase equilibrium between the polymer−toluene mixture in the rubbery state and the toluene vapor phase [11] [12]. It is important to note here that, since the system at hand is not endowed with specific self- and cross-hydrogen bonding (HB) interactions, the terms of the NRHB model associated with formation of HBs have been consistently set to be equal to zero. An excellent fitting was obtained considering only sorption (desorption) data in the lowest and highest temperature regions, where the polymer mixture is expected to be in a rubbery state (see the continuous red line in Figure 6.9). Small but significant deviations are instead observed for experimental data from model prediction in the intermediate temperature region, where the system is expected to be in the glassy state. In fact, the NRHB model has been developed for the equilibrium rubbery system and it is not expected to properly describe the thermodynamics of a system at the glassy state. As the modelling activity was not part of the

present doctorate program, this will never be explained in details; please refer to papers cited in literature, or to a paper from our groups that is currently under production for further details.

The rubber-to-glass transition has been then assumed to occur at that point in the isobaric curve for solute content where the difference between experimental data and equilibrium results obtained by using the NRHB model becomes significant. The exact location of this point has been taken as that where the departure becomes higher than 1% of the value of the experimental mass ratio. Obviously, this procedure is affected by a higher error when compared to the case of the procedure adopted for isothermal tests, and assumptions and calculation are required.

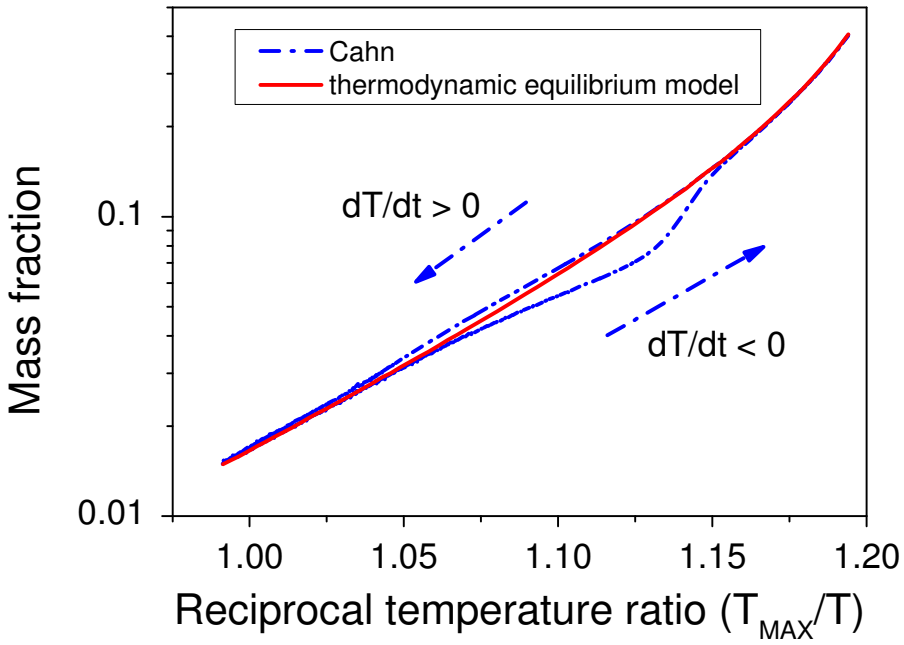

Figure 6. 9 Isobaric experiment at a toluene pressure of 36 mbar carried out between TMIN = 30°C and TMAX = 92°C. The red continuous line represents NRHB fitting of data in the rubbery regions. Dashed–dotted blue lines represent experimental data obtained by the protocol described as dynamic isobaric test.

In Table 6.3, values are reported for temperature and toluene mass fraction estimated at rubber-to-glass transition points as evaluated from the isobaric test.

Table 6.3 Values of T_g and corresponding toluene mass fraction determined from dynamic isobaric tests carried out at 36 mbar in the 30–92 °C range.

	T_g [°C]	toluene mass fraction
heating path	46 ± 8	0.105
cooling path	70 ± 8	0.036

As anticipated, two different rubber-to-glass transition points have been identified, along cooling and heating paths of the experiment, corresponding to higher and lower temperature limits for the glassy region at the assigned toluene pressure. Interestingly, the recovery of rubbery condition from the glassy state (glass-to rubber transitions) for both cooling and heating runs in isobaric experiments (see Figure 6.9) occurs at temperatures well beyond the transition points indicated in Table 6.3, parallel to what was shown for the same kind of recovery by isothermal experiments in sorption runs with respect to transition point retrieved after data from desorption runs.

6.4.4 Dynamic iso-activity tests

A third kind of dynamic experiments was performed in this work for the PS–toluene system, in which temperature was decreased at a prescribed rate, while toluene activity, was kept at an approximately constant value, by properly changing its pressure in the vapor phase. Its worth noting these experiments were performed at real isopiestic conditions: the term “iso-activity” was here used in order to differentiate experiments performed following classic pressure-jump steps, and these other tests where pressure and temperature were changed.

In detail, different iso-activity tests were performed by decreasing the system temperature at a rate of 2 °C/h and concurrently changing the pressure to maintain a constant value of the ratio between the actual pressure in the gaseous phase and the vapor pressure of toluene (p/p_0).

Figure 6.10 reports the results obtained in the case of toluene activity equal to 0.30. Similarly to the case of isothermal tests, in iso-activity experiments, there is evidence of a clear change for the

sensitivity of apparent solubility to the potential variable modulated in the test, as the latter is moved from higher to lower values. Indeed, the solubility coefficient in this case increases as the temperature decreases in a relatively narrow temperature interval (see arrows in Figure 6.10) from a negligible value registered at high temperature to a maximum value that appears to be substantially constant in the lower temperature range. The results are consistent with the assumption of one rubber-to-glass transition in the temperature range explored within the iso-activity experiment performed. In view of the features exhibited, results from these tests can be elaborated similarly to the case of isothermal experiments to identify the glass transition value for temperature (pressure) and solute content.

Results for three different iso-activity tests corresponding to the cases 0.11, 0.20, and 0.30 were collected, and here reported in Table 6.4, in terms of temperature, pressure, and toluene mass fraction at which rubber-to-glass transition occurred.

Table 6.4 Values of T_g and p_g and corresponding toluene mass fraction determined from dynamic iso-activity tests

toluene vapor activity	0.11	0.20	0.30
glass transition temperature [°C]	76	65	46
glass transition toluene pressure [mbar]	37.1	40.1	33.1
toluene mass fraction (solubility @ p_g)	0.029	0.054	0.083

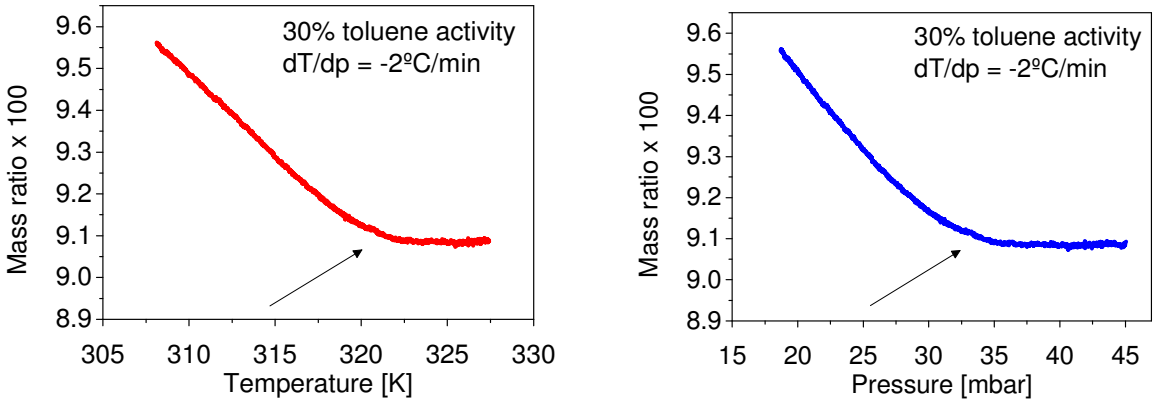

Figure 6. 10 Experimental results of dynamic iso-activity tests performed at a constant toluene activity equal to 0.3. Evolution of toluene mass ratio as a function of temperature (left) and of pressure (right).

6.4.5 Sorption induced glass transition over T-p couples

The entire set of data of rubber-to-glass transition points for manipulated process variables (T and p), as derived from the analysis of isothermal, isobaric, and iso-activity tests, is shown in the state diagram pictured in Figure 6.11. It is important to stress here that points represented in the plot have been identified only on the basis of desorption (isothermal tests and isobaric heating test) or sorption (isobaric cooling test and iso-activity tests) processes for which a continuous variation of process variable was imposed in order to induce a state change from equilibrium (rubbery) to non-equilibrium (glassy) conditions. Data have been retrieved from the analysis of results described above, essentially counting on the evidence of changes in the solubility coefficient in each experiment, defined as the sensitivity of the solute mass ratio to the manipulated process variable; furthermore, it has been shown in previous sections that the exact location of the transition point slightly depends on the rate at which the process variable is changed in the test and we should talk in terms of transition region rather than boundary. It is explicitly noted here that the transitions observed experimentally need to be interpreted as the experimentally accessible. Data for the low-pressure glass transition temperature of dry polystyrene, corresponding to the case of a null value of toluene pressure, have been added in Figure 6.11 to the results from dynamic sorption/desorption

experiments to represent the whole glassy region in the same diagram, according to the value provided by the producer.

It is noted that results from isobaric and iso-activity experiments are qualitatively consistent with those retrieved from isothermal experiments, although a non-negligible quantitative discrepancy is evident, that is likely due to the different procedure used to retrieve the transition points from isobaric experiment data as compared to isothermal and iso-activity tests. Most notably, the plot in Figure 6.11 confirms that the PS– toluene system is characterized by the so-called "type IV" behavior, and retrograde vitrification is apparent for toluene pressure and system temperature lower than 40 mbar and 60 °C, respectively [8] [9].

The diagram defines in detail the boundary of the glassy region around the maximum toluene pressure consistent with glassy conditions for polystyrene and indicates that the interval of toluene pressure for retrograde vitrification extends below 15 mbar. Furthermore, the state diagram in Figure 6.11 illustrates the number and nature of transitions the system experiences in different kinds of experiments.

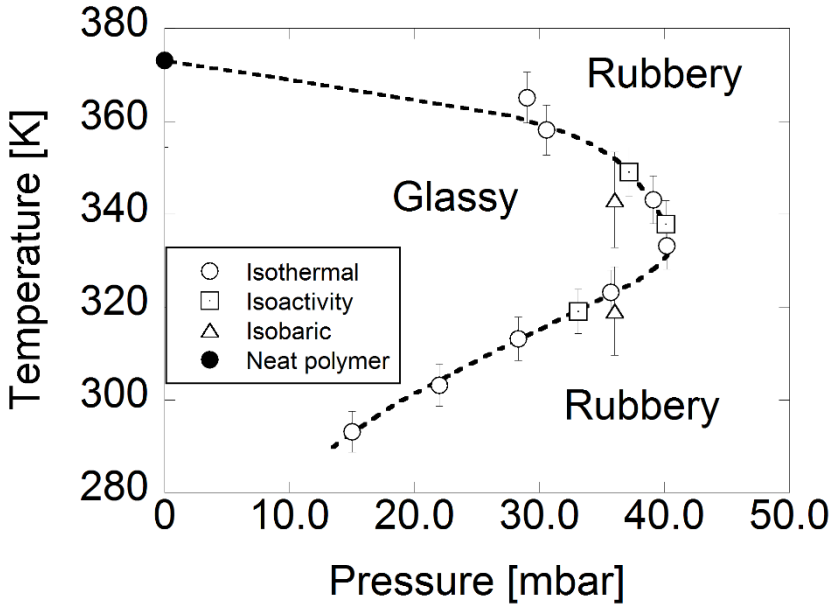

Figure 6. 11 Plot of rubber-to-glass transition points as determined from isothermal, isobaric, and iso-activity experiments. For isothermal experiments, results refer to tests performed at a pressure decrease rate equal to 0.16 mbar/min. For isobaric and iso-activity experiments, results refer to experiments performed at a rate of temperature change equal to 2 °C/h. The dotted curve is a guide to the eye.

It should be finally clarified that recovery of rubbery condition from glassy states through the same kind of mass transport process (e.g, isothermal and isobaric sorption tests in this work) exhibits a different behavior since it depends on the history of the process in the glassy state for which the non-equilibrium conditions can be observed for pairs of process variables outside the glassy domain in Figure 6.11 and a transition point cannot be actually identified in the same term as for rubber-to-glass transition.

References

[1] Pierleoni, D. *et al.* Analysis of a Polystyrene-Toluene System through "Dynamic" Sorption Tests: Glass Transitions and Retrograde Vitrification. *Journal of Physical Chemistry B* **121**, 9969-9981, doi:10.1021/acs.jpcb.7b08722 (2017).

[2] Pierleoni, D., Scherillo, G., Minelli, M., Mensitieri, G. & Doghieri, F. in *8th International Conference on Times of Polymers (TOP) and Composites.*(Amer Inst Physics, 2016).

[3] Doumenc, F., Bodiguel, H. & Guerrier, B. Physical aging of glassy PMMA/toluene films: Influence of drying/swelling history. *European Physical Journal E* **27**, 3-11, doi:10.1140/epje/i2008-10345-0 (2008).

[4] Greiner, R. & Schwarzl, F. Thermal contraction and volume relaxation of amorphous polymers. *Rheologica Acta* **23**, 378-395 (1984).

[5] Bruning, R. & Samwer, K. Glass-transition on long-time scales. *Physical Review B* **46**, 11318-11322, doi:10.1103/PhysRevB.46.11318 (1992).

[6] Schawe, J. E. K. Measurement of the thermal glass transition of polystyrene in a cooling rate range of more than six decades. *Thermochimica Acta* **603**, 128-134, doi:10.1016/j.tca.2014.05.025 (2015).

[7] Bawn, C., Freeman, R. & Kamaliddin, A. High polymer solutions. Part I.—Vapour pressure of polystyrene solutions. *Transactions of the Faraday Society* **46**, 677-684 (1950).

[8] Condo, P. D., Sanchez, I. C., Panayiotou, C. G. & Johnston, K. P. Glass-transition behavior including retrograde vitrification of polymers with compressed fluid diluents. *Macromolecules* **25**, 6119-6127, doi:10.1021/ma00049a007 (1992).

[9] Condo, P. D. & Johnston, K. P. Retrograde vitrification of polymers with compressed fluid diluents - experimental confirmation. *Macromolecules***25**, 6730-6732, doi:10.1021/ma00050a057 (1992).

[10] Grassia, L., Pastore Carbone, M. G. & D'Amore, A. Modeling of the Isobaric and Isothermal Glass Transitions of Polystyrene. *Journal of Applied Polymer Science***122**, 3752-3757, doi:10.1002/app.34789 (2011).

[11] Panayiotou, C., Pantoula, M., Stefanis, E., Tsivintzelis, I. & Economou, I. G. Nonrandom hydrogen-bonding model of fluids and their mixtures. 1. Pure fluids. *Industrial & Engineering Chemistry Research* **43**, 6592-6606, doi:10.1021/ie040114 (2004).

[12] Panayiotou, C., Tsivintzelis, I. & Economou, I. G. Nonrandom hydrogen-bonding model of fluids and their mixtures. 2. Multicomponent mixtures. *Industrial & Engineering Chemistry Research* **46**, 2628-2636, doi:10.1021/ie0612919 (2007).

Chapter 7

Analysis of dynamic isothermal desorption by modeling

7.1 Introduction

Methods defined in previous chapters allow for the experimental characterization of several different features related to structural relaxation in glassy polymers as induced by sorption/desorption of low molecular weight species. While results from the above procedures are of interest "per se" in the representation of characteristic properties of polymer/solute mixtures, their discussion and interpretation in modeling terms is also in order. The latter is indeed a necessary step toward the use of results from the experimental characterization to define tools which describe solvent induced relaxation phenomena for the case of a general sorption/desorption process in polymers. On the other hand, a comprehensive description of general out-of-equilibrium behavior of polymeric systems is far beyond the scope of the present work and attention will be confined here to simple empirical modeling approaches suitable for the representation of observed phenomena.

Essential ingredients of an empirical approach of this kind are the following:

- a reliable model for equilibrium thermodynamic properties of polymer/solute mixture as function of proper state variables for the system;

- a convenient set of order parameters for polymer/solute structure which allows for the distinction of different non-equilibrium states of the system below the glass transition temperature for the same externally applied potentials;
- constitutive equations for time evolution of order parameters at assigned variation of externally applied potentials for the polymer/solute systems.

Several different options are actually available for the selection of each kind of tool in the list above, from works presented within the fields of equilibrium and non-equilibrium thermodynamics of polymeric phases. A comparison between different possible choices for the points listed above will not be attempted here and the analysis of results from a specific selection of modeling tools will be directly given. In fact, the aim of the present discussion is the exemplification of a meaningful treatment of characterization results from experimental analysis described in the previous chapter, while the optimization of the modeling approach is left to possible future developments.

7.2 Modeling equilibrium thermodynamic properties

As it refers to the model for thermodynamic properties, the approach offered by the Perturbed-Chain-Statistical-Associating-Fluid-Theory (PC-SAFT) was considered in this work, in which molecules are described as chains of hard spheres which interact with each other both in unspecific and specific terms [1]. The corresponding representation of Helmholtz free energy A of the polymer/solute system as function of temperature T, volume and species mass density $\rho_{pol} = m_{pol}/V$ and $\rho_{sol} = m_{sol}/V$, according to the following scheme:

$$A^{PC-SAFT}\left(T,V,m_{pol},m_{sol}\right) = A^{IG}\left(T,V,m_{pol},m_{sol}\right) + A^{HC}\left(T,V,m_{pol},m_{sol}\right) + A^{DISP}\left(T,V,m_{pol},m_{sol}\right) + A^{HB}\left(T,V,m_{pol},m_{sol}\right) \quad [7.1]$$

where A^{IG} is the Helmholtz free energy for the corresponding ideal gas system at the same temperature, volume and species mass, while A^{HC}, A^{DISP} and A^{HB} are hard chain reference fluid, dispersion and hydrogen bonding contributions to the residual Helmholtz free energy.

For the case of non-associating components, as for the case of PS-Toluene pair, hydrogen bonding contribution to the free energy is dropped from the above list and remaining terms for energy density as function T, ρ_{pol} and ρ_{sol} , are all expressed in relation with three specific pure component and one binary parameters. Together with molar mass M_i, pure component characteristics used in PC-SAFT refer to segment diameter, mass and characteristic energy (σ_i, m_i, ε_i), while a binary parameter k_{ij} is used to interpret the ratio between interaction energy for non-homogeneous segment pair in the mixture with respect to geometrical average of corresponding homogeneous interaction.

Within the PC-SAFT framework, the equilibrium properties of the polymer solute mixtures at assigned temperature T, pressure p and solute to polymer mass ratio Ω, are then derived from Equation [7.1], after the system specific volume has been evaluated from the condition of minimum Gibbs free energy for given set $\{T, p, \Omega\}$.

PC-SAFT model is indeed a well-established tool for the representation of equilibrium properties of amorphous systems and proved to be very effective in the description of both simple fluids and solute/polymer systems [2].

The specific representation of equilibrium properties for PS-Toluene mixtures considered in this work was obtained through PC-SAFT model, after accounting for the pure component parameters retrieved by Müller et al. for the same system (values in table 7.1) and tuning the binary parameter as function of temperature for an optimal representation of equilibrium composition at high solute fugacity in the whole temperature range expected [3]. Results for k_{ij} after the corresponding best fit is also represented in Table 7.1.

Table 7.1 PC-SAFT parameters for PS-Toluene system

	Polystyrene	**Toluene**
M [g/mol]	300000	92.1
m [g/mol]	52.6	32.8
σ [Å]	4.11	3.72
ε/*k* [K]	267	286
χ	$-0.061 + 1.0\times10^{-4}$ T (T expressed in K; 290 K < T < 360 K)	

In Figure 7.1 results are shown for the comparison between apparent solubility measured in a dynamic desorption experiment for PS-Toulene systems at 20°C and corresponding correlation obtained from PC-SAFT model. As expected, good representation of experimental data are retrieved this way for the case of high solute fugacity mixtures, while increasing deviations of model predictions from experimental results are in evidence for the case of systems at lower solute content.

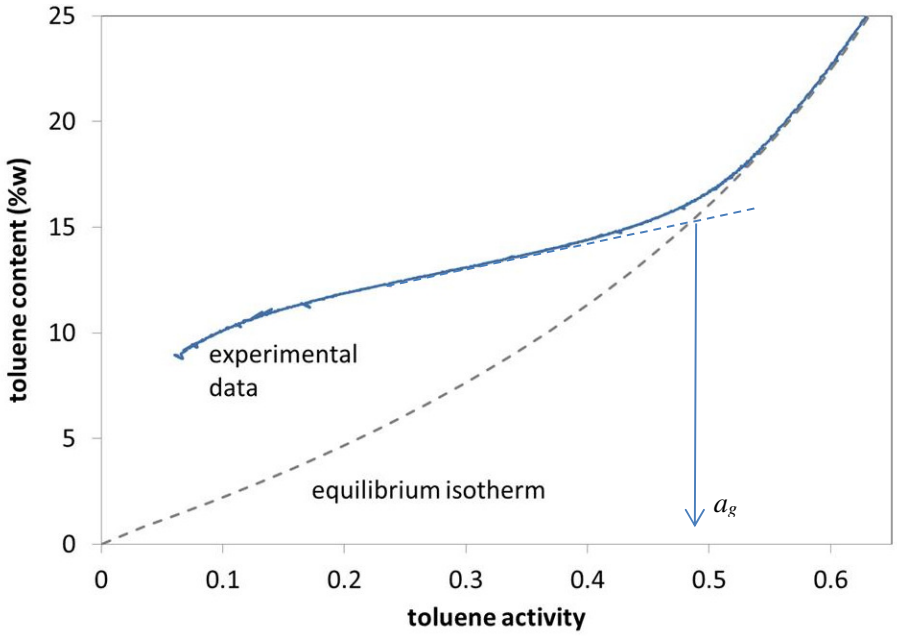

Figure 7. 1 Apparent solubility isotherm from dynamic desorption experiment and equilibrium solubility isotherm from PC-SAFT at 20°C

7.3 Modeling out-of-equilibrium thermodynamic properties

7.3.1 Thermodynamic approach to non-equilibrium state of polymer-solute systems

As anticipated in the introduction, deviations from equilibrium condition can be discussed through the above thermodynamic approach when one or more order parameters are selected to describe the departure from minimum Gibbs free energy conditions at assigned external potentials for the system. The simple assumption is considered in this work as suggested by the NET-GP model, for which the only order parameter needed to the description of the out-of-equilibrium conditions of glassy polymeric mixtures is the system volume [4]. According to this approach, the description of thermodynamic properties of the system in non-equilibrium conditions is obtained from the same expression for Helmholtz free energy as function and temperature and species density calculated for corresponding equilibrium. At assigned temperature and pressure, however, the out-of-equilibrium properties are evaluated releasing the constraint of minimum Gibbs free energy and accounting for the actual volume of the system. Indeed, NET-GP approach proved to be very successful in representing apparent gas and vapor solubility at pseudo-equilibrium in polymeric systems below the glass transition temperature, when independent information about the system volume is provided [5]. It is significant to observe that the model was satisfactorily used to represent the effect of different sample pre-treatments on apparent gas solubility in the glassy polymers, just accounting for the corresponding different value measured for volume per polymer mass. It is also useful to consider here that no additional parameter is needed to apply the NET-GP approach to the description of the out-of-equilibrium conditions of the polymer-solute system of interest and for the evaluation of its thermodynamic properties.

On the other hand, in the case of interest in this work, corresponding to conditions attained in dynamic desorption experiments, specific information about the actual volume of the system at each temperature and solute fugacity is not provided and an independent condition for the relation between the system volume and imposed external potentials is necessary. Ultimately, in view of the specific order

parameter considered in the NET-GP approach, a constitutive equation is required for time evolution of the volume at assigned variation of temperature, pressure and solute fugacity in the system.

7.3.2 Viscoelastic constitutive equation for volume changes in polymeric systems

In this work the attention was focused on the description of volume evolution of glassy polymers as imposed by assigned variation of temperature and pressure. Indeed, interesting results for the correlation of volume variation over time in PS as determined by isobaric temperature changes or isothermal pressure variations were obtained by Grassia and D'Amore, applying a non-linear viscoelastic model in which the relaxation time of the pure polymer is assumed to change with temperature and specific volume according to the following equation [6]:

$$\ln\left(\frac{\tau}{\tau_g}\right) = A\left[\frac{T_g V_g^{\gamma}}{T V^{\gamma}} - 1\right]^{\phi} \qquad [7.2]$$

In the above equation τ_g is the relaxation time at temperature T_g and specific volume V_g , while A, γ and ϕ are constant model parameters, whose values have been estimated by Grassia and D'Amore for PS after the analysis of both isothermal and isobaric volume relaxation experiments (see Table 7.2).

Table 7.2 Parameters for Grassia-D'Amore volume relaxation model in PS-toluene mixtures

	τ_g [s]	V_g [L/kg]	T_g [K]	A	β	γ	ϕ	χ
Polystyrene	1270	0.963	361	93.5	0.33	3.65	4.47	0.2

Scaling law in Equation [7.2] implies a simple power relation, interpreted by exponent γ , links temperature and specific volume at constant relaxation time for the case of pure polymer system. In order to apply the same model to the case of solute/polymer systems, the scaling law need to be updated to account for the presence of solute component. The latter can be actually considered as the last step in the process of building a model for the apparent solubility variation in dynamic desorption run examined in this work. To this specific aim, results for isothermal dynamic sorption experiments were analyzed to identify the volume of the system at glass transition as observed for assigned temperature. After the estimation of glass transition partial pressure/activity of the solute component (a_g in Figure 7.1), the volume per polymer mass V_g was calculated from the equilibrium density of the system as predicted by the PC-SAFT thermodynamic model. Results for V_g as function of temperature retrieved this way are reported in Table 7.3. The same data are plotted in Figure 7.3 (symbols) and compared with $V_g(T)$ relation identified by Grassia and D'Amore for pure PS volume relaxation (line). Deviations of data from PS-Toluene mixture at glass transition from extrapolation of $V_g(T)$ law for pure PS become larger when temperature decreases, parallel to the amount of solute content.

Table 7.3 glass transition solute content and volume per polymer mass from dynamic desorption experiments (desorption rate = 0.16 mbar/min)

T [°C]	W_{TOL} [g/100g PS]	V_{PS} (from EoS) [L/Kg]
20	16.9	1.114
40	13.7	1.087
50	9,9	1.051
60	7.5	1.031
70	5.3	1.013
80	3.3	0.997

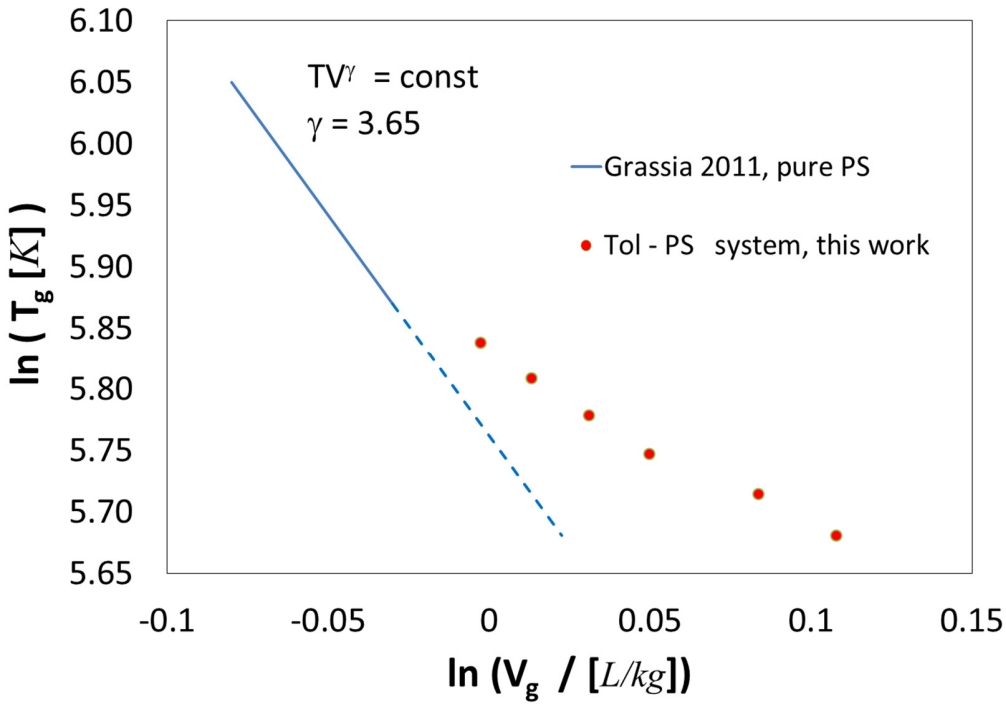

Figure 7. 2 System volume per polymer mass at glass transition from isobaric cooling experiments in pure PS (solid line) and from isothermal dynamic desorption experiment in PS-Toluene mixture

7.3.3 New scaling law for T-V relation at glass transition

In view of the above observation for the deviation of volume to polymer mass at glass transition, it is here assumed that a relation corresponding to Equation [7.2] could be used to identify glass transition point for PS-Toluene system, when $V_g(T)$ is substituted by a linear function of solute content as represented hereafter:

$$V_g(T) \rightarrow \frac{V}{m_{pol}} - V_{sol}^{*}\,\Omega \qquad [7.3]$$

The above relation can be interpreted in such a way that the effective volume available to the polymeric species in the mixture does not correspond to the entire system volume, as the presence of the solute

prevents the polymeric chain to take advantage of a part of the volume in the measure of V_{sol}* per unit mass.

Correlation of re-scaled volume per polymer mass versus temperature is shown in Figure 7.3 and results show that a reasonable agreement is obtained with data estimated for pure polystyrene, when a value of V_{TOL}* is taken as 0.54 *L/kg*.

7.4 Model for apparent solubility in isothermal dynamic desorption experiments

When the model of Grassia and D'Amore is specialized for the case of isothermal change in solute fugacity and implemented with the above scaling law for relaxation time, the following equation is obtained for the volume per polymer mass V in isothermal desorption experiments:

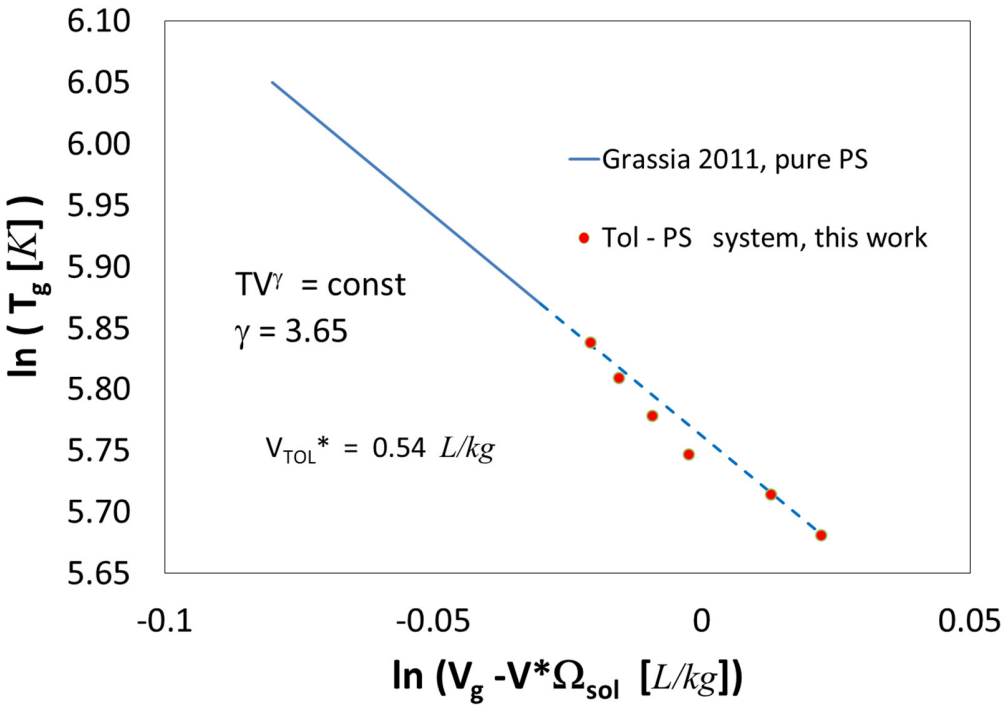

Figure 7. 3 Revised T-V scaling law for volume per polymer mass at glass transition in PS-toluene mixtures

$$V\left(T,f,m_{pol}\right) = V^{EQ}\left(T,f,m_{pol}\right)+\left(1-\chi\right)\int_{f}^{f_0}\left\{\frac{\partial V^{EQ}}{\partial f}\times \right.$$
$$\left.\exp\left[-\left(\int_{f'}^{f}\frac{1}{\left(-df/dt\right)}\frac{1}{\tau_g}\exp\left[-\frac{A}{\phi}\left[\left(\frac{T_g}{T}\left(\frac{V_g}{V/m_{pol}-V^{*}_{Tol}\Omega}\right)^{\gamma}\right)^{\phi}-1\right]\right]df''\right)^{\beta}\right]\right\}df' \qquad [7.4]$$

Where V^{EQ} is the equilibrium value for V at imposed solute fugacity f for the assigned temperature, β is a stretching factor for relaxation spectrum and χ is an adjustable parameter which interprets the fugacity effect over volume at very high relaxation times. It should be noted that the above equation holds for the case the solute fugacity is changed at assigned rate d*f*/dt , starting from an equilibrium condition at solute fugacity f_0.

The model for the apparent solubility in isothermal desorption experiments is thus obtained by coupling Equation [7.4] with the phase equilibrium conditions of NET-GP model, implemented for PC-SAFT description of equilibrium thermodynamic properties:

$$f = \frac{RT}{V/m_{sol}}\exp\left(\frac{M_{sol}}{RT}\frac{\partial\left(A^{HC}+A^{DISP}\right)}{\partial m_{sol}}\right)_{T,V,m_{pol}} \qquad [7.5]$$

Modeling description was thus attempted through the solution of Equations [7.4] and [7.5], for assigned temperature and rate of variation of solute fugactity, for the case of initial fugacity f_0 higher than the corresponding glass transition value, setting all parameters in the viscolelastic model to values Grassia and D'Amore retrieved from pure PS relaxation experiments (see Table 7.2) and allowing the only parameter χ to be used as adjustable.

Results from the modelling correlation (value of adjustable parameter χ also shown in Table 7.2) are reported in Figure 7.4 and compared with experimental values retrieved in this work from dynamic desorption experiments. Comparison show that the model allows for a rather accurate representation of apparent solubility measured in this kind of experiment in which the glassy region is explored at assigned rate of variation for solute fugacity. This is encouraging both with respect the validity of the modeling approach and for the significance of the information that can be retrieved form the novel experimental protocol for the characterization of structural relaxation properties as set up in this work.

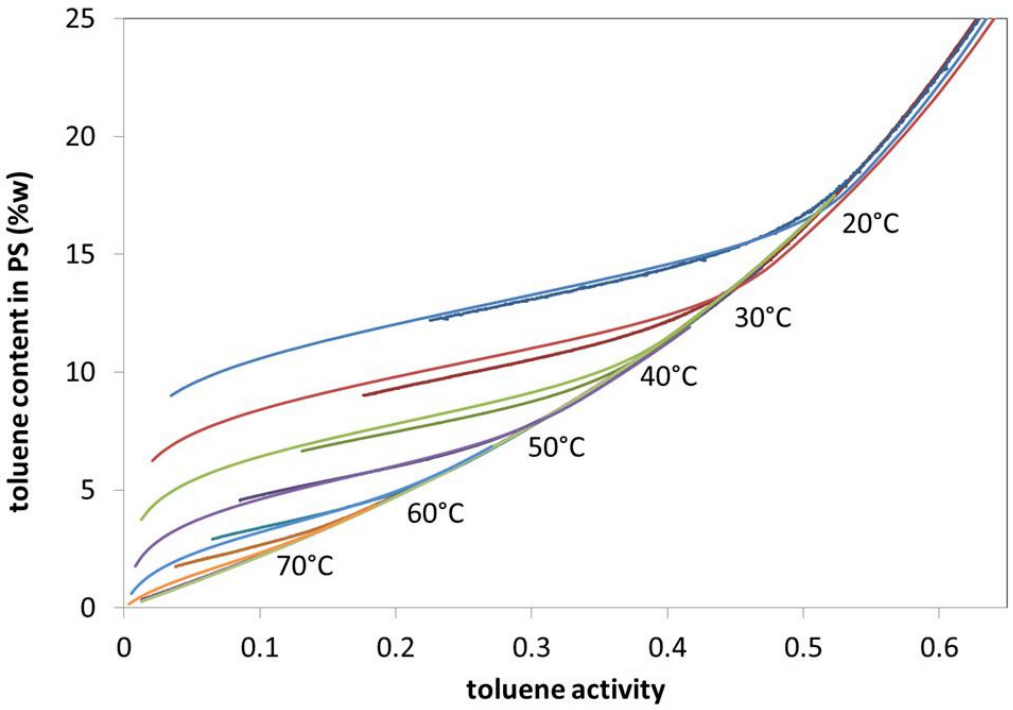

Figure 7. 4 Comparison between experimental values and modeling results for dynamic desorption isotherms at 0.16 mbar/min (modeling curves extended to lower activity values with respect to curves from experimental runs)

References

[1] Gross, J. & Sadowski, G. Perturbed-chain SAFT: An equation of state based on a perturbation theory for chain molecules. Industrial & Engineering Chemistry Research 40, 1244-1260, doi:10.1021/ie0003887 (2001).

[2] Gross, J. & Sadowski, G. Modeling polymer systems using the perturbed-chain statistical associating fluid theory equation of state. Industrial & Engineering Chemistry Research 41, 1084-1093, doi:10.1021/ie010449g (2002).

[3] Mueller, F., Naeem, S. & Sadowski, G. Toluene Sorption in Poly(styrene) and Poly(vinyl acetate) near the Glass Transition. Industrial & Engineering Chemistry Research 52, 8917-8927, doi:10.1021/ie302322t (2013).

[4] Doghieri, F. & Sarti, G. C. Nonequilibrium lattice fluids: A predictive model for the solubility in glassy polymers. Macromolecules 29, 7885-7896, doi:10.1021/ma951366c (1996).

[5] Baschetti, M. G., Doghieri, F. & Sarti, G. C. Solubility in glassy polymers: Correlations through the nonequilibrium lattice fluid model. Industrial & Engineering Chemistry Research 40, 3027-3037, doi:10.1021/ie000834q (2001).

[6] Grassia, L., Pastore Carbone, M. G. & D'Amore, A. Modeling of the Isobaric and Isothermal Glass Transitions of Polystyrene. Journal of Applied Polymer Science 122, 3752-3757, doi:10.1002/app.34789 (2011).

Chapter 8

Isochoric experiments on colloids

8.1 Introduction

The present chapter is about the experience carried out during the mandatory foreign experience provided for in the doctoral program. A 9-month period was spent at the Department of Chemical Engineering at Whitacre College of Engineering, Texas Tech University in Lubbock, Texas (USA), under the supervision of prof. Gregory B. McKenna. Professor McKenna is without any doubt one of the maximum experts in the field of glassy dynamics research, as well as nanorheology and advanced rheometry. Thanks to his amazing activity over the last 30 years, professor McKenna significantly contributed to a wide knowledge of both soft and hard matter through lots of highly cited papers. In return for his efforts he was awarded in 2009 with the Bingham Medal, the highest world award in the rheology field, just to mention one of the credits professor McKenna received in his past career that will certainly continue at extraordinary high level for long.

On the performed research activity with dr. McKenna, the focus shifted to other sorption-related phenomena than the case described in previous chapter. Great efforts were spent, in particular, on developing a novel advance experimental method for macroscopic effects related to molecular dynamics in glass-former colloids. An innovative set of experiments were performed, which required to accurately design and assemble a real measuring instrument and accessories, and everything was purposely made starting from basic key components, in order to meet specific

related to the use of colloids at desired conditions. This work was also previously presented at the 89th Annual Meeting of The Society of Rheology, held in Denver, CO, in October 2017.

8.2 Basis on glassy colloids

The first studies on colloids date back to the nineteenth century, and shall be attributed to Francesco Selmi, who had a professorship among other institutions at the University of Bologna during his prestigious career [1] [2]. He first noted the existence of substances who never show a crystalline form, and generates transparent viscous liquid mixtures when dispersed, property which distinguishes those new "pseudo-solutions" from emulsions (that were already well-known at that time). Referring to the jelly, curdled characteristic state on these new materials, in 1861 Thomas Graham christened these substances "colloids" and the "colloidal condition of matter"; his paper focused on liquid diffusion phenomena, and particularly addressed to the insight into use colloids as medium for liquid diffusion and separations, then the connection between sorption behavior and colloids goes back to early times [3].

Nowadays the term "colloid" refers to a wide range of multiphasic substances with a variety of chemical compositions, e.g. inorganic or organic molecules, but even states of matter: the early view is now outdated, and also some kinds of emulsions or suspensions are referred as colloids [4]. The main thing so different materials have in common is a highly stable and homogeneous multiphase structure. Colloids are composed by small particles (roughly 10 nm to 10 μm in size), which can be in the solid, liquid or gaseous state, dispersed in a continuum phase, which is a key-player in the colloid properties or even in the colloidal nature itself (e.g. solid particles requiring specific solvents properties to be suspended).

Referring to colloids in general terms, there are plenty of examples in our day life of these systems, as lotions, milk, sprays, cremes and salad dressings, and even in our body, as blood or advanced medical and surgical devices, all the way up to aerosols for industrial use. It is due to this large

spectrum of properties that colloids found applications in a wide range of fields, but here is focused the use in laboratories as models of matter: since the 1960's colloids have proved to be a useful tool, as analogous structures to atomic structures. More recently, glass-former colloids were involved in the glassy dynamics research field, as Pusey and Van Megen first described a colloidal glass, but especially they showed how colloids can behave like molecular glasses, on the limit of time scales long enough to ensure many collisions between colloidal particles [5] [6].

The significant relevance of this finding can be expressed as multiple advantages on using colloids instead of common glassy materials in research, as glassy colloids can be convenient in terms of an highly tunable chemical synthesis, on an ease induction of a metastable state and its persistency (allowing long observations), and above all the accessibility to long-time relaxation rates of density fluctuations: in atomic glasses this occurs at 10^{11} s^{-1}, while in colloids it can be obtained in the order of seconds [7] [8]. However, Di et al. recently raised doubts on this analogy between molecular liquids and colloids glassy states [9]. Through a classic approach based on Kovacs experiments previously discussed in Chapter 3, they demonstrated a peculiar behavior of a colloidal glass-former, in particular in its structural recovery for which the time required to reach a pseudo-stable state after a jump experiment seemed to be temperature-insensitive; hence the analogy between these quite different structures is still an open question.

Volume fraction was shown as the controlling parameter for the glass transition in colloids. As the available volume for colloidal particles decreases, the viscosity increases due to collisions between particles, up to a critical volume fraction which is the analogous of the glass transition temperature, so that is commonly referred as "glass transition volume fraction". This mechanism is easy to figure out, as suggested by Hunter and Weeks who assimilated the colloidal glass transition to an evaporating ink bucket in : ink is composed by particles in water; if water gradually evaporates, it is easy to imagine that viscosity will continuously increase until the ink is still dump but will never flows easily [4]. This mechanism was described as the ideal "hard-sphere" glass behavior, as the

colloid dynamic is the same of simulations from Alder and Wainwright in 1957 for equilibrium phase behavior of assemblies of equal-sized hard spheres [6]. However, colloids also showed a variety of solid-non-crystalline arrested states, which apparently seem unrelated each other [10]. This is due to a possible variety of interaction between particles, which for this reason can be generally classified as “attractive” or not. The ability to create long-distance interactions between each other generates a solid-like structure at volume fractions below the characteristic glass transition value, and this state can be referred as attractive gel or attractive glass, while in absence of interactions just steric interactions occur and the case is called “repulsive gel”. It is beyond the scope of this thesis to go into detail of different definitions, but this is nonetheless an ongoing discussion in the field [10] [11] [12] [13].

As volume fraction sterically regulates the state of colloidal matter, the theoretical phase transition values are independent on the specific material, in the limit of ideal hard spheres and repulsive interactions. This apparently represents a remarkable difference in glass transition temperature and volume fraction concepts. Under these assumptions, general ranges where defined for phases as reported in Figure 6.1, where reported values were obtained from simulated hard spheres [4]. Crystallization in colloids can be avoided if the sample is somewhat polydisperse, it means spheres shall have a size distribution, and this influences the precise volume fraction values [14]. Things are much more complicated for other systems as attractive particles, for which phase diagrams become much more complicated as significant shifts occur from theoretical values, and even other variables as aggregation and temperature play a fundamental role on phase transition [15].

This work focuses on glass-former colloids, and particularly on the same multiphase material used from Di et al. in a recent work on structural recovery, constituted by polymeric double-layered spheres with a hard-core and soft-shell [16]. This and other similar kinds of systems attracted considerable interest as they show a responsive character to external conditions, e.g. temperature, that could be used for multiple applications [17]. When suspended, these “smart” particles exhibit a

characteristic lower critical solution temperature (LCST), below which the external polymer phase becomes soluble in the surrounding medium, leading to a particle volume growth [18].

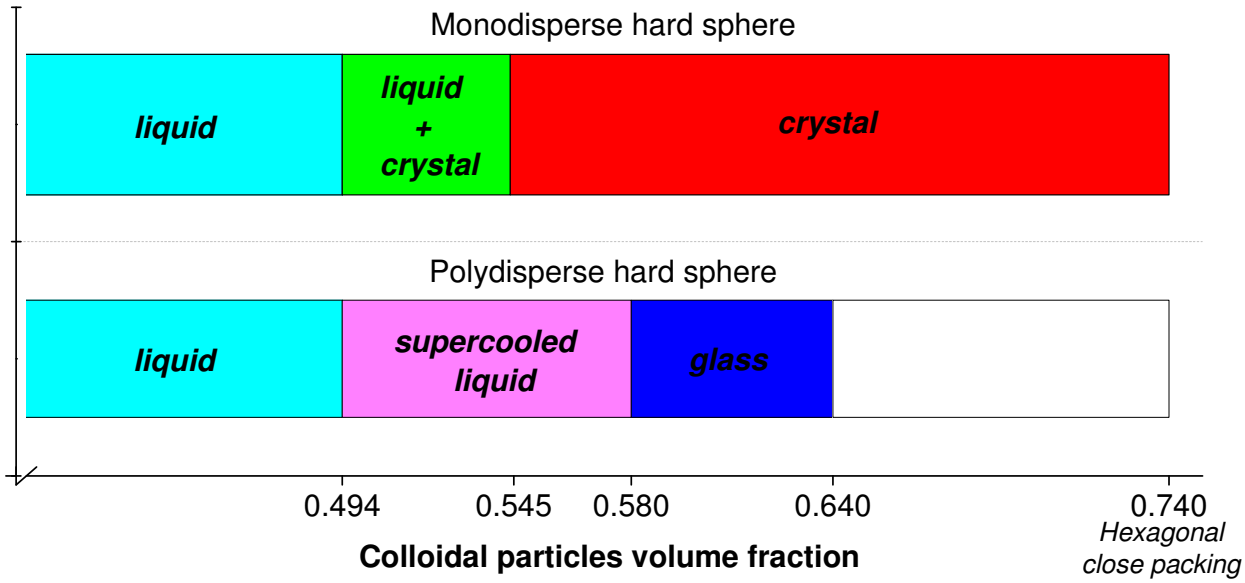

Figure 8. 1 Phase diagram of for had sphere colloids

These materials are commonly referred as "soft particle colloids", and a glassy-like state is obtained when the concentration is high enough to approach a nominal glass transition. The latter is then attributed to an increment of volume fraction on cooling. By both rheological and diffusing wave spectroscopy experiments, the relaxation time increases dramatically with apparent volume fraction, and this is consistent with the approach of a glass transition volume fraction into the sample [16].

A significative example of misgiving about thermo-responsive particles is represented by the apparent volume fraction value corresponding to the glass transition. A significative method for

volume fraction estimation over temperature T was described for thermo-sensitive particles from Di et al. as:

$$\varphi(T) = \varphi_{collapsed} \cdot \left(\frac{D(T)}{D_{collapsed}} \right)^3 \quad [6.1]$$

where D and φ represents particles diameter and volume fraction respectively, while "collapsed" subscript indicates the particle state at high temperature, when diameter takes the minimum value as the surrounding medium phase is insoluble [9].

One of the strongest motivations to the experimental activity described below regarded an unclear aspect related to apparent volume fraction calculated under specific conditions, namely high concentration colloids demonstrated values larger than 1 into the glassy state verified by experiments. This points to a structure where particles are in contact with each other, and a significant deformation can be supposed. Please refer to the following results section for clearer explanation, also supported by experimental evidences. This and other aspects were considered in the design of experiments reported in this Chapter.

8.3 Apparatus description

An ambitious challenge to achieve additional information on dynamics in glassy colloids, developing a novel experimental method specifically dedicated to soft stimuli-responsive colloidal particles, was approached during the foreign period. This project was indeed developed to find answers to trivial questions here introduced, regarding the colloidal glassy state.

Due to the absorption mechanism described for thermosensitive particles, the whole colloid volume is usually considered additive even in the glassy state, then none of volume change can theoretically be associated to the glass transition as it is caused by steric effects, in case of repulsive particles. But as the apparent volume fraction shows values larger than 1, these aspects are inconsistent to some extents, as volume shall increase for fast transitions, and then a slight decrease could be supposed due to particles softness. However, detailed measurements of the whole colloid volume behavior are not available in the knowledge of the author.

Besides the volume behavior at isobaric cooling, another relevant condition in glass transition that is actually less considered in common experimental practice is the isochoric behavior. Indeed, whilst isochoric conditions are on basis of computer simulations and few relevant industrial processes, an insidious experimental practice restricts this kind of experiments. Examples of isochoric experiments on molecular glasses were described on literature, first by Colucci et al. who demonstrated the existence of the isochoric glass transition; other analysis then followed about similarities and differences between isochoric and more common isobaric transitions [19] [20] [21]. The isochoric colloidal glass transition is yet unknown, but there are not known reasons to neglect its existence, and great benefits could be obtained from this kind of investigation, e.g. for the isochoric molecular glasses studies in case of similar behaviors, on comprehensive modelling of glass transition, or achievements on the colloidal glassy state per se.

The apparatus assembled in dr. McKenna's lab was purposely designed for isochoric experiments on colloids. Common isochoric experiments are usually performed using confining liquids, as already described in Chapter 3 for isobaric dilatometry. These methods are not readily adaptable to the study of colloid systems, an alternative measuring technique was hence adopted. The basic concept for measurement was taken from Merzlyakov, who developed a closed-volume system for thermal pressure, cure and thermally-induced stress on epoxy resins [22]. A similar instrument was here replicated and improved in order to examine the colloidal systems, viz., experimental

sensitivity and precision. A stainless steel thick-walled tube was derived from high-pressure fittings (up to 60000 PSI, HiP High Pressure Equipment Co.), and used as sample chamber, where samples shall be poured in the fluid state. Tubes were closed through opportune high-pressure connections and caps, as schematized in Figure 6.2; this volume constituted the fixed volume for isochoric tests, were a glassy state would be induced into the sample by means of temperature jump exploiting particles thermo-sensitivity, and internal pressure measured as observation variable. The cylindrical geometry was chosen in order to have an isostatic tension state, which means the solid-like specimen are subjected during tests to uniform normal forces.

The inner pressure was indirectly acquired measuring the induced tube deformation by foil strain gauges (350Ω nominally, Micro Measurements, Vishay Precision Group, Inc.) opportunely fixed in the outer tube surface with a two-component epoxy-phenolic adhesive (Micro Measurements M-Bond 610). Strain gauges are sensors capable of high-precision strain measurements, high reliability and flexibility of use. The gauge has an intrinsic resistance to electric current flow, and it is incorporated in a foil; a deformation on the support (tube) deforms the foil, and the gauge resistance changes correspondingly. Depending on the gauge material, there is a linear relationship between strain ε and resistance difference ΔR:

$$G_f = \frac{\Delta R / R}{\Delta L / L} = \frac{\Delta R / R}{\varepsilon} \qquad [6.2]$$

G_f is commonly referred as “gauge factor”, an intrinsic material property, and for common foil gauge materials like the ones used here is about 2. As tubes are produced with a well-controlled high thickness, pressure inside the tube can be evaluated from strain by stress relationship for thick-walled cylindrical geometry, then from relative resistance change from Equation [6.2]:

$$\varepsilon_{hoop} = \frac{p \cdot b^2(2-\upsilon)}{E \cdot (a^2 - b^2)} = \frac{\Delta R / R}{G_f} \qquad [6.3]$$

where E and υ are stainless steel elastic modulus and Poisson coefficient respectively, a the outer tube diameter and b the inner one [22]. Equation [6.3] refers to the hoop which is the selected strain direction for measurements (Gauges are direction-sensitive), because this is the most deformed by pressure, then maximum sensitivity reached. It is worth noting that as pressure is measured by volume deformation, tests shall be construed as pseudo-isochoric tests; however, the thick tube wall guarantees a small deviation from ideal isochoric conditions, estimated in a relative volume difference of 10^{-6} per MPa of pressure jump.

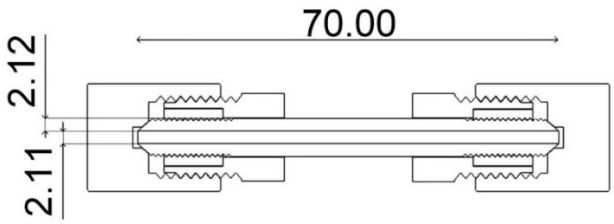

Figure 8. 2 Scheme of thick-walled tubes used as sample chamber

A resistance can be measured as voltage drop across an electrified material crossed by a well-known current, but direct absolute measurements are not sensitive. For accurate measurements of resistance difference, a dedicated circuitry was required according to the Wheatstone bridge scheme [23]. Please refer to Figure 8.3, where the circuit scheme is reported, while reading the following description. A full bridge-configuration circuit was built using two stable high-precision foil resistors (350 Ω, VPG Foil Resistors, Vishay Precision Group, Inc.) opportunely soldered on a

prototype board, and placed inside a circuit box. These resistances were connected in series, while two identical gauge series form a parallel branch.

During operations, electric tension is applied to the poles of parallel branches, and voltage is acquired between series elements: point A through foil resistors, and point B through gauges. Bridge theory requires elements and branches with identical resistance: this neglects any current flow on each element and branch, and correspondingly to a null tension between points A and B. Any resistance change in elements causes a potential difference, that can be measured to detect the resistance drop. Under reasonable approximations, e.g. small voltage, a theoretical linear relationship can be derived from Kirchhoff's circuit laws to relate the voltage measurement $\Delta V_{A\text{-}B}$ to the relative resistance difference at the measuring gauge on tube [22]. However, as this procedure assumes approximate values for gauge factor, pressure was evaluated in experiments from voltage measurements according to Equations [6.2] and [6.3] as follows:

$$p = f(a, b, E, \upsilon, R, G_f, V_{\text{ex}}, bridge) \cdot \Delta V_{A-B} = k \cdot \Delta V_{A-B} \qquad [6.4]$$

where V_{ex} is the excitation voltage, viz., tension applied to parallel branches, and k is a constant value determined by calibration: measuring tube was connected to a hydraulic circuit filled with silicone oil and equipped with manometer and pressure accumulator, and the calibration constant measured for successive pressurizations in the 0-10000 psi range.

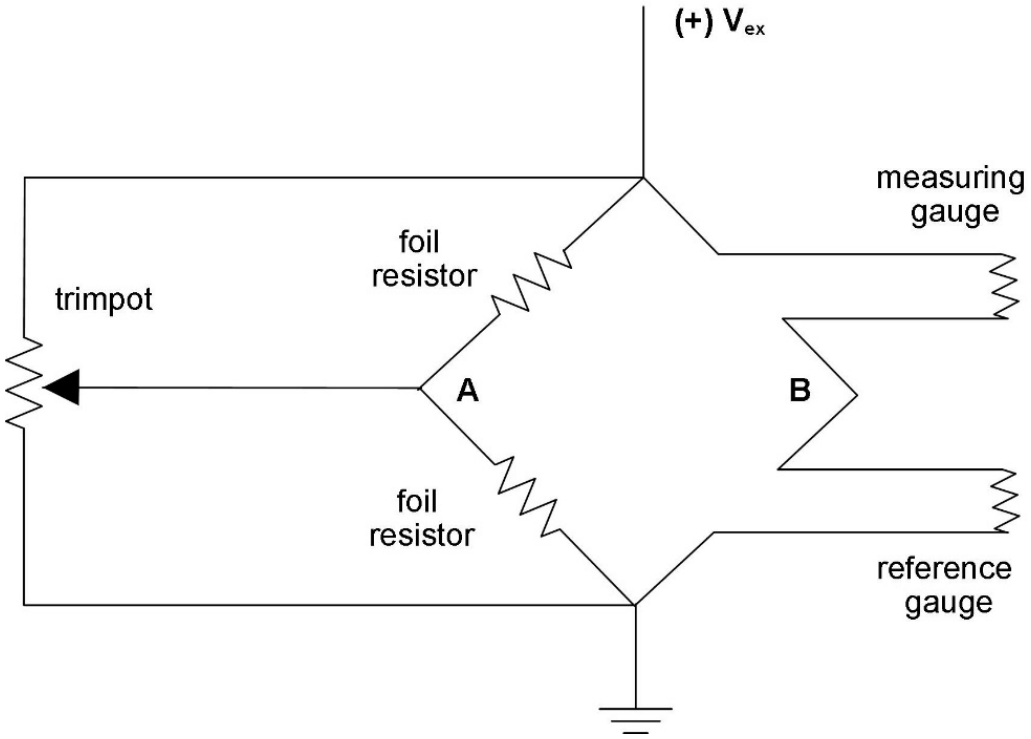

Figure 8. 3 Scheme of the applied Wheatstone bridge, in full-bridge configuration, and balancing trimpot added n the left-hand side branch.

As similar gauges are required for the right-hand side branch in Figure 8.3, an equivalent tube-gauge system was built as a reference: this completes the bridge, but it is useful as in the bridge configuration it compensates effects from variables affecting resistance other than tube strain due to pressurization, as temperature effects both on tube (due to thermal expansion effect), and on gauge; the reference system must be at relative null pressure and placed close to the measuring system.

In any case, gauges must be pre-strained to be fixed on tubes, and this operation is much complicated for films rigidity, curvature radius and small dimensions involved. This unfortunately caused small differences that required a temperature calibration anyway, to characterize the temperature effect on signal that needed to be filtered from experiments results. Since linear relationship requires an almost balanced bridge (whilst real bridges cannot reach a perfect balancing), a precision foil voltage partitioner (trimpot, 10kΩ, Vishay) was placed in parallel

configuration to the bridge, in order to balance even small differences between the bridge components.

It is also important to note on circuit assembly that, despite foil resistors are purposely produced and sold for high stability over time and temperature, a significative instability ascribed to environmental temperature oscillation was acquired within the sensitivity reached from the apparatus here described. In order to eliminate this undesired effect, the bridge circuit box was equipped with a small heater, built with axial-lead resistors (330 Ω) connected in a parallel circuit. These were driven with a 12V power source and a K-type thermocouple, placed inside the box and connected to a commercial temperature controller (Omega Engineering, Inc.), working with On/Off logic and set at 25°C; a sufficient amount of current for heat emission was provided to resistors with a Field Effect Transistor (MOSFET), which allows current flowing from power source through the heater depending on the signal from the temperature controller (see also details on MOSFETs below).

The voltage measuring system is completed by a digital lock-in amplifier. This instrument provides an oscillating signal of well-controlled frequency and amplitude, and it can be used for voltage measurement. The instrument is frequency-sensitive, it means the voltage is measured just at the same frequency generated for circuit excitation: this allowed to filter all the noise at different frequencies and remarkably increase the instrumental sensitivity. Excitation signal was set at optimized values of 1.5 V and 10 Hz; optimization accounted for maximum voltage applied to gauges to avoid Joule effects, and mid-frequency for white noise reduction and avoid deviations caused by real resistors effects [24]. The output from lock-in amplifier is, in particular, expressed as in-phase X and quadrature Y components, or in magnitude R and phase θ components in order to remove the phase dependency from voltage measurements:

$$X = V_{ex}\cos\theta \; ; \; Y = V_{ex}\sin\theta \; ; \; R = \sqrt{X^2 + Y^2} \; ; \; \theta = \arctan\left(\frac{Y}{X}\right) \qquad [6.5]$$

Amplifier and trimpot were set to have a phase angle close to 0 rad and minimize the magnitude, with a special attention to avoid sign inversion in the X and Y components, which can affect the voltage conversion. The system here described reached really-high sensitivity of 0.1 μV, or 10^{-7} in terms of strain units, and 0.2 MPa with described thick-walled tubes (in measuring operations order).

Experiments on colloids require the best control on temperature, due to the high particles sensitivity in terms of apparent volume fraction vs. temperature. To allow both high and low temperature measurements needed by most of glass-former colloids, but also to ensure a fine control in a low-thermal inertia small chamber, a Peltier thermo-electric cooler module was designed, assembled and used to both heat and cool the system (12V, 5A). A Peltier module is composed by a series of doped semi-conductors, and it is used to produce heat flux by electric current: when a voltage difference is applied through a junction of different conductors, a temperature difference is generated due to heat flux (for a reversed Seebeck effect). This causes a temperature increment in one side of the electrified junction, but also a decrement in the opposite side. Since reversing the voltage difference (electric current flow direction) the heat flux direction also results reversed, the same setup can be exploited for both cool and heat operations. A metallic plate and a heat sink were fixed to the opposite surfaces of the Peltier module with screws and thermal grease for efficient heat exchange: the metallic plate was used as tubes support and for temperature control, while the heat sink is needed for heat dispersion in the opposite side of Peltier module. A cover was tailor-made with plexiglass and insulating materials to be placed on top of tubes support, and also equipped with an electric fun took apart for reuse from a hold computer, in order to improve heat exchange inside the chamber, then avoid thermal gradients potentially caused by the exchanging surface. For the sake of

completeness, a dry air flow was forced into the chamber to improve the signal reliability; reasons for this solution will be explained in a further work, when explanatory results from ongoing experiments will be available.

For temperature control into the sample chamber, the Peltier plate was driven by a 12 V power source took apart from an old computer, a H-bridge and an accurate temperature measurement system. The H-bridge is a bridge circuit able to control an electric current flux in any direction; in this work the bridge was built by p and n-doped MOSFETs transistors (TO220 type, FQP27P06 and IRLB8721 respectively). For the sake of clarity, transistors are semiconductor devices used to switch or amplify electric currents: in the described circuit, the MOSFETs were used as digital power switches. When a positive voltage is applied to an insulated gate, the semiconductor stack constituting these devices changes the resistivity ranging between extremely high values (insulating, switch closed) to low values (switch open), depending on the doping type: in p-doped MOSFETs a positive voltage causes a depletion layer, so current cannot flows, while in n-doped ones it enhances layers conductivity, then current can flow through the transistor. Connecting transistors in an alternated configuration, represented in Figure 8.4, allows to control the voltage applied to mid-points (where the Peltier module was represented) by means of two signals, and neglects any shortening possibility due to errors. When gate signals are both “on” (or “off”), poles are at same voltage, and current cannot flows through transistors or the Peltier. On the contrary, opposite signals shall cause current crosses the module, and the flow direction is determined by the pin order.

Here an Arduino Uno board (Adafruit®) was used to control the circuit. As Arduino pins cannot provide voltage higher than 5V, and this is not enough to control the available MOSFETs at 12V, bipolar junction transistors (BJT, 2N2222 type) were added to the H-bridge circuit, and gates voltage controlled by the same 12V power supply. This configuration has a safety function, since overvoltage to Arduino pins is avoided in case of components failure. Resistance were purposely optimized to regulate voltage on the basis of components performances.

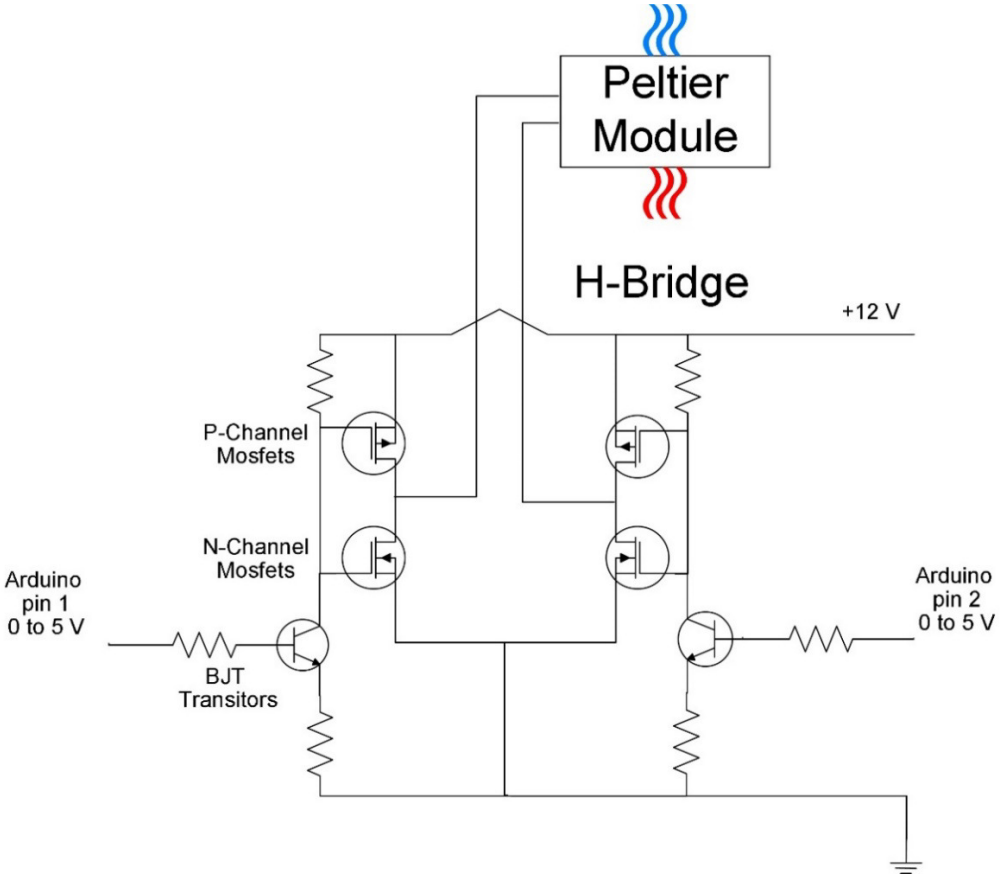

Figure 8. 4 Scheme of H-bridge used to drive the Peltier module.

The temperature measurement system was built with a K-type thermocouple put in touch with measuring tube during tests, and connected to a module board (Adafruit®) equipped with a MAX31956 thermocouple amplifier. This is a cold junction compensated amplifier, universal for non-linearities and calculation handling, with a great sensitivity up to $7.8 \cdot 10^{-3}$ K. The Arduino board was opportunely programmed for SPI communication (Serial Peripheral Interface, a standard synchronous serial communication interface) in order to acquire temperature values from the amplifier, and transmit values to a computer. A Labview® Virtual Instrument was purposely created for voltage and temperature acquisition and besides, temperature values are used to generate pin output for Peltier control with a developed code. This is based on a PID algorithm modified to

work with an on/off logic, required by the Peltier for reliability reasons: threshold values were adopted for output determination from PID error output. The whole system demonstrated an ability to control system temperature within ±0.1 K from set point.

8.4 Materials and methods

Polystyrene (PS)-core poly N-isopropylacrylamide-acrylic acid (PNIPAm-AA)-shell colloidal particles dispersed in water where used as model glass-former colloid, at a weight fraction of 16% as one of the most interesting system from the previous work: this colloid is the same described by Di et al., who adopted the synthesis process developed by Ballauff and co-workers. [16] [25] [26] In brief, sodium dodecyl sulfate (Sigma-Aldrich), NIPAm and styrene monomer were added to ultrapure water in a flask, and here heated to 80 ^{o}C. Polymerization was then induced by addition of potassium persulfate (KPS, 99%, Sigma-Aldrich) previously solved in water, and the system stirred for long time before cooling down to room temperature and filtering. PS-core particles were then purified by dialysis following a specific high-efficiency procedure. In order to form the shell, dispersed PS particles were further diluted with ultrapure water, then spiked with NIPAm, N,N-methylenebisacrylamide (99%, Sigma-Aldrich) and acrylic acid monomer (99%, Sigma Aldrich), heated to 80 ^{o}C, then again spiked with KPS aqueous solution as initiator. When reaction is over, the system was cooled down and suspension purified following a time-consuming dialysis protocol. Core-shell PS-PNIPAm-AA particles in water obtained from this recipe showed a hairy structure cross-linked to the shell, with dangling chains at the surface; this confer softness and thermo-sensitivity to particles, preserving repulsive character [27]. The particles hydrodynamic diameter was then measured on the batch by dynamic light scattering (DLS, Nanotrac® 250, Macrotrac, Inc.), equipped with water bath and thermostat (± 0.1 K). For further details, please refer to previous works.

For isochoric experiments, 16% wt. PS-PNIPAM-AA colloid was poured into the measuring tube, on which surface a strain gauge was previously fixed with high-stability epoxy-phenolic resin, and cured for long-term and temperature stability. The specific gauge-tube couple when connected to the measuring instrument required prior trimpot balancing, temperature and pressure calibrations, then was ready for filling operations. An oven set at 45 ºC was used to heat the colloid to reach a fluid behavior, then it was withdrawn with a disposable syringe without needle, and measuring tube was filled using a small rubber hose as syringe adaptor. Sample was squeezed through the back cap before tightening, then the front cap was tightened after pouring excess of sample into the dead-end, in order to avoid presence of air inside the system.

Filled tube was then connected to the measuring system, and heated up to 40 ºC and kept at constant temperature until a stable signal was reached. Attempts were made to measure the absolute starting pressure set into the tube after filling operations; however, these resulted not trustworthy within the required sensitivity (as will explained later).

A maximum temperature rate for the isochoric system set was previously determined by experiments with water. Since relaxation phenomena are avoided in water, temperature ramps where performed at constant rate (controlled by the Labview Virtual Instrument) within the 40 to 15 ^{o}C range, then temperature was kept constant to verify if stable apparent pressure values were obtained. Undesired effects were obtained from temperature ramps up to 20 ºC/h, lower rates were hence adopted for experiments on colloids as a precaution.

During experiments, after high-temperature stabilization temperature was decreased in order to impose the glass transition at well-controlled rate, as one of variable of interest for glassy dynamics. Cooling ramps were performed at 5 K/h starting from 40 ºC, well above the glass transition (about 30.1 ºC, see below), down to prescribed low temperature. Here ramps were stopped in order to acquire the pressure behavior over time in the glassy state, as commonly done in dilatometry experiments described in Chapter 3.

Other preliminary experiments were performed on another colloid for reasons of availability expediency. This was a soft particles PNIPAm-AA, a glass-former colloid made of softer particles as there is not PS core inside. On this system, tested at 7% wt. fraction, an alternative isothermal procedure was performed exploiting the same apparatus. A measuring tube was purposely modified to connect one side to a small bellow-sealed valve (Swagelok®), whose body was fixed to the tailor-made plexiglass cover so as to operate on the valve handle during measurements. The tube was charged with colloid at high pressure, using a pressure accumulator previously filled with PNIPAm-AA at fluid state. During filling operations, the system was connected to the measuring equipment to finely acquire the pressure increment, then disconnected and placed inside the thermo-regulated chamber for testing. Here a constant temperature of 25 ºC was imposed to the system, purposely chosen below the glass transition temperature measured at environmental pressure. After stabilization, the valve was used to quickly release the pressure inside the tube, by rapid opening. Valve was then manually closed as fast as possible to measure the pressure behavior at isochoric conditions. This method is targeted to demonstrate relaxation phenomena into the colloidal glassy state, as the pressure jump shall induce the glass transition as well as the temperature jump, exploiting the particles baro-sensitivity already described by several authors on literature, e.g. Lietor-Santos et al. who described the pressure effect on hydrodynamic diameter on PNIPAm [28]. This method was previously tested with water, to ensure the absence of undesired effects on the signal: results showed stable pressure values, confirming the lack of side effects.

8.5 Results

DLS results obtained for PS-PNIPAm-AA particles here used were previously published from Di et al. and reported in Figure 8.5 for the clarity sake. Here experimental data were also accompanied by colloid apparent volume fraction values calculated for the colloidal system used (16% wt.) from Equation [6.1], where a polynomial function (black line) was used for $D(T)$.

First, the thermal sensitivity of these particles is confirmed as the diameter increases with temperature decrements: diameter values start from an almost constant collapsed value of 95 nm at temperatures higher than 45 ºC, and increase up to 220 nm at 20 ºC. It is worth noting that the behavior represented by hydrodynamic diameter concerns highly diluted suspensions, because DLS measurements require extremely low concentration, while the calculated volume fraction refers to the 16% wt. colloid (high concentration). That being said, apparent volume fraction values larger than unity were obtained, referring to temperature lower than 25 ºC. This temperature range resulted below the glass transition threshold, which was measured slightly higher than 30.1 ºC in the previous work (occurring at apparent volume fraction well above the theoretical value for hard spheres from literature, $\varphi = 0.58$) [4] [16]. These high-volume fraction values express the particle volume occupied (from high dilution expansions) at each temperature value, with reference to the volume occupied by the colloid when particles are in the collapsed state (high temperature). This hence figures a complex swelling behavior when colloid is cooled down to temperatures lower than 25 ºC, and a consequent volume relaxation might occur due to particles softness.

Isochoric tests were performed on the colloid at same conditions assumed for volume fraction calculation; for the sake of brevity here are reported just most notable achievements.

In Figure 8.6 are reported experiments carried out at 5 K /h constant cooling rate starting from 40 ºC. In particular, the dark-blue (greatest slope) curve refers to a test performed on PS-PNIPAm-AA filled into the tube following the procedure previously described. The same pseudo-linear constant decrement with an average slope of 0.49 MPa/K was obtained even for test repeated to lower temperatures down to 20 ºC, confirming good reproducibility, and this resulted lower than the thermal pressure behavior obtained from the dispersant phase alone, water, when tested at same conditions (dashed line). This demonstrates colloidal particles reduce the overall thermal behavior when dispersed, and this can be ascribed to particles softness.

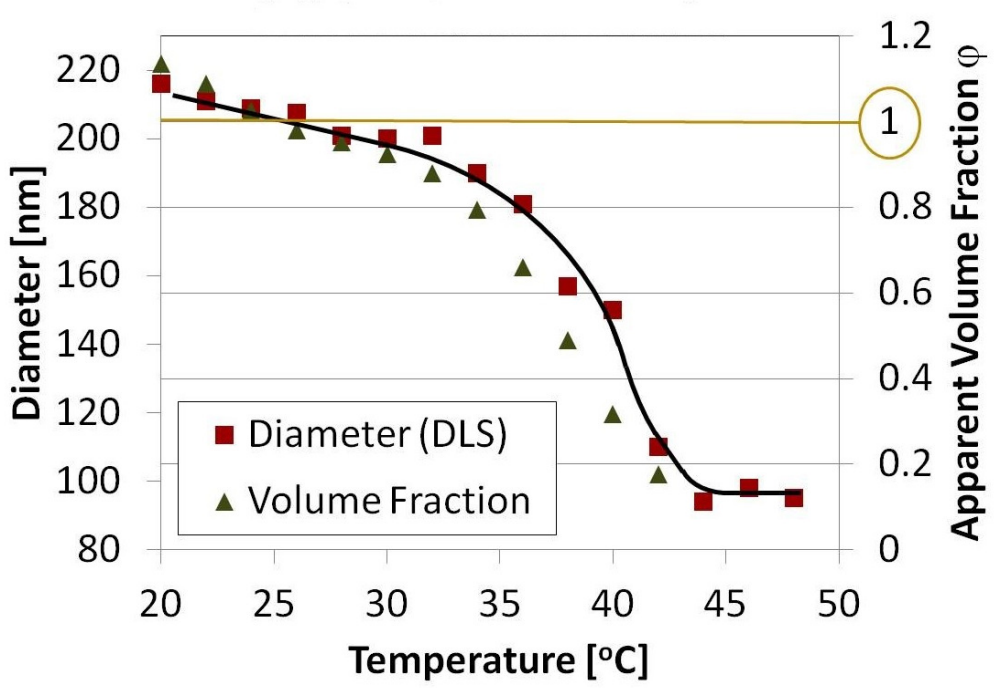

Figure 8. 5 PS-PNIPAm-AA particles hydrodynamic diameter acquired by DLS over temperature, and apparent volume fraction values for the colloid here used in isochoric temperature ramp experiments. Black line represents the polynomial function implemented in Equation [6.1] for apparent volume fraction of 16% wt. dispersion (values from [16])

Furthermore, curves seemed not revealing differences into the thermal-pressure behavior at temperatures which showed a glassy behavior in the previous work [16]. This might be interpreted as prove of opposite scenarios, as it could result from a peculiar behavior of the colloidal glassy state, which is much different from the isochoric molecular glassy behavior described by Colucci et al., or alternatively the absence of transition in the conditions range tested: further investigations were then attempted for a better explanation [19].

As glass transition could be inhibited from particles baro-sensitivity effects, tube pressure was reduced through the following procedure. After tests, the same filled tube was disconnected from measurement system and heated inside the oven previously used for filling operations. Then the top cap was unscrewed and sample excess in the dead-end regulated by a clean needle before closing again for further tests: absence of air inside the volume cannot be guaranteed, but certainly this

procedure reduces the starting pressure of tests. Because apparent pressure measured after connection slightly increased compared to previous value, it was concluded that filling operations much affected the signal reproducibility within small values measured, then estimation of pressure inside the tube were avoided and results were consequently expressed in terms of pressure difference.

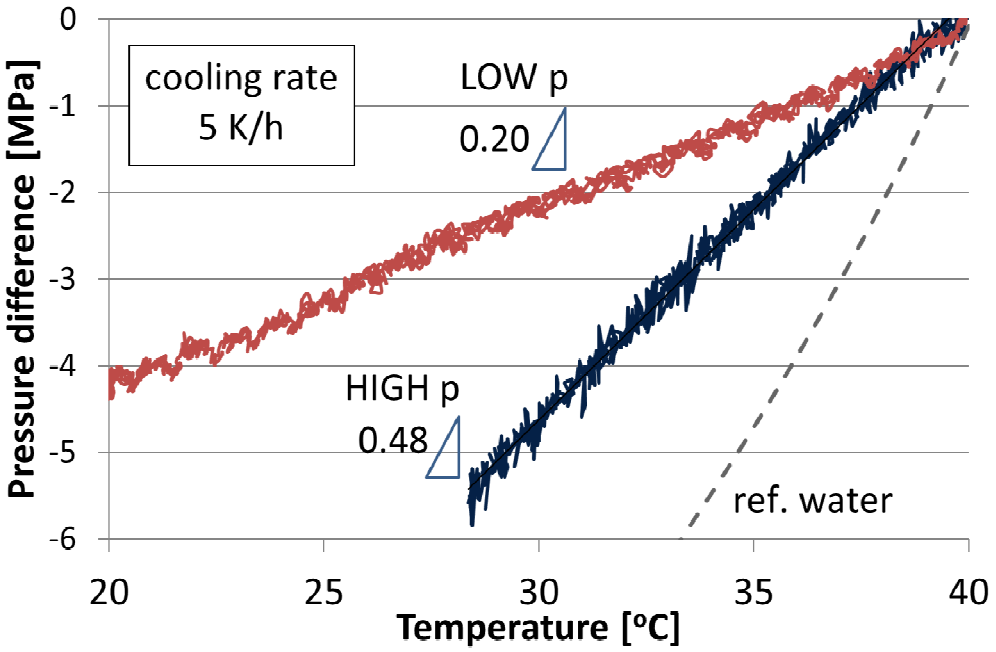

Figure 8. 6 Thermal pressure behavior of PS-PNIPAm-AA colloid at different pressures measured at 5 K/h cooling rate, and compared with water.

Reproducible results obtained after the described depressurizing procedure are represented by the red curve (lowest slope) in Figure 8.6. Lower pressure value into the tube generated a qualitatively similar pseudo-linear behavior, confirmed down to 20 ºC, but the slope significantly decreased with respect to values obtained al lower pressure. It should be observed that presence of air into the system is excludes, because a significative pressure decrement was observed: air must neglect any measurement because its high compressibility). The system showed hence an improved softness conferred by lower pressure values, confirming the baro-sensitive behavior of this kind of colloids. In the same way, systems like the one here tested could be exploited for aqueous dispersions with

reduced thermal pressure behavior, or even reduced thermal expansion effect if the same regulating mechanism is confirmed in isobaric conditions, and so forth.

The need of a deeper knowledge on the joint temperature-pressure effect was here demonstrated, to properly assess the apparent volume fraction reached during isochoric experiments. Nevertheless, values larger than 1 are not excluded, and unfortunately these experiments were not fully explanatory for colloidal glassy state due to not allowable pressure measurements. The system here used then needs modification for better determinations for absolute pressure measurements; these were never implemented in the framework of this thesis for time constrains.

Alternative isothermal experiments described in the previous section were also carried out. An alternative measuring tube was equipped with a manual valve to stimulate glass transition by pressure jump, and results from PNIPAm-AA at 25 ºC are reported in Figure 8.7. Data were acquired after a pressure jump from 35 MPa to atmospheric pressure, induced by quick depression using the manual valve; as tube was filled when connected to the measuring instrument, pressure values here refer to the real pressure inside the tube, and time is referred to the valve closure. For the sake of completeness, early point were cut as strong disturbs into the signal were introduced for manual operations required. It is worth noting that the same protocol was applied to water, obtaining a constant signal at null relative pressure, as it could be expected.

On colloid, a fast pressure increment was obtained immediately after valve closure, and this seemed released within $4 \cdot 10^5$ s. It is worth speculating a bit this is what could be expected from a swelling system, which relaxes the internal stress in a finite relaxation time. This can prove the glassy state induced after pressure jump at isothermal conditions, since the colloid easy flowed into the tube during filling operations under pressure, and an aging dynamic was showed at isochoric conditions after transition. However, more robust protocol shall be followed to erase uncertainty on fast dynamics and instability on signal from manual operations here performed in this preliminary

experiment. Better results achievements could open to deep investigations on variables effects on this relaxation process.

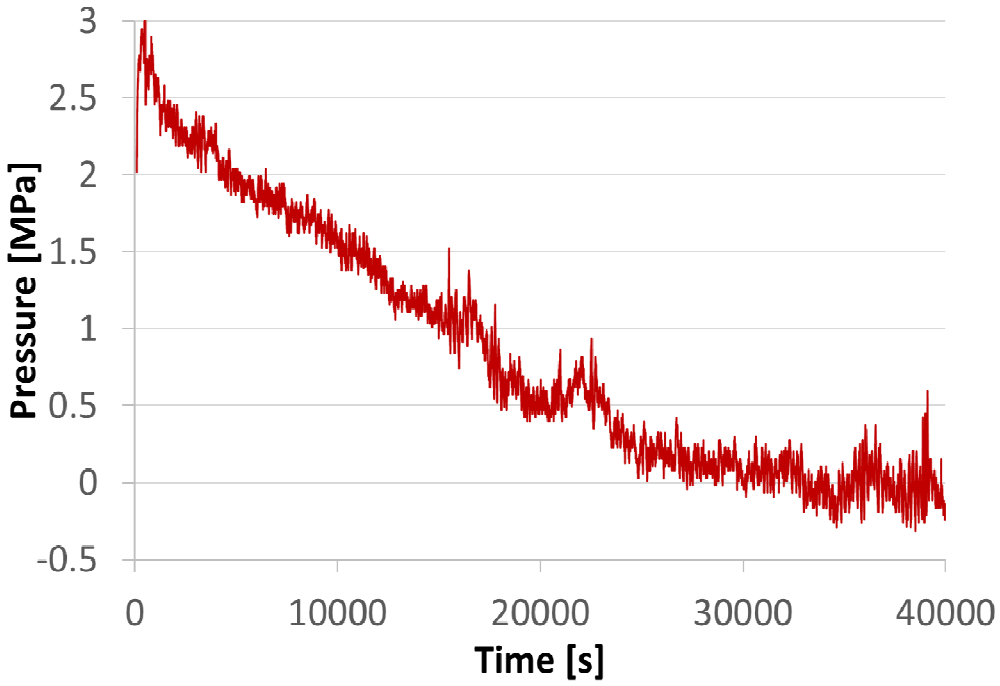

Figure 8. 7 Results from isochoric measurements on PNIPAm-AA particles in water, at 25 °C after pressure jump down to atmospheric pressure

References

[1] Annuario della Regia Università di Bologna – Anno Scolastico 1867-1868, Bologna, p. 9

[2] Guareschi, I. *Francesco Selmi e la sua opera scientifica / memoria del socio Icilio Guareschi*. (V. Bona, 1911).

[3] Graham, T. Liquid diffusion applied to analysis. *Philosophical transactions of the Royal Society of London* **151**, 183-224 (1861).

[4] Hunter, G. L. & Weeks, E. R. The physics of the colloidal glass transition. *Reports on Progress in Physics* **75**, 30, doi:10.1088/0034-4885/75/6/066501 (2012).

[5] Pusey, P. N. & van Megen, W. Phase-behavior of concentrated suspensions of nearly hard colloidal spheres. *Nature* **320**, 340-342, doi:10.1038/320340a0 (1986).

[6] Pusey, P. N. Colloidal glasses. *Journal of Physics-Condensed Matter* **20**, 6, doi:10.1088/0953-8984/20/49/494202 (2008).

[7] Sciortino, F. & Tartaglia, P. Glassy colloidal systems. *Advances in Physics***54**, 471-524, doi:10.1080/00018730500414570 (2005).

[8] van Megen, W. & Pusey, P. N. Dynamic light-scattering study of the glass-transition in a colloidal suspension. *Physical Review A* **43**, 5429-5441, doi:10.1103/PhysRevA.43.5429 (1991).

[9] Di, X. J. *et al.* Signatures of Structural Recovery in Colloidal Glasses. *Physical Review Letters* **106**, 4, doi:10.1103/PhysRevLett.106.095701 (2011).

[10] Dawson, K. A. The glass paradigm for colloidal glasses, gels, and other arrested states driven by attractive interactions. *Current Opinion in Colloid & Interface Science* **7**, 218-227, doi:10.1016/s1359-0294(02)00052-3 (2002).

[11] Bonn, D., Kellay, H., Tanaka, H., Wegdam, G. & Meunier, J. Laponite: What is the difference between a gel and a glass? *Langmuir* **15**, 7534-7536, doi:10.1021/la990167+ (1999).

[12] Tanaka, H., Meunier, J. & Bonn, D. Nonergodic states of charged colloidal suspensions: Repulsive and attractive glasses and gels. *Physical Review E* **69**, 6, doi:10.1103/PhysRevE.69.031404 (2004).

[13] Royall, C. P., Williams, S. R. & Tanaka, H. The nature of the glass and gel transitions in sticky spheres. *arXiv preprint arXiv:1409.5469* (2014).

[14] Bolhuis, P. G. & Kofke, D. A. Monte carlo study of freezing of polydisperse hard spheres. *Physical Review E* **54**, 634-643, doi:10.1103/PhysRevE.54.634 (1996).

[15] Trappe, V., Prasad, V., Cipelletti, L., Segre, P. N. & Weitz, D. A. Jamming phase diagram for attractive particles. *Nature* **411**, 772-775, doi:10.1038/35081021 (2001).

[16] Di, X. J., Peng, X. G. & McKenna, G. B. Dynamics of a thermo-responsive microgel colloid near to the glass transition. *Journal of Chemical Physics***140**, 9, doi:10.1063/1.4863327 (2014).

[17] Nayak, S. & Lyon, L. A. Soft nanotechnology with soft nanoparticles. *Angewandte Chemie-International Edition* **44**, 7686-7708, doi:10.1002/anie.200501321 (2005).

[18] Ballauff, M. & Lu, Y. "Smart" nanoparticles: Preparation, characterization and applications. *Polymer* **48**, 1815-1823, doi:10.1016/j.polymer.2007.02.004 (2007).

[19] Colucci, D. M. *et al.* Isochoric and isobaric glass formation: Similarities and differences. *Journal of Polymer Science Part B-Polymer Physics* **35**, 1561-

1573, doi:10.1002/(sici)1099-0488(19970730)35:10<1561::aid-polb8>3.0.co;2-u (1997).

[20] Yang, L., Srolovitz, D. J. & Yee, A. F. Molecular dynamics study of isobaric and isochoric glass transitions in a model amorphous polymer. *The Journal of chemical physics* **110**, 7058-7069 (1999).

[21] McKenna, G. B. Mechanical rejuvenation in polymer glasses: fact or fallacy? *Journal of Physics-Condensed Matter* **15**, S737-S763, doi:10.1088/0953-8984/15/11/301 (2003).

[22] Merzlyakov, M., Simon, S. L. & McKenna, G. B. Instrumented thick-walled tube method for measuring thermal pressure in fluids and isotropic stresses in thermosetting resins. *Review of Scientific Instruments* **76**, 7, doi:10.1063/1.1930069 (2005).

[23] Hoffmann, K. *Applying the wheatstone bridge circuit*. (HBM, 1974).

[24] Park, S. & Lee, Y. J. Precision Electrical Measurement Experiment Using a Lock-in Amplifier that is Suitable for Science and Engineering Undergraduates. *New Physics: Sae Mulli* **65**, 328-332, doi:10.3938/NPSM.65.328 (2015).

[25] Dingenouts, N., Norhausen, C. & Ballauff, M. Observation of the volume transition in thermosensitive core-shell latex particles by small-angle X-ray scattering. *Macromolecules* **31**, 8912-8917, doi:10.1021/ma980985t (1998).

[26] Kim, J. H. & Ballauff, M. The volume transition in thermosensitive core-shell latex particles containing charged groups. *Colloid and Polymer Science***277**, 1210-1214, doi:10.1007/s003960050512 (1999).

[27] Crassous, J. J. *et al.* Direct imaging of temperature-sensitive core-shell latexes by cryogenic transmission electron microscopy. *Colloid and Polymer Science* **286**, 805-812, doi:10.1007/s00396-008-1873-3 (2008).

[28] Lietor-Santos, J.-J. et al. Deswelling microgel particles using hydrostatic pressure. Macromolecules 42, 6225-6230 (2009).

Chapter 9

Critical thesis review

The hope on writing a PhD thesis is undoubtedly to transmit the amount of work carried out over years with passion and sometimes even sacrifice, but at the same time to keep professional detachment in order to report data and analysis objectively. For this reason, it is worth noting there is so much to do for a good comprehension of glassy dynamics showed, or just a complete development of what the basic idea beyond this project are capable of. And then, this section would summarize achievements, but also underline weak points and further improvement.

A major result from this work is the set-up of a new experimental protocol to perform vapour sorption/desorption experiments in glassy polymers in which boundary conditions are changed at prescribed and controllable rate, while the specimen sorbs/desorbs the mobile component under negligible concentration gradients. This ultimately allows for a characterization of sorption kinetics as dictated by structural relaxation mechanism only, which in turn may be solicited at different characteristic frequencies, by changing the rate of variation in time of boundary conditions.

Data from the new characterization procedure have been collected for the case of PS-toluene system in the form of different series of sorption (isothermal) and desorption curves (isothermal, isobaric and iso-activity) across the glass transition point. Information for glass transition point and for ratio between characteristic relaxation times at different conditions can be retrieved from the direct analysis of output in experiments performed at different rate of change of controlled variable. Further analysis of data can be performed to characterize the spectrum of structural relaxation and determine its dependence on temperature, volume and concentration, for which a relaxation model need to be considered.

Good interpretation of desorption curves from dynamic-ramp experiments were obtained through the use of the model by Grassia and D'Amore for volume relaxation as it was set-up for the interpretation of pure polymer species behaviour. Relevant achievements are the successful modelling of multiple rate curves, and predictions on the solvent induced transition obtained at different experimental temperatures. However, great efforts shall be spent in modelling sorption curves obtained, with a special mention to results from sorption runs from glassy state. This kind of problem is still waiting for a satisfactory modelling approach, although some attempts were already performed following ideas similar to those explained in Chapter 8.

Dynamic sorption experiments expressed useful output and various advantages with respect to classic protocols, and the belief of cross-analysis with results from dry tests was successfully supported. Other experiments are nevertheless fundamentals in order to strongly promote this idea, as example exploiting the technique with other materials, penetrants, or polymers with slightly different structural properties. In addition to this, significant unexpected behaviours were observed, e.g. Non-equilibrium state above the glass transition, and volumetric response from same dynamic protocols could bring major benefits to obtained results: both these elements requires further investigations and additional equipment to be developed.

On isochoric experiments, results can represent to some extent revolutionary concepts on peculiar behavior of responsive particles and glass-former colloids. As a matter of facts, results from isochoric experiments demonstrated peculiar behaviours of smart particle systems, as baro-sensitivity and the thermal-pressure behavior. These specific features might also be suitable even for applied research, viz. applications exploiting particles for pressure/volume self-equilibrating systems. However, some equipment improvements are required for more robust data, that in the period spent were not implemented for time constrains. In the context of isochoric experiments on colloids, a student has been trained for further development of the project, as part of another ongoing thesis work.

Bibliography

Akay, M. Aspects of dynamic mechanical analysis in polymeric composites. *Composites Science and Technology* **47**, 419-423, doi:10.1016/0266-3538(93)90010-e (1993).

Alcoutlabi, M., Banda, L., Kollengodu-Subramanian, S., Zhao, J. & McKenna, G. B. Environmental Effects on the Structural Recovery Responses of an Epoxy Resin after Carbon Dioxide Pressure Jumps: Intrinsic Isopiestics, Asymmetry of Approach, and Memory Effect. *Macromolecules* **44**, 3828-3839, doi:10.1021/ma1027577 (2011).

Alcoutlabi, M., Briatico-Vangosa, F. & McKenna, G. B. Effect of chemical activity jumps on the viscoelastic behavior of an epoxy resin: Physical aging response in carbon dioxide pressure jumps. *Journal of Polymer Science Part B-Polymer Physics* **40**, 2050-2064, doi:10.1002/polb.10263 (2002).

Alfrey, T., Wiederhorn, N., Stein, R. & Tobolsky, A. Some studies of plasticized polyvinyl chloride. *Journal of Colloid Science* **4**, 211-227 (1949).

Ballauff, M. & Lu, Y. "Smart" nanoparticles: Preparation, characterization and applications. *Polymer* **48**, 1815-1823, doi:10.1016/j.polymer.2007.02.004 (2007).

Baschetti, M. G., Doghieri, F. & Sarti, G. C. Solubility in glassy polymers: Correlations through the nonequilibrium lattice fluid model. *Industrial & Engineering Chemistry Research* **40**, 3027-3037, doi:10.1021/ie000834q (2001).

Bauer, C. *et al.* Capacitive scanning dilatometry and frequency-dependent thermal expansion of polymer films. *Physical Review E* **61**, 1755-1764, doi:10.1103/PhysRevE.61.1755 (2000).

Bawn, C., Freeman, R. & Kamaliddin, A. High polymer solutions. Part I.—Vapour pressure of polystyrene solutions. *Transactions of the Faraday Society* **46**, 677-684 (1950).

Berens, A. & Hopfenberg, H. Diffusion and relaxation in glassy polymer powders: 2. Separation of diffusion and relaxation parameters. *Polymer* **19**, 489-496 (1978).

Berens, A. & Hopfenberg, H. Induction and measurement of glassy - state relaxations by vapor sorption techniques. *Journal of Polymer Science Part B: Polymer Physics* **17**, 1757-1770 (1979).

Bodiguel, H. & Fretigny, C. Viscoelastic properties of ultrathin polystyrene films. *Macromolecules* **40**, 7291-7298, doi:10.1021/ma070460d (2007).

Bolhuis, P. G. & Kofke, D. A. Monte carlo study of freezing of polydisperse hard spheres. *Physical Review E* **54**, 634-643, doi:10.1103/PhysRevE.54.634 (1996).

Bonavoglia, B., Storti, G., Morbidelli, M., Rajendran, A. & Mazzotti, M. Sorption and swelling of semicrystalline polymers in supercritical CO2. *Journal of Polymer Science Part B: Polymer Physics* **44**, 1531-1546 (2006).

Bonn, D., Kellay, H., Tanaka, H., Wegdam, G. & Meunier, J. Laponite: What is the difference between a gel and a glass? *Langmuir* **15**, 7534-7536, doi:10.1021/la990167+ (1999).

Bos, A., Punt, I. G. M., Wessling, M. & Strathmann, H. CO2-induced plasticization phenomena in glassy polymers. *Journal of Membrane Science* **155**, 67-78, doi:10.1016/s0376-7388(98)00299-3 (1999).

Boyer, R. & Spencer, R. Thermal Expansion and Second - Order Transition Effects in High Polymers: Part I. Experimental Results. *Journal of Applied Physics* **15**, 398-405 (1944).

Briatico-Vangosa, F. & Rink, M. Dilatometric behavior and glass transition in a styrene-acrylonitrile copolymer. *Journal of Polymer Science Part B-Polymer Physics* **43**, 1904-1913, doi:10.1002/polb.20476 (2005).

Bruning, R. & Samwer, K. Glass-transition on long-time scales. *Physical Review B* **46**, 11318-11322, doi:10.1103/PhysRevB.46.11318 (1992).

Cahn, L. Electromagnetic balance. United State patent (1965).

Camera-Roda, G. & Sarti, G. C. Mass-transport with relaxation in polymers. *Aiche Journal* **36**, 851-860, doi:10.1002/aic.690360606 (1990).

Colucci, D. M. *et al.* Isochoric and isobaric glass formation: Similarities and differences. *Journal of Polymer Science Part B-Polymer Physics* **35**, 1561-1573, doi:10.1002/(sici)1099-0488(19970730)35:10<1561::aid-polb8>3.0.co;2-u (1997).

Condo, P. D. & Johnston, K. P. Retrograde vitrification of polymers with compressed fluid diluents - experimental confirmation. *Macromolecules* **25**, 6730-6732, doi:10.1021/ma00050a057 (1992).

Condo, P. D., Sanchez, I. C., Panayiotou, C. G. & Johnston, K. P. Glass-transition behavior including retrograde vitrification of polymers with compressed fluid diluents. *Macromolecules* **25**, 6119-6127, doi:10.1021/ma00049a007 (1992).

Crank, J. *The mathematics of diffusion*. (Oxford university press, 1979).

Crassous, J. J. *et al.* Direct imaging of temperature-sensitive core-shell latexes by cryogenic transmission electron microscopy. *Colloid and Polymer Science* **286**, 805-812, doi:10.1007/s00396-008-1873-3 (2008).

Dawson, K. A. The glass paradigm for colloidal glasses, gels, and other arrested states driven by attractive interactions. *Current Opinion in Colloid & Interface Science* **7**, 218-227, doi:10.1016/s1359-0294(02)00052-3 (2002).

Debenedetti, P. G. & Stillinger, F. H. Supercooled liquids and the glass transition. *Nature* **410**, 259-267, doi:10.1038/35065704 (2001).

Di, X. J., Peng, X. G. & McKenna, G. B. Dynamics of a thermo-responsive microgel colloid near to the glass transition. *Journal of Chemical Physics* **140**, 9, doi:10.1063/1.4863327 (2014).

Di, X. J. *et al.* Signatures of Structural Recovery in Colloidal Glasses. *Physical Review Letters* **106**, 4, doi:10.1103/PhysRevLett.106.095701 (2011).

Dingenouts, N., Norhausen, C. & Ballauff, M. Observation of the volume transition in thermosensitive core-shell latex particles by small-angle X-ray scattering. *Macromolecules* **31**, 8912-8917, doi:10.1021/ma980985t (1998).

Doghieri, F. & Sarti, G. C. Nonequilibrium lattice fluids: A predictive model for the solubility in glassy polymers. *Macromolecules* **29**, 7885-7896, doi:10.1021/ma951366c (1996).

Domack, A. & Johannsmann, D. Plastification during sorption of polymeric thin films: a quartz resonator study. *Journal of applied physics* **80**, 2599-2604 (1996).

Doumenc, F., Bodiguel, H. & Guerrier, B. Physical aging of glassy PMMA/toluene films: Influence of drying/swelling history. *European Physical Journal E* **27**, 3-11, doi:10.1140/epje/i2008-10345-0 (2008).

Ferry, J. D. *Viscoelastic properties of polymers*. (John Wiley & Sons, 1980).

Fetters, L. J., Hadjichristidis, N., Lindner, J. S. & Mays, J. W. Molecular-weight dependence of hydrodynamic and thermodynamic properties for well-defined linear-polymers in solution. *Journal of Physical and Chemical Reference Data* **23**, 619-640 (1994).

Filler, R. L. & Vig, J. R. Long-term aging of oscillators. *Ieee Transactions on Ultrasonics Ferroelectrics and Frequency Control* **40**, 387-394, doi:10.1109/58.251287 (1993).

Frenkel, Y. I. Kinetic theory of liquids. (1955).

Frisch, H. Sorption and transport in glassy polymers–a review. *Polymer Engineering & Science* **20**, 2-13 (1980).

Fukao, K. & Miyamoto, Y. Slow dynamics near glass transitions in thin polymer films. *Physical Review E* **64**, 9, doi:10.1103/PhysRevE.64.011803 (2001).

Gast, T. Development of the magnetic suspension balance. *Measurement* **4**, 53-62 (1986).

Graham, T. Liquid diffusion applied to analysis. *Philosophical transactions of the Royal Society of London* **151**, 183-224 (1861).

Grassia, L., Pastore Carbone, M. G. & D'Amore, A. Modeling of the Isobaric and Isothermal Glass Transitions of Polystyrene. *Journal of Applied Polymer Science* **122**, 3752-3757, doi:10.1002/app.34789 (2011).

Grassia, L., Pastore Carbone, M. G., Mensitieri, G. & D'Amore, A. Modeling of

density evolution of PLA under ultra-high pressure/temperature histories. *Polymer* **52**, 4011-4020, doi:10.1016/j.polymer.2011.06.058 (2011).

Greiner, R. & Schwarzl, F. Thermal Contraction and Volume Relaxation of Amorphous Polymers. *Rheologica Acta* **23**, 378-395, doi:10.1007/BF01329190 (1984).

Gross, J. & Sadowski, G. Perturbed-chain SAFT: An equation of state based on a perturbation theory for chain molecules. *Industrial & Engineering Chemistry Research* **40**, 1244-1260, doi:10.1021/ie0003887 (2001).

Gross, J. & Sadowski, G. Modeling polymer systems using the perturbed-chain statistical associating fluid theory equation of state. *Industrial & Engineering Chemistry Research* **41**, 1084-1093, doi:10.1021/ie010449g (2002).

Guareschi , I. *Francesco Selmi e la sua opera scientifica / memoria del socio Icilio Guareschi*. (V. Bona, 1911).

Han, W. & McKenna, G. in *Proceedings of the SPE ANTEC.* 1822.

Hoffmann, K. *Applying the wheatstone bridge circuit*. (HBM, 1974).

Hunter, G. L. & Weeks, E. R. The physics of the colloidal glass transition. *Reports on Progress in Physics* **75**, 30, doi:10.1088/0034-4885/75/6/066501 (2012).

Jacques, C., Hopfenberg, H. & Stannett, V. in *Permeability of Plastic Films and Coatings* 73-86 (Springer, 1974).

Jean, Y. C. *et al.* Glass transition of polystyrene near the surface studied by slow-positron-annihilation spectroscopy. *Physical Review B* **56**, R8459-R8462 (1997).

Jiang, Z., Imrie, C. T. & Hutchinson, J. M. An introduction to temperature modulated differential scanning calorimetry (TMDSC): a relatively non-mathematical approach. *Thermochimica Acta* **387**, 75-93, doi:10.1016/s0040-6031(01)00829-2 (2002).

Kauzmann, W. The nature of the glassy state and the behavior of liquids at low temperatures. *Chemical Reviews* **43**, 219-256 (1948).

Keddie, J. L., Jones, R. A. L. & Cory, R. A. Size- dependent depression of the glass-transition temperature in polymer-films. *Europhysics Letters* **27**, 59-64, doi:10.1209/0295-5075/27/1/011 (1994).

Kim, D. J., Caruthers, J. M. & Peppas, N. A. Penetrant transport in cross-linked polystyrene. *Macromolecules* **26**, 1841-1847, doi:10.1021/ma00060a008 (1993).

Kim, J. H. & Ballauff, M. The volume transition in thermosensitive core-shell latex particles containing charged groups. *Colloid and Polymer Science* **277**, 1210-1214, doi:10.1007/s003960050512 (1999).

Koh, Y. P., McKenna, G. B. & Simon, S. L. Calorimetric glass transition temperature and absolute heat capacity of polystyrene ultrathin films. *Journal of Polymer Science Part B-Polymer Physics* **44**, 3518-3527,

doi:10.1002/polb.21021 (2006).

Koh, Y. P. & Simon, S. L. Enthalpy Recovery of Polystyrene: Does a Long-Term Aging Plateau Exist? *Macromolecules* **46**, 5815-5821, doi:10.1021/ma40112361 (2013).

Koros, W. J. & Paul, D. Design considerations for measurement of gas sorption in polymers by pressure decay. *Journal of Polymer Science Part B: Polymer Physics* **14**, 1903-1907 (1976).

Kovacs, A. Applicability of the free volume concept on relaxation phenomena in the glass transition range. *Rheologica Acta* **5**, 262-269 (1966).

Kovacs, A., Stratton, R. A. & Ferry, J. D. Dynamic mechanical properties of polyvinyl acetate in shear in the glass transition temperature range. *The Journal of Physical Chemistry* **67**, 152-161 (1963).

Kovacs, A. J. La contraction isotherme du volume des polymères amorphes. *Journal of Polymer Science Part A: Polymer Chemistry* **30**, 131-147 (1958).

Kovacs, A. J. in *Fortschritte der hochpolymeren-forschung* 394-507 (Springer, 1964).

Kruger, K. M. & Sadowski, G. Fickian and non-Fickian sorption kinetics of toluene in glassy polystyrene. *Macromolecules* **38**, 8408-8417, doi:10.1021/ma050353o (2005).

Li, G., Lee-Sullivan, P. & Thring, R. W. Determination of activation energy for glass transition of an epoxy adhesive using dynamic mechanical analysis. *Journal of Thermal Analysis and Calorimetry* **60**, 377-390, doi:10.1023/a:1010120921582 (2000).

Lietor-Santos, J.-J. *et al.* Deswelling microgel particles using hydrostatic pressure. *Macromolecules* **42**, 6225-6230 (2009).

Lunkenheimer, P., Schneider, U., Brand, R. & Loidl, A. Glassy dynamics. *Contemporary Physics* **41**, 15-36, doi:10.1080/001075100181259 (2000).

Madkour, S. *et al.* Decoupling of Dynamic and Thermal Glass Transition in Thin Films of a PVME/PS Blend. *Acs Macro Letters* **6**, 1156-1161, doi:10.1021/acsmacrolett.7b00625 (2017).

Mathot, V. *et al.* The Flash DSC 1, a power compensation twin-type, chip-based fast scanning calorimeter (FSC): First findings on polymers. *Thermochimica Acta* **522**, 36-45, doi:10.1016/j.tca.2011.02.031 (2011).

McBain, J. & Bakr, A. A new sorption balance1. *Journal of the American Chemical Society* **48**, 690-695 (1926).

McKenna, G. B. Mechanical rejuvenation in polymer glasses: fact or fallacy? *Journal of Physics-Condensed Matter* **15**, S737-S763, doi:10.1088/0953-8984/15/11/301 (2003).

McKenna, G. B. Ten (or more) years of dynamics in confinement: Perspectives for 2010. *European Physical Journal-Special Topics* **189**, 285-302,

doi:10.1140/epjst/e2010-01334-8 (2010).

Menges, G. & Thienel, P. Pressure - specific volume - temperature behavior of thermoplastics under normal processing conditions. *Polymer Engineering & Science* **17**, 758-763 (1977).

Merzlyakov, M., Simon, S. L. & McKenna, G. B. Instrumented thick-walled tube method for measuring thermal pressure in fluids and isotropic stresses in thermosetting resins. *Review of Scientific Instruments* **76**, 7, doi:10.1063/1.1930069 (2005).

Miyazaki, T., Nishida, K. & Kanaya, T. Thermal expansion behavior of ultrathin polymer films supported on silicon substrate. *Physical Review E* **69**, 6, doi:10.1103/PhysRevE.69.061803 (2004).

Morris, D. R. & Sun, X. Water - sorption and transport properties of Nafion 117 H. *Journal of Applied Polymer Science* **50**, 1445-1452 (1993).

Mueller, F., Naeem, S. & Sadowski, G. Toluene Sorption in Poly(styrene) and Poly(vinyl acetate) near the Glass Transition. *Industrial & Engineering Chemistry Research* **52**, 8917-8927, doi:10.1021/ie302322t (2013).

Nayak, S. & Lyon, L. A. Soft nanotechnology with soft nanoparticles. *Angewandte Chemie-International Edition* **44**, 7686-7708, doi:10.1002/anie.200501321 (2005).

O'Donnell, K. P. & Woodward, W. H. H. Dielectric spectroscopy for the determination of the glass transition temperature of pharmaceutical solid dispersions. *Drug Development and Industrial Pharmacy* **41**, 959-968, doi:10.3109/03639045.2014.919314 (2015).

Odani, H., Hayashi, J. & Tamura, M. Diffusion in glassy polymers. II. Effects of polymer-penetrant interaction; diffusion of ethyl methyl ketone in atactic polystyrene. *Bulletin of the Chemical Society of Japan* **34**, 817-821 (1961).

Panayiotou, C., Pantoula, M., Stefanis, E., Tsivintzelis, I. & Economou, I. G. Nonrandom hydrogen-bonding model of fluids and their mixtures. 1. Pure fluids. *Industrial & Engineering Chemistry Research* **43**, 6592-6606, doi:10.1021/ie040114 (2004).

Panayiotou, C., Tsivintzelis, I. & Economou, I. G. Nonrandom hydrogen-bonding model of fluids and their mixtures. 2. Multicomponent mixtures. *Industrial & Engineering Chemistry Research* **46**, 2628-2636, doi:10.1021/ie0612919 (2007).

Paul, D. Gas sorption and transport in glassy polymers. *Berichte der Bunsengesellschaft für physikalische Chemie* **83**, 294-302 (1979).

Pavesi, E. *Mass Transport and Stress Field in Polymer-Solute Systems: Analysis and Solutions of Coupled Problems*, ALMA MATER STUDIORUM Università di Bologna, Bologna (Italy), (2017).

Pierleoni, D. *et al.* Analysis of a Polystyrene-Toluene System through "Dynamic" Sorption Tests: Glass Transitions and Retrograde Vitrification. *Journal of Physical Chemistry B* **121**, 9969-9981,

doi:10.1021/acs.jpcb.7b08722 (2017).

Pierleoni, D., Scherillo, G., Minelli, M., Mensitieri, G. & Doghieri, F. in *8th International Conference on Times of Polymers (TOP) and Composites.* (Amer Inst Physics, 2016).

Potts, J. R., Dreyer, D. R., Bielawski, C. W. & Ruoff, R. S. Graphene-based polymer nanocomposites. *Polymer* **52**, 5-25, doi:10.1016/j.polymer.2010.11.042 (2011).

Punsalan, D. & Koros, W. J. Drifts in penetrant partial molar volumes in glassy polymers due to physical aging. *Polymer* **46**, 10214-10220 (2005).

Pusey, P. N. Colloidal glasses. *Journal of Physics-Condensed Matter* **20**, 6, doi:10.1088/0953-8984/20/49/494202 (2008).

Pusey, P. N. & van Megen, W. Phase-behavior of concentrated suspensions of nearly hard colloidal spheres. *Nature* **320**, 340-342, doi:10.1038/320340a0 (1986).

Rahman, M. S. & Al-Saidi, G. S. Thermal Relaxation of Gelatin and Date Flesh Measured by Isothermal Condition in Differential Scanning Calorimetry (DSC) and its Relation to the Structural and Mechanical Glass Transition. *International Journal of Food Properties* **13**, 931-944, doi:10.1080/10942912.2010.489210 (2010).

Rajendran, A. *et al.* Simultaneous measurement of swelling and sorption in a supercritical CO2-poly(methyl methacrylate) system. *Industrial & Engineering Chemistry Research* **44**, 2549-2560, doi:10.1021/ie049523w (2005).

Reiser, A., Kasper, G. & Hunklinger, S. Pressure-induced isothermal glass transition of small organic molecules. *Physical Review B* **72**, 7, doi:10.1103/PhysRevB.72.094204 (2005).

Rim, Y. S., Bae, S. H., Chen, H. J., De Marco, N. & Yang, Y. Recent Progress in Materials and Devices toward Printable and Flexible Sensors. *Advanced Materials* **28**, 4415-4440, doi:10.1002/adma.201505118 (2016).

Rodriguez, E. L. in *Assignment of the Glass Transition* (ASTM International, 1994).

Royall, C. P., Williams, S. R. & Tanaka, H. The nature of the glass and gel transitions in sticky spheres. *arXiv preprint arXiv:1409.5469* (2014).

Ruegg, M., Luscher, M. & Blanc, B. Hydration of native and rennin coagulated caseins as determined by differential scanning calorimetry and gravimetric sorption measurements. *Journal of Dairy Science* **57**, 387-393 (1974).

Park, S. & Lee, Y. J. Precision Electrical Measurement Experiment Using a Lock-in Amplifier that is Suitable for Science and Engineering Undergraduates. *New Physics: Sae Mulli* **65**, 328-332, doi:10.3938/NPSM.65.328 (2015).

Saeki, S., Holste, J. & Bonner, D. Sorption of organic vapors by polystyrene. *Journal of Polymer Science Part B: Polymer Physics* **19**, 307-320 (1981).

Sauerbrey, G. Verwendung von Schwingquarzen zur Wägung dünner Schichten und zur Mikrowägung. *Zeitschrift für Physik A Hadrons and Nuclei* **155**, 206-222 (1959).

Schawe, J. E. K. Measurement of the thermal glass transition of polystyrene in a cooling rate range of more than six decades. *Thermochimica Acta* **603**, 128-134, doi:10.1016/j.tca.2014.05.025 (2015).

Schult, K. A. & Paul, D. R. Techniques for measurement of water vapor sorption and permeation in polymer films. *Journal of Applied Polymer Science* **61**, 1865-1876, doi:10.1002/(sici)1097-4628(19960912)61:11<1865::aid-app2>3.0.co;2-h (1996).

Sciortino, F. & Tartaglia, P. Glassy colloidal systems. *Advances in Physics* **54**, 471-524, doi:10.1080/00018730500414570 (2005).

Seborg, C. & Stamm, A. J. Sorption of Water Vapor by Paper-Making Materials I—Effect of Beating1. *Industrial & Engineering Chemistry* **23**, 1271-1275 (1931).

Sencadas, V., Lanceros-Mendez, S., Serra, R. S. I., Balado, A. A. & Ribelles, J. L. G. Relaxation dynamics of poly(vinylidene fluoride) studied by dynamical mechanical measurements and dielectric spectroscopy. *European Physical Journal E* **35**, 11, doi:10.1140/epje/i2012-12041-x (2012).

Shenoy, A. Single-event cracking temperature of asphalt pavements directly from bending beam rheometer data. *Journal of Transportation Engineering* **128**, 465-471 (2002).

Struik, L. C. E. Physical Aging in Plastics and other Glassy Materials. *Polymer Engineering and Science* **17**, 165-173, doi:10.1002/pen.760170305 (1977).

Struik, L. C. E. Volume relaxation in polymers. *Rheologica Acta* **5**, 303-311 (1966).

Struik, L. C. E. Physical aging in amorphous polymers and other materials. (1977).

Tanaka, H., Meunier, J. & Bonn, D. Nonergodic states of charged colloidal suspensions: Repulsive and attractive glasses and gels. *Physical Review E* **69**, 6, doi:10.1103/PhysRevE.69.031404 (2004).

Tanaka, Y., Asano, H. & Okuya, Y. Enthalpy relaxation near the glass transition for comb-like polymer: Power law relaxation revealed by DSC experiment. *Journal of Non-Crystalline Solids* **363**, 147-151, doi:10.1016/j.jnoncrysol.2012.11.050 (2013).

Tong, H. & Saenger, K. Bending - beam study of water sorption by thin poly (methyl methacrylate) films. *Journal of applied polymer science* **38**, 937-950 (1989).

Trappe, V., Prasad, V., Cipelletti, L., Segre, P. N. & Weitz, D. A. Jamming phase diagram for attractive particles. *Nature* **411**, 772-775, doi:10.1038/35081021 (2001).

Tribone, J. J., Oreilly, J. M. & Greener, J. Pressure-jump volume-relaxation studies of polystyrene in the glass-transition region. *Journal of Polymer Science Part B-Polymer Physics* **27**, 837-857, doi:10.1002/polb.1989.090270409 (1989).

Tsvigu, C., Pavesi, E., De Angelis, M. G. & Baschetti, M. G. Effect of relative humidity and temperature on the gas transport properties of 6FDA-6FpDA polyimide: Experimental study and modelling. *Journal of Membrane Science* **485**, 60-68, doi:10.1016/j.memsci.2015.02.032 (2015).

van Megen, W. & Pusey, P. N. Dynamic light-scattering study of the glass-transition in a colloidal suspension. *Physical Review A* **43**, 5429-5441, doi:10.1103/PhysRevA.43.5429 (1991).

Vieth, W. & Sladek, K. A model for diffusion in a glassy polymer. *Journal of Colloid Science* **20**, 1014-1033 (1965).

Vig, J. R., Walls, F. L. & Ieee. in *IEEE/EIA International Frequency Control Symposium and Exhibition.* 30-33 (Ieee, 2000).

Visser, T. & Wessling, M. When do sorption-induced relaxations in glassy polymers set in? *Macromolecules* **40**, 4992-5000, doi:10.1021/ma070202g (2007).

Vogt, B. D., Lin, E. K., Wu, W. L. & White, C. C. Effect of film thickness on the validity of the Sauerbrey equation for hydrated polyelectrolyte films. *Journal of Physical Chemistry B* **108**, 12685-12690, doi:10.1021/jp0481005 (2004).

Vrentas, J. S., Duda, J. L. & Hou, A. C. Anomalous sorption in poly(ethyl methacrylate). *Journal of Applied Polymer Science* **29**, 399-406, doi:10.1002/app.1984.070290137 (1984).

Vrentas, J. S., Duda, J. L. & Ling, H. C. Free-volume theories for self-diffusion in polymer solvent systems .1. Conceptual differences in theories. *Journal of Polymer Science Part B-Polymer Physics* **23**, 275-288, doi:10.1002/pol.1985.180230204 (1985).

Wajid, A. On the accuracy of the quartz-crystal microbalance (QCM) in thin-film depositions. *Sensors and Actuators a-Physical* **63**, 41-46, doi:10.1016/s0924-4247(97)80427-x (1997).

Wallace, W. E., Vanzanten, J. H. & Wu, W. L. Influence of an impenetrable interface on a polymer glass-transition temperature. *Physical Review E* **52**, R3329-R3332 (1995).

Walsh, D. & Zoller, P. *Standard pressure volume temperature data for polymers*. (CRC Press, 1995).

White, C. C. & Schrag, J. L. Theoretical predictions for the mechanical response of a model quartz crystal microbalance to two viscoelastic media: A thin sample layer and surrounding bath medium. *The Journal of Chemical Physics* **111**, 11192-11206 (1999).

Wilcock, J. & Campbell, D. A sensitive bending beam apparatus for measuring

the stress in evaporated thin films. *Thin Solid Films* **3**, 3-12 (1969).

Williams, D. A magnetic susceptibility balance suspension. *Thermochimica Acta* **24**, 243-246 (1978).

Wong, H. C., Campbell, S. W. & Bhethanabotla, V. R. Sorption of benzene, toluene and chloroform by poly(styrene) at 298.15 K and 323.15 K using a quartz crystal balance. *Fluid Phase Equilibria* **139**, 371-389, doi:10.1016/s0378-3812(97)00158-1 (1997).

Xie, L. *et al.* Positronium formation as a probe of polymer surfaces and thin-films. *Physical Review Letters* **74**, 4947-4950, doi:10.1103/PhysRevLett.74.4947 (1995).

Yang, L., Srolovitz, D. J. & Yee, A. F. Molecular dynamics study of isobaric and isochoric glass transitions in a model amorphous polymer. *The Journal of chemical physics* **110**, 7058-7069 (1999).

Zhang, C., Guo, Y. L., Shepard, K. B. & Priestley, R. D. Fragility of an Isochorically Confined Polymer Glass. *Journal of Physical Chemistry Letters* **4**, 431-436, doi:10.1021/jz302002v (2013).

Zhang, Y., Gangwani, K. K. & Lemert, R. M. Sorption and swelling of block copolymers in the presence of supercritical fluid carbon dioxide. *Journal of Supercritical Fluids* **11**, 115-134, doi:10.1016/s0896-8446(97)00031-4 (1997).

Zhao, J., Simon, S. L. & McKenna, G. B. Using 20-million-year-old amber to test the super-Arrhenius behaviour of glass-forming systems. *Nature Communications* **4**, 6, doi:10.1038/ncomms2809 (2013).

Zhao, J.-H., Kiene, M., Hu, C. & Ho, P. S. Thermal stress and glass transition of ultrathin polystyrene films. *Applied Physics Letters* **77**, 2843-2845 (2000).

Zhao, J.-H., Ryan, T., Ho, P. S., McKerrow, A. J. & Shih, W.-Y. On-wafer characterization of thermomechanical properties of dielectric thin films by a bending beam technique. *Journal of Applied Physics* **88**, 3029-3038 (2000).

Zheng, Y. & McKenna, G. B. Structural recovery in a model epoxy: Comparison of responses after temperature and relative humidity jumps. *Macromolecules* **36**, 2387-2396, doi:10.1021/ma025930c (2003).

Zhou, J. M. & Lucas, J. P. Hygrothermal effects of epoxy resin. Part II: variations of glass transition temperature. *Polymer* **40**, 5513-5522, doi:10.1016/s0032-3861(98)00791-5 (1999).